The Pennsylvania State University

The Graduate School

Department of Energy and Mineral Engineering

DESIGN OF AN EFFECTIVE WATER-ALTERNATING-GAS (WAG) INJECTION PROCESS USING ARTIFICIAL EXPERT SYSTEMS

A Thesis in

Energy and Mineral Engineering

by

Jaehyun Ma

Submitted in Partial Fulfillment
of the Requirements
for the Degree of

Master of Science

May 2010

*The thesis of Jaehyun Ma was reviewed and approved by the following:

Turgay Ertekin
Professor of Petroleum and Natural Gas Engineering
George E. Trimble Chair in Earth and Mineral Sciences
Thesis Advisor

Luis Felipe Ayala
Assistant Professor of Petroleum and Natural Gas Engineering

John Yilin Wang
Assistant Professor of Petroleum and Natural Gas Engineering

Yaw Yeboah
Professor and Department Head of Energy and Mineral Engineering

*Signatures are on file in the Graduate School

ABSTRACT

Numerical reservoir simulators are commonly used to simulate the water-alternating-gas process for hydrocarbon reservoir. However, a reservoir simulation study can only provide information about the expected reservoir performance and also be time-consuming work. This research presents a screening tool to suggest a set of design parameters that can optimize the WAG process. A commercial reservoir simulator and the neural network toolbox of publicly available software are used in the study.

A number of different five spot scenarios were simulated using a commercial program. These scenarios are associated with different reservoir conditions that include initial water saturation, formation thickness, porosity and permeability. They are also involved various design parameters, that is, well spacing, water-gas ratio, alternating frequency, alternating slug size and bottom hole pressure. The reservoir performance is expressed with recovery efficiency and abandonment time. These simulation results and functional links are used to build an artificial neural network of water-alternating-gas process.

In this study, an artificial neural network is implemented to construct neuro-simulation tools for screening and designing water-alternating-gas process. These tools generated in this study are effectively able to recognize the connection between the reservoir characteristics and hydrocarbon production performance of the WAG process in order to forecast proper operating conditions. They can also serve to provide a relatively narrow range of possible scenarios and reduce the time for conventional reservoir simulations.

TABLE OF CONTENTS

LIST OF FIGURES

LIST OF TABLES

ACKNOWLEDGEMENTS

First of all, I would like to express my sincere gratitude to Dr. Turgay Ertekin, who supported me to complete my journey of this project and provided me with valuable guidance of petroleum engineering. His patience, friendship and kindness will be another precious lesson for my life. I extend my gratitude to Dr. Luis F. Ayala and Dr. John Yilin Wang for serving as committee members.

I also would like to express appreciation to my company, Korea Gas Corporation for providing me with good opportunity to study Petroleum and Natural Gas Engineering in Pennsylvania State University.

Finally, special thanks to my fellow graduate students and my family, especially my wife.

Chapter 1

INTRODUCTION

Primary recovery is oil production by only natural reservoir energy sources such as water drive, solution gas drive, fluid expansion, gas-cap drive and gravity drainage. The amount of oil produced from primary recovery mainly depends on different types of the reservoir but, recovery efficiency is mostly small. Several enhanced oil recovery (EOR) methods have been studied and applied to improve oil production. These methods typically refer to injecting agents like water, steam or gas into the reservoir for increasing oil displacement efficiency. However, each process has couple of disadvantages that still decrease the overall oil recovery efficiency. Unfavorable mobility ratio between oil and water on the displacement front results in low sweep efficiency in the traditional water flooding method. And also strong capillary forces leave high residual oil saturation in the reservoir. The mobility ratio between injected gas and the displaced oil in gas injection method is even worse than that of water flooding process resulting in reduced sweep efficiency and viscous fingering. Water-Alternating-Gas (WAG) injection technique was introduced to solve these problems. The combined mobility of water-gas system is lower than that of injected water or even gas alone. Therefore, the mobility ratio between displacing agent and displaced oil in the WAG process is improved. In this technique water injection reduces viscous fingering and early breakthrough, and gas injection decreases residual oil saturation of water injection process.

Reservoir simulation has played an important role to evaluate an operational scheme of oil recovery and to assess its economic value. The estimation of reservoir performance from simulation studies suggests a good selection of operating conditions under specific reservoir characteristics. However, the simulation result from the given oil field cannot be universally applicable to other fields because reservoir characteristics or conditions are different in each field.

Furthermore, conducting extensive simulation runs is a highly time-consuming task and also needs well-trained simulation engineers. Therefore, it is almost infeasible for every candidate reservoir to be evaluated by traditional numerical simulators for the purpose of proposing appropriate reservoir developing schemes owing to limited time and experts.

An artificial neural network (ANN) is developed in order to overcome such difficulties of common reservoir simulations and also to provide a practical and divert access to the solutions. An ANN is an adaptive system in which its structure can be changed through training period like biological neural networks. In this study, ANN technology is considered to find out the complicated connection between inputs and outputs of reservoir performance mechanism. An inverse application of the universal expert system is constructed to provide proper field development plan and design parameters for a given reservoir with certain characteristics. This inverse looking ANN can reduce time and energy involved in evaluating the candidate reservoirs.

Chapter 2

LITERATURE REVIEW

2. 1 Enhanced Oil Recovery (EOR)

Enhanced oil recovery (EOR) is oil production normally by injecting certain agents into the reservoir to increase recovery efficiency. EOR includes all kinds of oil recovery methods such as drive, push-pull and well treatment. EOR also covers all three stages of oil recovery from primary to secondary and tertiary recovery. Primary recovery typically means the oil production by natural forces such as water drive, solution gas drive, fluid expansion, gas-cap drive and gravity drainage. Secondary recovery involves water flooding, gas injection to maintain reservoir pressure after primary recovery. Tertiary recovery refers to any techniques implemented, for example solvent injection, chemicals, and/or thermal energy after secondary recovery [Lake, 1989].

Increasing demands of petroleum related energy suggest a strong reason to develop advanced EOR technologies. The possibility of producing substantial amount of additional oil from EOR has been proven through various studies. One of the researches studied from U.S. National Petroleum Council shows potential of the enhanced oil recovery processes which could enlarge the current domestic hydrocarbon reserves by approximately 40 per cent and increase the production rate by almost 2 times [Stosur, J. J. George, 2007]. Table 2-1 illustrates three stages of oil recovery processes [Green & White, 1998].

Table 2- 1: Three stage of enhanced oil recovery (reproduced from Green & White, 1998)

Hydrocarbon Recovery Process		
Primary Recovery	Solution Gas Drive	
	Gas Cap Drive	
	Natural Water Drive	
	Gravity Drainage	
	Fluid and Rock Expansion	
Secondary Recovery	Gas Injection	
	Water flooding	
Tertiary Recovery	Thermal	Steam Injection
		In Situ Combustion
		Hot Water Injection
	Chemical	Polymer Flooding
		Surfactant Flooding
		Carbonated Water Flooding
	Solvent	Hydrocarbon Miscible Flooding
		CO_2 miscible Flooding
		CO_2 Immiscible Flooding
		Nitrogen Flooding
		Flue Gas Injection

2. 1. 1 Mobility Effect

If two fluids exist in the reservoir such as oil and gas, there are two properties to determine relative flowing rates of both phases. The effective permeability of oil and gas is directly proportional to each flowing rates, whereas the viscosity inversely affects each of the flowing rates. Therefore, flowing rates is clearly described by calculating effective permeability ratio and viscosity ratio which is expressed as a mobility ratio [Craft and Hawkins, 1959]. The definition of mobility ratio is given by Eq. **2.1**:

$$\frac{q_g}{q_o} = \frac{\left(\frac{k_g A \Delta p}{\mu_g L}\right)}{\left(\frac{k_o A \Delta p}{\mu_o L}\right)} = \frac{\left(\frac{k_g}{\mu_g}\right)}{\left(\frac{k_o}{\mu_o}\right)} = \frac{\lambda_g}{\lambda_o} = \text{Mobility Ratio (M)} \qquad \textbf{(2.1)}$$

Favorable mobility ratio refers to the case that mobility ratio is less than one, whereas unfavorable mobility ratio indicates that mobility ratio is more than one. The mobility ratio between injected gas and displaced oil in gas injection method is usually unfavorable to sweep efficiency since most gases have such low viscosities as compared to that of oil. The viscosity of CO_2, for example, is about 0.03 cp at 1,500 psia and at 110 °F [Green & White, 1998]. The viscosity of volatile oils typically ranges from 0.25 to 3 cp and the viscosity of black oils reach up to 100 cp [Abhijit Y. Dandekar, 2006]. The mechanism of displacement process is dramatically different according to whether the mobility ratio is greater or smaller than one. If the mobility ratio is less than one, there is almost no penetration of displacing agents into the displaced oil bank resulting in stable fronts and also efficient displacing process. However, large mobility ratio allows the displacing solvents to penetrate into the displaced oil causing unstable zones and viscous fingering which reduce oil displacement [Green & White, 1998].

2. 1. 2 Miscible Displacement Processes

Two components are miscible if they can mix completely without forming an interface between them [Lake, 1989]. The displacement efficiency primarily depends on miscibility between oil and displacing materials in the miscible displacement processes [Green & White, 1998]. Main purpose of the miscible displacement processes is to reduce interfacial tension between oil and displacing solvents to its lowest possible extent bringing minimum residual oil saturations.

Miscible displacement processes are subdivided into two categories which are first-contact-miscible (FCM) and multiple-contact-miscible (MCM) with respect to its miscibility. FCM process means that injected fluids can be blended directly with reservoir oils in all proportions and their mixture maintains single phase. On the other hand, MCM process yields two phases and forms a transition zone between oil and displacing fluids. However, all fluid compositions in the transition zone keep their miscibility by repeated contact of oil and injected solvents [Stalkup, 1983].

Research to find out optimal injecting agents tested several materials such as natural gas, flue gas, nitrogen or mixture of these. Relatively high injection pressure and the composition requirement for miscibility restrict the number of possible reservoir where miscible displacement processes can be applied. Carbon dioxide (CO_2) is quite a proper agent for this process since CO_2 requires lower injection pressures and easily available [Carcoana, 1992].

2. 1. 3 The Water-Alternating-Gas Process (WAG)

The WAG process was originally developed to increase recovery efficiency of gas injection by mostly injecting water. Unfavorable mobility ratio between injected gas and the

displaced oil in the miscible displacement processes result in viscous fingering and unstable zone on the flood front. The traditional water flooding also has disadvantages which are unfavorable mobility ratio and strong capillary forces causing high residual oil saturation. Injecting water and gas in an alternative manner can generate reduced mobility of two phases which is even lower than water mobility. High residual oil saturation from water injection can be avoided by using miscible gas owing to phase transitions and inter phase mass transfer between oil and gas [Bedrikovetsky et al, 1996 ; Christensen et al, 2001].

2. 1. 3. 1 Classification of WAG Process

WAG process can be conveniently divided according to miscibility and/or operating method as well. Most of this process has been found to be miscible displacement process, but there exists uncertainty to distinguish between miscible and immiscible WAG. Miscible WAG process should use relatively high injection pressure to maintain the reservoir pressure above the minimum miscibility pressure (MMP). Most miscible WAG has a close well spacing and has been implemented onshore field. Immiscible WAG injection can be useful to the reservoir where gravity-stable gas injection is not possible due to limited gas availability or some reservoir properties such as low dip or strong heterogeneity [Christensen, 2001].

Hybrid WAG injection refers to the process in which a large amount of gas is first injected and then typical WAG operations are followed. Simultaneous water-gas injection called SWAG has been introduced to improve injectivity problems which occurred in high injection rate and/or high permeability reservoir [Rogers & Grigg, 2000].

2. 1. 3. 2 Analysis of WAG Performance with Different Water-Gas Ratio (WGR)

Optimum injection rate of both phases in WAG process has been studied on the miscible water-CO_2 process. There are five different regimes for water-gas injection depending on different water-gas (CO_2) ratio which makes different structure of mixture zones and also different displacement mechanisms. Studies show that injecting high rates of water, that is, higher Water-Gas-Ratio (WGR) results in more favorable mobility ratio. On the other hand, lower WGR reduces the residual oil saturation and the velocity of the front which extends waterless production period. Based on these results, there should be optimum WGR that provides the more stable displacement front and better recovery factor at the same time.

If the WGR is the highest, it is called carbonized water flooding in which all the gas injected is dissolved into water. The structure of mixing zone is such that there is displaced oil bank followed by CO_2 free water-oil bank and then carbonized water. This regime has advantages over the conventional water flooding like the lower residual oil saturation due to the solubility of CO_2. The longer waterless production time and increased oil production after breakthrough are other factors to contributing to the better performance than the water flooding.

When the WGR is less than the one in carbonized water flooding called piston-like displacement, some of the injected CO_2 is dissolved in water and some maintains gas phase resulting in two phase's fluid. The residual oil saturation becomes even lower since free CO_2 works as a solvent. Furthermore, the velocity of the front is reduced making longer waterless production period.

As decreasing more water injection rate, oil saturation on the front is increased and the waterless production period is extended so that the recovery factors are improved.

As the WGR comes close to the lowest value, fluid acts like miscible gas injection process. Displacement instability and viscous fingering occur due to unfavorable mobility ratio. Figure 2-1 shows the displacement mechanism of five regimes.

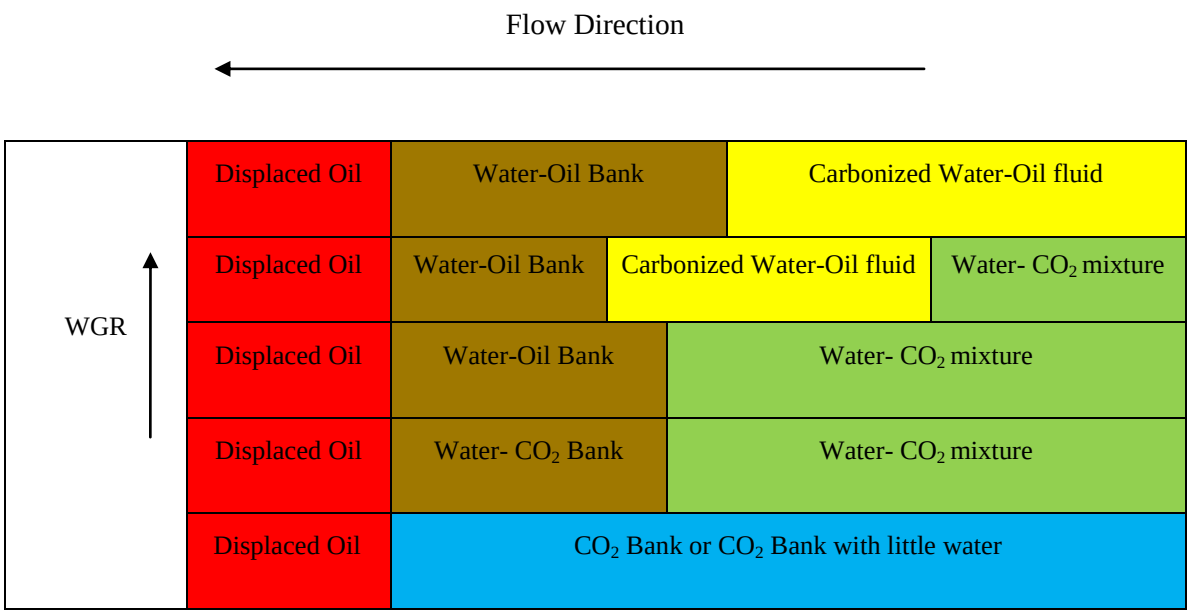

Figure 2- 1: The displacement mechanism of five regimes (adapted from Bedrikovetsky, 1996)

According to this study, the upper value of WGR can be calculated from the fact that the higher the WGR the more favorable mobility ratio. The lower value of WGR can be estimated observing that the lower the WGR the higher the recovery factor [P. Bedrikovetsky et al, 1996].

2. 2 Reservoir Simulation using Computer Programming

Reservoir simulation has been developed to forecast the hydrocarbon reservoir performance combining physics, mathematics, reservoir engineering and computer programming. Petroleum engineers need to calculate performance of oil and gas reservoir under different

characteristics and various operating conditions. It is necessary to estimate the ultimate recovery and total operating period of the candidate reservoir before developing since the capital cost of project can reach hundreds of millions of dollars. Reservoir simulation investigates the economic development scheme reducing the risk related to expensive investment and maximizing profits.

There has been considerable growth of the reservoir simulation technology with advance of computing powers which broaden applicability of simulation, improve reservoir characterization techniques and upgrade complicated oil recovery techniques. Mathematical equations in the form of partial-differential equations are used to calculate the performance of the reservoir. These equations used in the simulator are formulated in an attempt to incorporate the most important physical phenomena taking place in the reservoir, for example, the flow of fluids separated into as many as three phases (oil, water and gas), mass transfer between phases and the effects of viscous, capillary and gravity forces. This method also takes into account various rock properties, fluid properties and relative permeability effects as well.

If the problems that the reservoir simulator deals with are simple enough to be solved analytically (exactly), the solution would provide exact value of the pressure and production rates with continuous function of time and position. Because most reservoir analysis involves complicated problems, numerical (approximate) solutions are more efficient than analytical approach. Numerical methods produce the approximate solutions which give reservoir performance prediction at discrete locations in the reservoir.

There are several ways to categorize the reservoir simulators. According to the type of reservoir and fluids, reservoir simulators can be divided into two categories namely as black-oil and compositional models. In black-oil models, compositional changes of the reservoir fluids are considered not to have influence on recovery and mass transfer is an exclusive function of pressure. Compositional simulators are applicable to the reservoir which is responsive to

compositional changes such as primary depletion of volatile oil and gas condensate reservoir, pressure maintenance processes and multi-contact miscible displacement.

Reservoir simulators can also be classified with regard to recovery processes. Primary and secondary recovery processes are simulated using black-oil models. Tertiary recovery methods such as chemical flooding can be modeled by specialized compositional simulators that have conservation equations for individual chemical components. Thermal processes are investigated using thermal recovery simulators that solve energy balance equation along with the mass balance equations [Ertekin et al., 2001].

2. 3 Overview of an Artificial Neural Network (ANN)

An artificial neural network is a signal processing technology that imitates the operation of a biological neural system. Although computer power is tremendously developed, there are certain limits by which the need of an artificial neural network is underlined. An artificial neural network has several advantages over the conventional data processing methods based on computer programming. An ANN can solve the problems that a sequential program cannot take care of. An ANN learns through training period just like a biological organism so that it does not need to be reprogrammed. Traditional computer programming is typically useful to specific problems and it should be changed according to each different problems. But an ANN can be implemented in wide range of application to produce solutions for various problems saving time and personnel.

2. 3. 1 The Structure of an Artificial Neuron

A biological neuron has three main components of its structure, that is, the cell body or soma, the dendrites and the axon. The cell body is the center of the cell. Many dendrites stem from the cell body receiving signals from other neurons. The axon delivers electric signals produced at the axon hillock down its length. Neuron uses these electric signals called action potentials to carry information to the brain. Figure 2-2 shows schematic of biological neurons [Hagan et al., 1996].

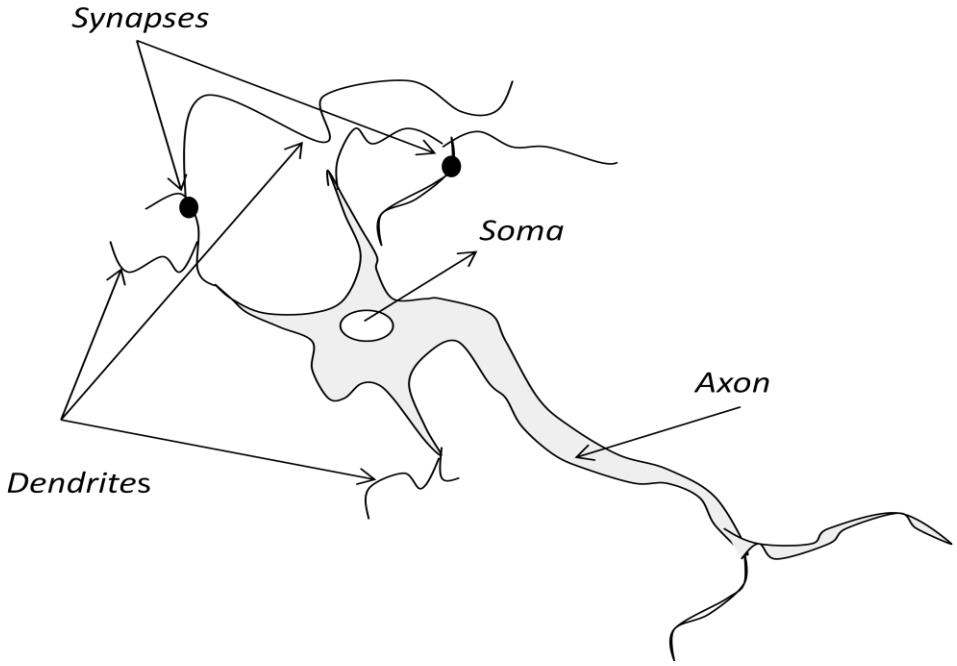

Figure 2- 2: Schematic of biological neurons (adapted from Hagan et al., 1996)

There are also three main elements to build an artificial neural network which has similarity with a biological network. First of all, the synapses of the neuron are represented as weights which describe how strongly the connection is made between an input and a neuron.

Each input X shown in Figure 2-3 is multiplied by a weight W which is determined during an iterative training process. Next, summarizing junction 'Σ' collects all the inputs 'X*W+b'. Finally, transfer function 'F' decides magnitude of the output of the neuron 'y' through modification of those inputs. These outputs indicate electrical signals called action potentials [Fausett, 1994].

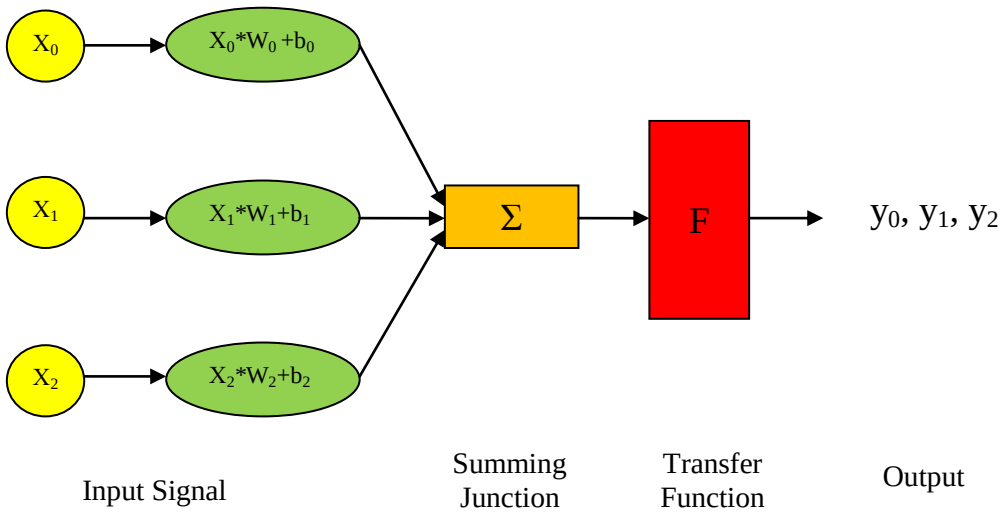

Figure 2- 3: Schematic of an artificial neuron

2. 3. 2 The Structure of Networks

The structure of an artificial neural network commonly falls into two kinds which are single-layer and multilayer networks. In a single-layer network, there is only one input and one output layer that are linked to each other with one layer of connection weights. The multilayer system has one input and one output layer and several internal layers called hidden layers. It is true that more layers the network has the more complicated problems to be solved. However,

multilayer systems need relatively longer periods for training compared to single layer counterpart [Minakowski, 2008]. Figure 2-4 shows each structure of a single-layer and a multilayer network.

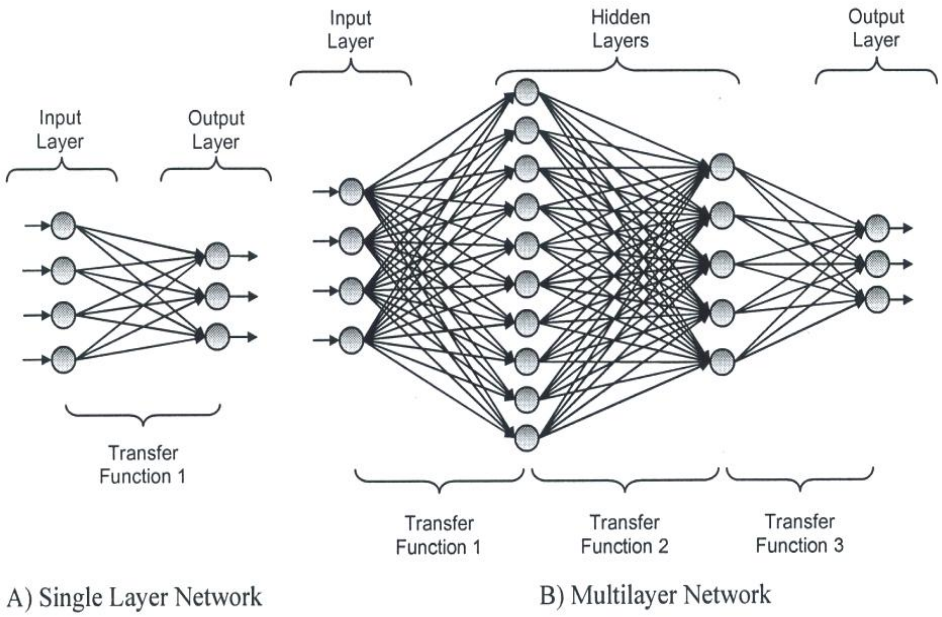

Figure 2- 4: Structures of single-layer and multilayer networks (adapted from Minakowski, 2008)

2. 3. 3 Transfer Functions

The transfer functions yield the action potentials by responding artificial neurons. A pure linear transfer function generates output of a neuron "a" which is equal value of its input "n" as given in Eq. 2-2:

$$a = \mathrm{n} \tag{2. 2}$$

A threshold or bias is sometimes involved in this linear transfer function. The bias "b" constantly adds another weight to the input of the neuron [Fausett, 1994]. The linear transfer function is applied to the output layer because it allows the network to generate its output within the desired limits without de-normalizing them. Figure 2-5 shows two types of linear functions.

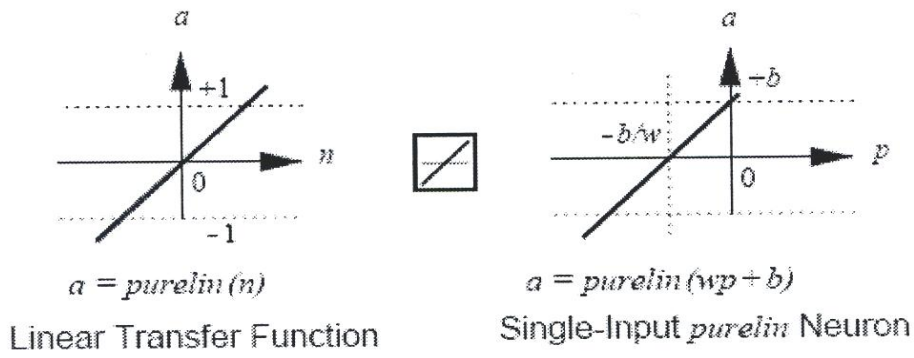

Figure 2- 5 : Linear transfer function (reproduced from Hagan et al., 1996)

Sigmoid functions are nonlinear transfer functions that deals with more complicated problems compared to linear functions. The log-sigmoid and the hyperbolic tangent sigmoid function are the typical ones applying back propagation training method.

The log-sigmoid function reads the input signal, which can be any values between positive and negative infinity, activates neurons and generates its output at the range of 0 and 1. The output of the log-sigmoid transfer functions is given in Eq. 2.3 and Figure 2-6.

$$a = \frac{1}{1 + e^{-n}} \qquad \textbf{(2.3)}$$

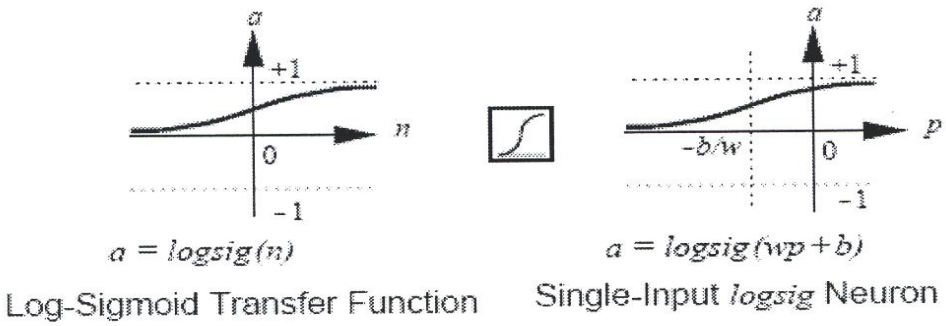

Figure 2- 6: Log-sigmoid transfer function (reproduced from Hagan et al., 1996)

The hyperbolic tangent sigmoid transfer functions, shown in Eq. 2.4 and Figure 2.7, produce its outputs with value between -1 and 1.

$$\mathrm{a} = \frac{e^{n} - e^{-n}}{e^{n} + e^{-n}} \qquad \textbf{(2.4)}$$

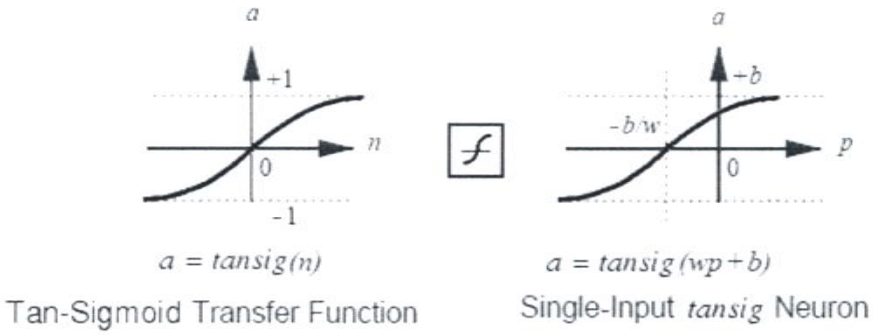

Figure 2- 7: Hyperbolic tan-sigmoid transfer function

2. 3. 4 Training of an Artificial Neural Network

The weights express the strength of the connection between an input and a neuron, for instance, negative value of weights for inhibitory connections and positive values for excitatory connections. These weights are decided through an iterative training session.

In general, network training process can be classified into two categories which are supervised learning and unsupervised learning. In supervised learning, pattern or input vector is provided with an associated target or output vector. The weights are initially set to zero or to a small value. Then, these weights are changed iteratively by a learning algorithm until the calculated output target is close to the given target. Unsupervised learning refers output unit is trained by reacting to clusters of pattern within the input. The network has to find out statistically clear characteristics of the input on its own. The difference between those two training methods is the existence of a priori set of categories into which the patterns are to be classified [Minakowski, 2008]. For the present study, supervised learning is used with sets of input pattern and output target produced using a commercial reservoir simulator.

2. 3. 5 Multilayer Feedforward Networks with Back Propagation

Multilayer feedforward network with back propagation is the most common learning process in neural network [Maren et al., 1990 & Patterson, 1995]. This type of network always connects neurons of each layer in forward direction. The back propagation refers to a supervised learning process which is utilized in this multilayer networks. The learning mechanism of the back propagation process is the Generalized Delta Rule, a generalized form of the Least Mean Squared (LMS) rule. This rule applies the optimization of the weights and biases of each layer for the purpose of reducing the difference between the network outputs and the desired targets.

Three main stages are involved in this feedforward back propagation method. The forward feeding of the input through the network is the first stage in which input pattern is introduced to the input layer and the information flow through the hidden layers to the output layer. Transfer functions modify the information in each layer. Back propagation is the next stage in which network response is compared to the desired output to estimate the gradient of the error of the network. The errors calculated are then propagated from the output layer to the inner layer, and finally these errors allow proper adjustment of the connection weights. Several iterations of this process decrease the error of the network [Ali, 1994].

2. 3. 6 Convergences and Training Efficiency

Convergence problems occur when the network calculates a lower value of total error than the one in the previous iteration without achieving an overall minimum error. As a result, the network memorizes the training data sets and cannot generate appropriate outputs. Early stopping is a typical method to avoid the network memorization related problems. In this method validation data set is provided into the network along with the training data set. Thus, the network can be trained independently while the error of the validation set is monitored. When the networks begin overtraining, the validation error starts increasing and the training error keeps decreasing. The training process is then stopped [Demuth et al., 2007 & Maren et al., 1990].

There are several ways to improve learning efficiency. One common method is to optimize the number of neuron in hidden layers. Also, applying functional links to the input and/or output layer allows the network to interpret the data through various angles and thus help to improve the training efficiency. The learning rate can also have influence on the training efficiency. Large learning rates result in faster training with some fluctuation and small learning

rates decrease learning speed with more stabilization. A high momentum parameter is another way for increasing the speed of convergence.

Chapter 3

STATEMENT OF THE PROBLEM

The water-alternating-gas (WAG) process is developed to overcome several individually characteristic disadvantages of water injection and gas injection methods. Unfavorable mobility ratio between oil and water or gas on the displacement front reduces sweep efficiency. Injected water formulates strong capillary forces leaving high residual oil saturation. Low viscous gases involve viscous fingering and early breakthrough. Alternative injection of two phases results in improved mobility ratio between displaced oil and injected fluids. Thus stable displacement front of WAG can effectively increase the ultimate recovery efficiency.

Reservoir simulations are commonly utilized to evaluate different field development plans with field data for given reservoirs. However, the simulation results generated for a specific oil field are not readily applicable to other reservoirs since reservoir characteristics and operating conditions are different. Reservoir assessment using simulation techniques even requires significant amount of time and well-trained experts. Furthermore, available guidelines for WAG process do not propose detailed operating conditions for various candidate reservoirs.

In this study, an artificial neural network is brought to overcome such difficulties of common reservoir simulation as time and expert limitation allowing easy access to the solutions. Inverse application of ANN provides the optimized operating conditions to achieve certain reservoir performance for a given field.

Chapter 4

RESERVOIR MODEL

Numerical reservoir simulation is a common method to forecast oil and gas reservoir performance under various conditions. With simulation results, petroleum engineers can decide the most efficient way of developing the reservoir under consideration. Reservoir simulation can also serve to reduce the investment risk by optimizing production schemes.

There are two basic elements needed to build a reservoir simulation, which are design parameters and reservoir characteristics. Design parameters refers to well pattern, injection rates of injection wells and bottom hole pressure of a production well. In order to calculate injection rates, there are four parameters to be determined such as well spacing, alternating slug size, alternating frequency and water-gas ratio. These parameters can be determined by engineers according to development plans. On the other hand, reservoir characteristics indicate rock properties, fluid properties and hydrocarbon formation such as types of oil, initial water saturations, formation thickness, porosity and permeability. Reservoir characteristics are unique values for specific field and cannot be effectively modified.

Since an artificial neural network demands a large number of data to increase prediction accuracy, various reservoir simulations were made using a commercial reservoir simulator. Homogeneous and isotropic conditions are applied for simplifications which do not reduce the accuracy for numerical model.

4. 1 Fluid Types and Initial Reservoir Conditions

Black-oil formulation is chosen to develop this study. Black-oil models are often used in modeling the most common type of oil reservoirs. This type of oil normally contains heavy

hydrocarbon elements such as heptanes plus fraction. Table 4-1 shows PVT composition that was taken from the literature.

Table 4- 1: Molar composition of typical black-oil (adapted from Minakowski, 2008)

	CO_2	N_2	C1	C2	C3	iC4	nC4	iC5	nC5	C6	C7+	MW
Black Oil (PVT#1)	0.91	0.16	36.47	9.67	6.95	1.44	3.93	1.44	1.41	4.33	33.29	218

Most of WAG process using CO_2 has been reported as miscible drive from field experiences [Christensen, 2001]. Initial reservoir conditions should be determined to satisfy minimum miscible pressure and temperature. In general, deeper reservoirs tend to involve high pressure and temperature which maintain miscible displacement conditions. This study utilizes the temperature profile of the reservoirs in the Malay Basin to decide initial reservoir temperature. Figure 4-1 shows the frequency of reservoir temperature measured in the Malay Basin. Since 220°F has the highest frequency, the reservoir temperature of this research is all fixed at 220°F.

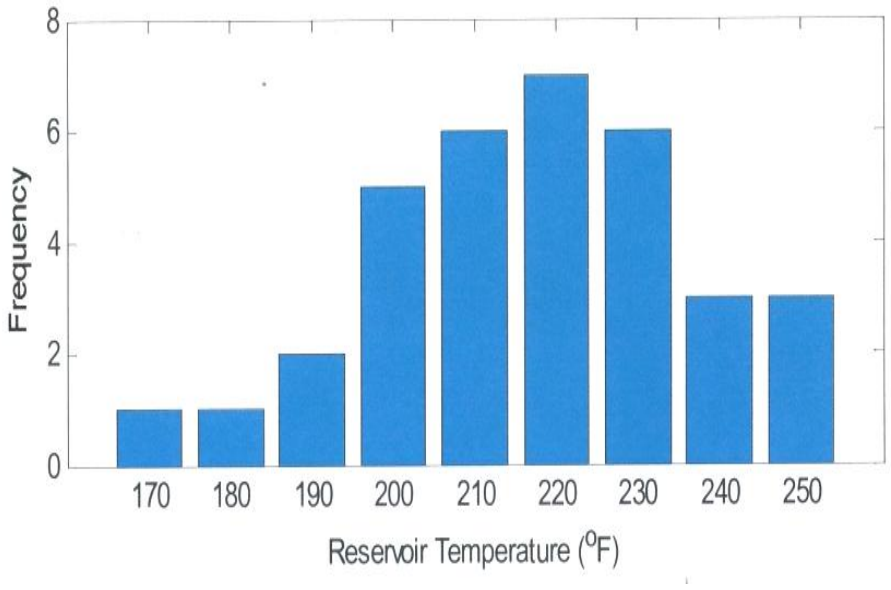

Figure 4- 1: Reservoir temperature in the Malay basin (from Teletzke et al., 2005)

The initial reservoir pressure should then correspond with keeping miscible displacement conditions at the temperature of 220°F. In order to decide minimum miscible pressure (MMP) of CO_2, this study applies the results obtained using slim-tube test that generates minimum miscible pressure as a function of temperature. This test introduces a correlation to predict CO_2 MMP and suggests that only temperature has crucial influence on CO_2 MMP. Figure 4-2 shows CO_2 MMP [Yellig & Metcalfe, 1980]. According to the graph below, minimum miscible pressure is about 2900 psia at the temperature of 220°F. The initial reservoir pressure of this study is set at 5000 psia so that pressure drop around producing wells does not affect miscible conditions.

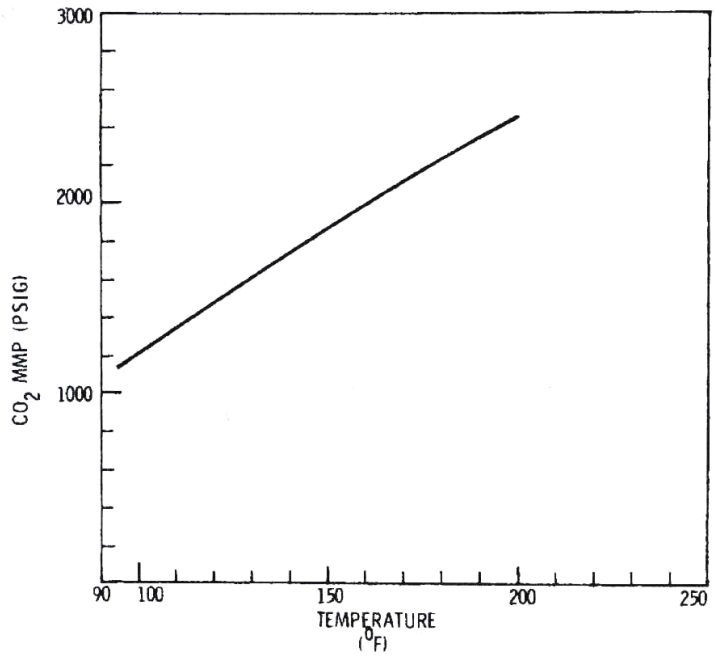

Figure 4- 2: CO_2 MMP (from Yellig & Metcalfe, 1980)

4. 2 Well Pattern

Most of field application of WAG process chooses 5-spot pattern because this well pattern makes a fairly close well spacing and is effective to maintain miscible drive operations. It is true that off-shore reservoir utilizes relatively spare well pattern since drilling related cost is expensive. However, off shore WAG is still considered pilot project and onshore WAG is a routine operation [Christensen, 2001]. Thus, five-spot well pattern is fixed for the present study. Figure 4-3 gives a good example of popularity of 5-spot pattern for onshore WAG operations.

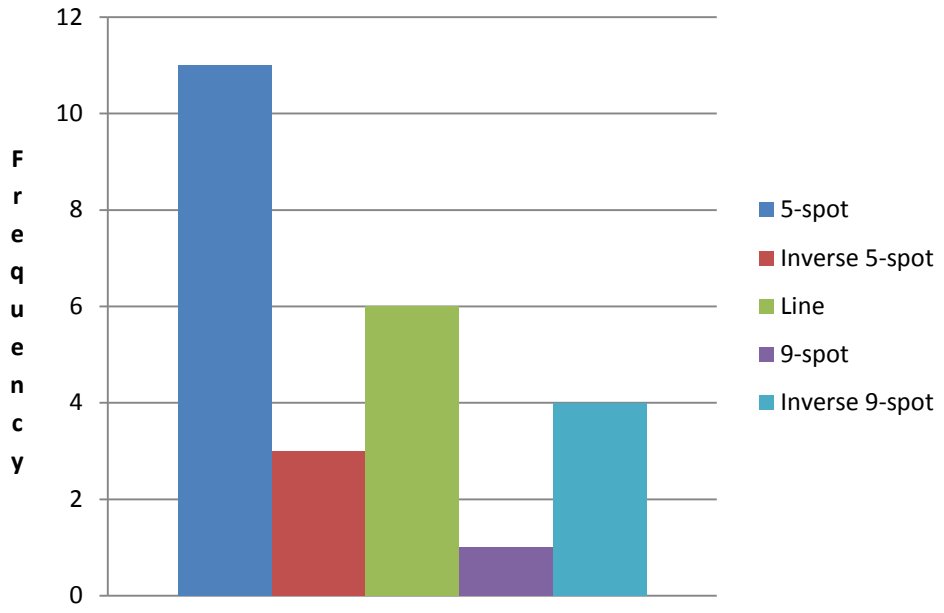

Figure 4- 3: The number of field operations utilizing WAG according to well patterns (reproduced from Christensen, 2001)

4. 3 Grid Block Dimensions

In order to decide the optimum number of grid blocks for numerical simulation, five different grid block sizes were tested. As the number of grid blocks is increased, the simulation takes the longer time. Thus, the number of grid blocks is attempted to be minimized without decreasing the accuracy of the runs. Tests were performed on three different well spacing which are 20, 104 and 200 acres for black-oil. The number of grid blocks tried was 9×9, 15×15, 25×25, 35×35 and 45×45 with 4 layers. The properties used to produce these test are presented in Table 4-2.

Table 4- 2: Simulation properties for optimum number of grid blocks

Area (acres)	20	104	200
WAG Ratio	0.6	1	3.1
Alternating Frequency (days)	90	60	45
Alternating CO2 Size (% PV)	1.5	1.4	0.4
BHP Producer (psia)	3500	3000	3250
Thickness (ft)	560	200	50
Porosity (%)	15	40	25
Permeability (md)	10	100	10
Initial Water Saturation (%)	15	15	40

Figure 4-4 shows the recovery efficiency and abandonment time with regard to the number of grid blocks utilized. It is noted that the results do not make noticeable difference between number of grid blocks 15×15 and 45×45 in each three tests. But, 9×9 grid dimension yields an obvious deviation for both the recovery efficiency. Thus, 15×15 grid block size is used for present study to reduce considerable amount of computational time without sacrificing the accuracy.

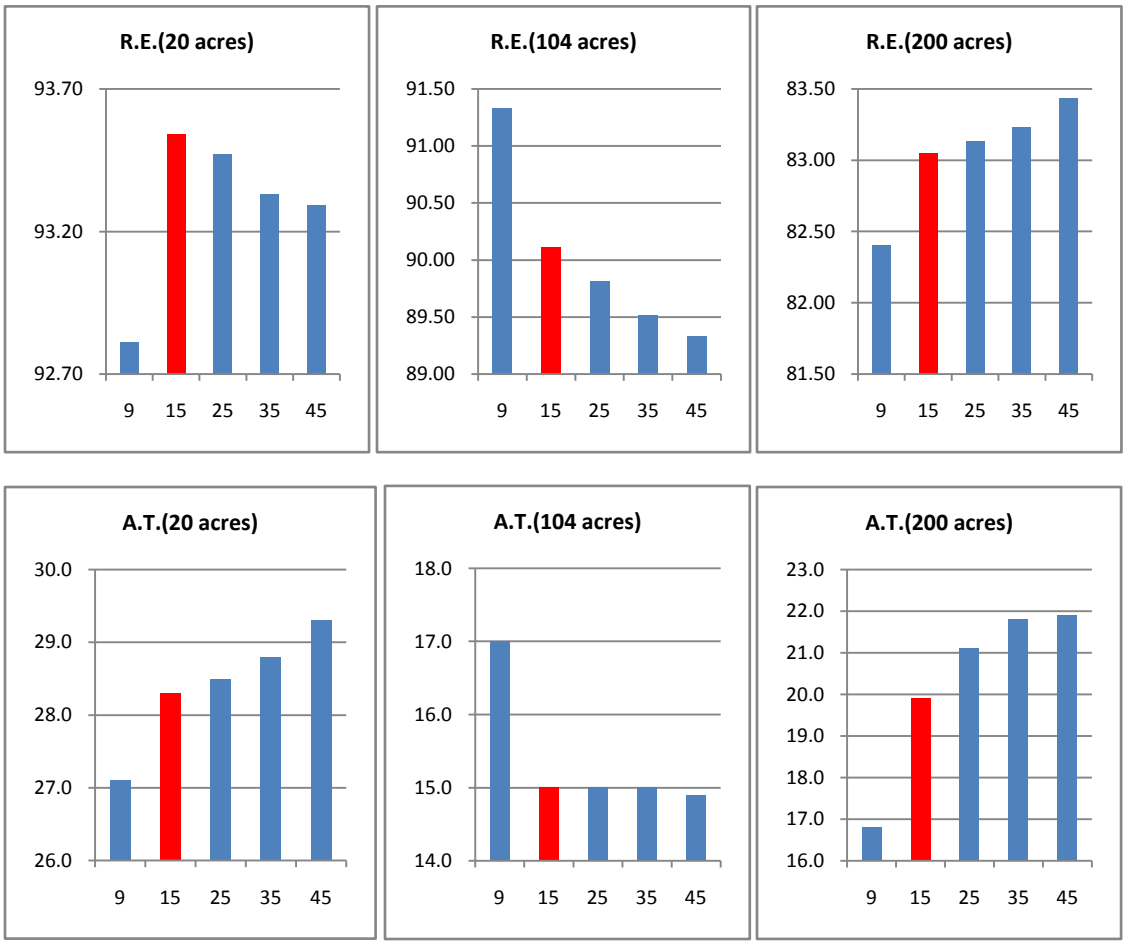

Figure 4- 4: Sensitivity analysis on the number of grid blocks used in describing the computational domain for different pattern sizes

4. 4 Reservoir Layering and Well Completion

In order to account for gravitational effects, all reservoir simulation models consist of four layers associated only with the hydrocarbon zone or pay zone. All the reservoirs are initially saturated with water and oil. Thus, initially free gas zone does not exist in the reservoir. There is no aquifer included in this model. Both production well and injection wells are completed in all four layers. Figure 4-5 illustrates a 3D grid model of 5-spot pattern having four layers.

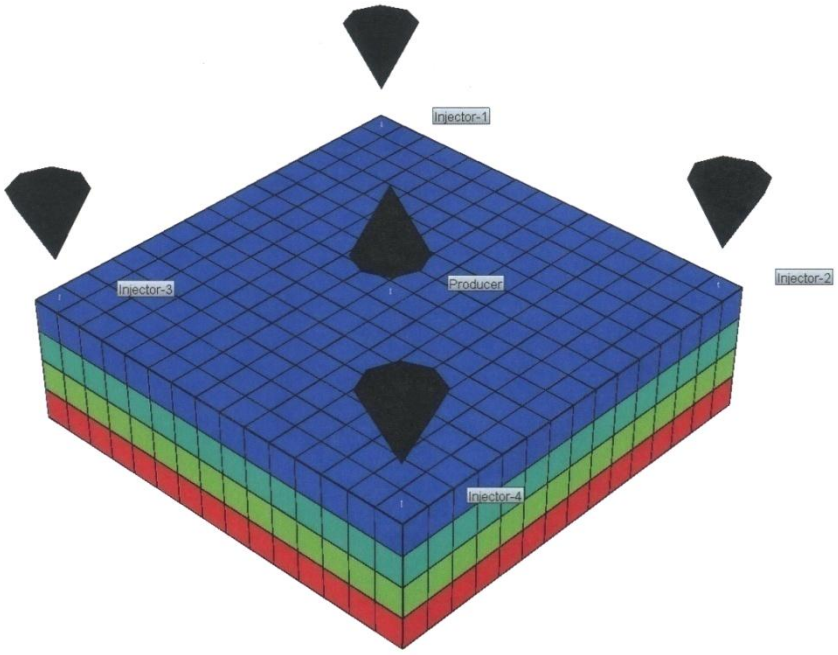

Figure 4- 5: 3D grid model and layering

4. 5 Relative Permeability and Capillary Pressure

The relative permeability data for present study is the properties of sandstone rock which is the most common type of hydrocarbon formation applied WAG injection [Christensen, 2001]. Figure 4-6 indicates WAG applications according to rock types. The water-oil and gas-oil relative permeability curves are generated using Corey's correlations [Corey, 1954]. This three- phase relative permeability curve shown in Figure 4-7 is fixed in all reservoir simulations.

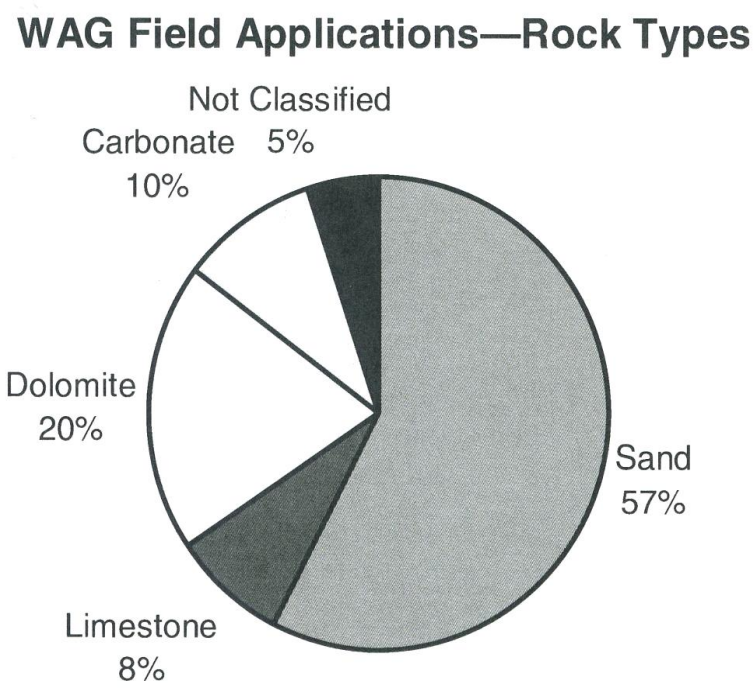

Figure 4- 6: WAG field applications according to rock types (adapted from Christensen, 2001)

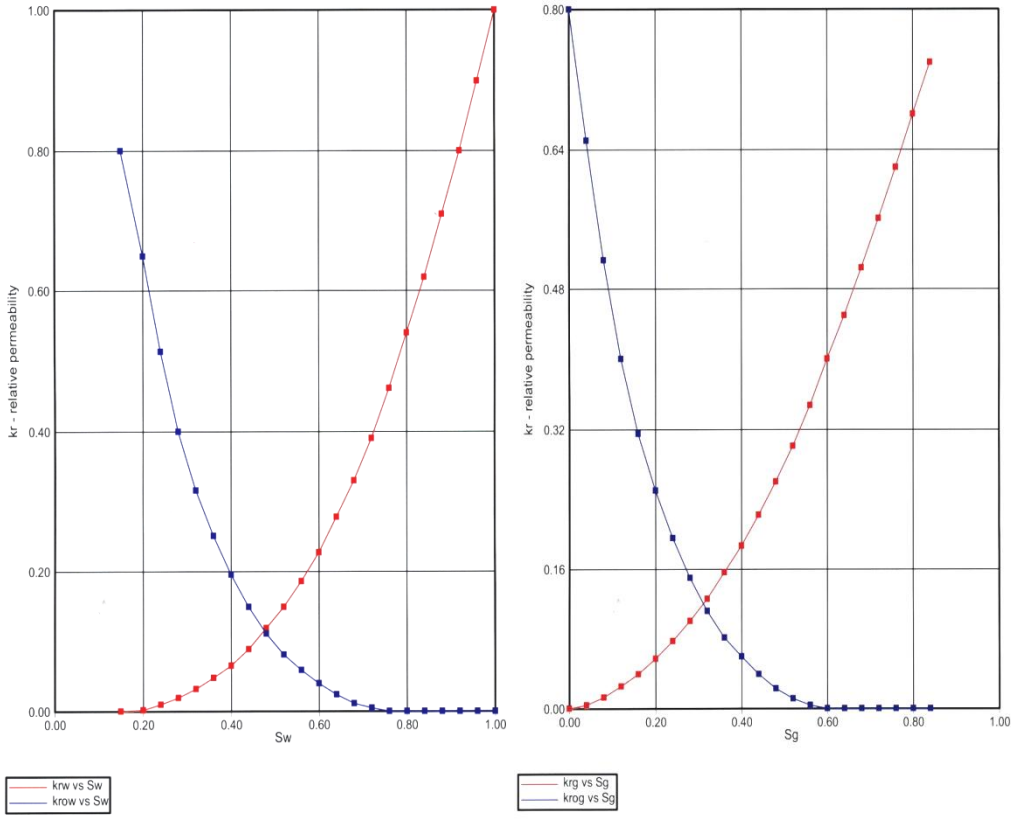

Figure 4- 7: Water-oil & gas-oil relative permeability curves

4. 6 Operational Conditions of WAG Process

The operational conditions refer to the parameters used to decide well performance. There are a couple of parameters such as well spacing, water-gas ratio, alternating frequency, alternating slug size and bottom hole pressure. It is true that a well can be operated by controlling either its pressure or flow rates. However, recovery efficiency and abandonment time mostly depend on injection rates in WAG process and minimum miscible pressure should be maintained around a producing well. Thus, an injection well is controlled by its injection rates and a

producing well is monitored by bottom hole pressure to achieve high performance for this WAG process.

There are four different parameters utilized in deciding the injection rates. First of all, water-gas injection ratio for this study is fixed in the range of 0.5 to 4 representing the typical values from field experience. If water-gas ratio is too small, then unstable front and viscous fingering is problematic. If water-gas ratio is too large, then high residual oil saturations reduce the amount of cumulative oil production. Next, the slug size of alternating CO_2 used changes from 0.1 to 2 % of pore volume which is also regular range from field experiences. In order to decide proper alternating slug size, abandonment time should be taken into account. When alternating slug size of both water and gas is too small, then obviously it would take relatively long time to reach ultimate recovery. The alternating frequency for water-gas injection can be 30, 60 and 90 days. Too short frequency gives infeasible conditions from the perspective of field operations, whereas the WAG advantages would be lost by alternating both phases with a too long interval. Lastly, well spacing should be determined without losing miscible displacement conditions since a relatively close distance of wells provide a good control of reservoir pressure and thus WAG performance. Numerical simulations for this study are implemented on well spacing that ranges from 20 acres up to 200 acres.

On the other hand, in order to evaluate the optimum bottom hole pressure of a producing well, miscible displacement process should be considered. Bottom hole pressure of a producing well should be below the initial reservoir pressure to produce oil by pressure drawdown and also more than minimum miscibility pressure to reduce detrimental effect on miscible conditions. Bottom hole pressure of a producing well is fixed at the range of 3000-4000 psia since minimum miscible pressure of CO_2 is about 2900 psia at the temperature of 220°F according to the Figure 4-2.

The abandonment condition is set at the time when the water cut reaches 90 % at the producing well.

Chapter 5

DEVELOPMENT OF AN ANN BASED PREDICTION TOOL

A series of WAG process scenarios are simulated for black-oil using properties within certain ranges. This information is utilized in designing and training different architectures to construct an artificial neural network. Three considerations are discussed in this chapter: selection of inputs and outputs, training of the artificial neural network, and finally the accuracy analysis to evaluate the performance of networks.

5. 1 Inputs and Outputs

While reservoir performance depends on the reservoir characteristics such as fluid properties and rock properties, production of oil is furthermore controlled by different operating schemes such as well pressures and/or flow rates. A commercial simulator predicts the reservoir performance of a specific hydrocarbon field using reservoir natural characteristics and field development plans. Forward looking ANN also forecasts the reservoir performance by feeding the reservoir characteristics and field operating schemes. However, the main purpose of this study is to establish a screening tool to evaluate WAG process by the inverse application of ANN. Thus, the accomplishment of this purpose is based on suggesting a good selection of design parameters to achieve certain reservoir performance from given reservoir natural characteristics.

There are two different groups of input variables to build the inverse neural network. One is the reservoir characteristics that are summarized in Table 5-1. The rock properties are permeability, thickness and porosity. The fluid properties are type of oil that is black-oil for this

study. Reservoir temperature, initial reservoir pressure and initial water saturation are also included in the reservoir characteristics.

Table 5- 1: Reservoir characteristics as input variables

	min	mid	max
Type of Oil	Black-oil (PVT #1)		
Formation Thickness (ft)	50	200	560
Porosity (%)	15	25	40
Permeability (md)	10	100	500
Initial Reservoir Pressure (psia)	5000		
Reservoir Temperature (°F)	220		
Initial Water Saturation (%)	15	-	40

The other group of input is reservoir performances that are obtained from a commercial simulator. Simulations provide cumulative oil production curve as a function of time. The reservoir performance can be expressed by recovery efficiency that is the cumulative oil production divided by original oil in place. One significant observation is that abandonment time can be different for given reservoir even though the recovery efficiency is similar. Thus, recovery efficiency and abandonment time consist of this group of input. Figure 5-1 shows one of the oil production curves.

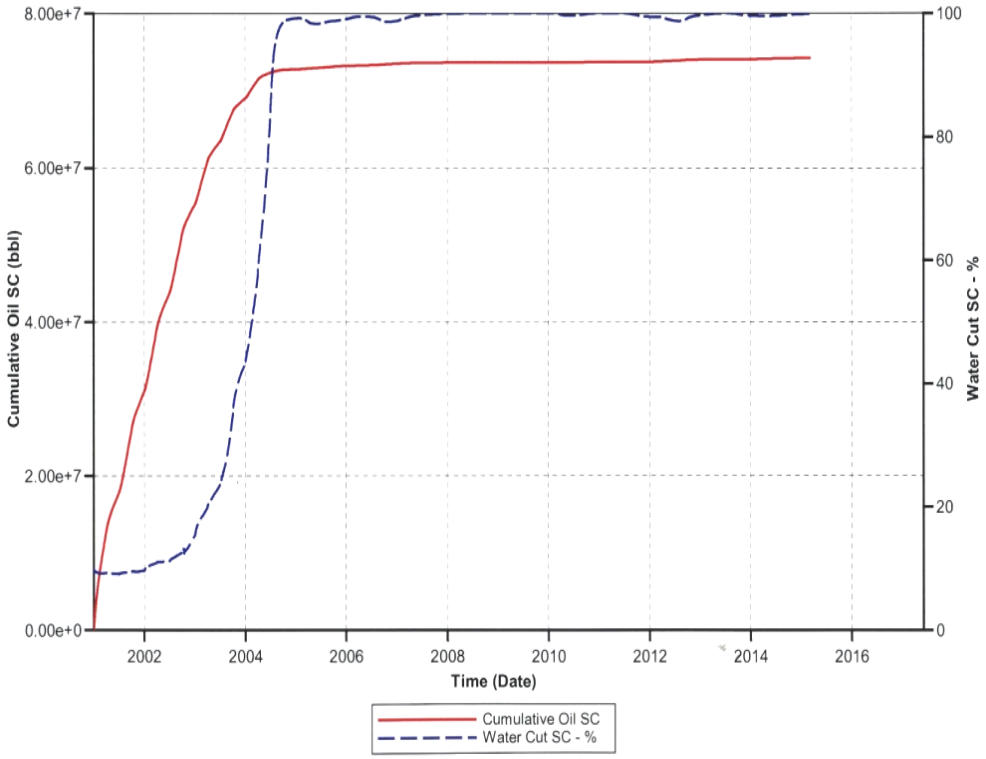

Figure 5- 1: Oil production curve

The inverse neural network is then constructed to yield the field development plans called design parameters which consist of well spacing, water-CO_2 injection ratio, alternating frequency, alternating slug size and bottom hole pressure of a producing well. This study generates three respective networks according to 30, 60 and 90 days of alternating frequency. Table 5-2 shows output variables and each ranges.

Table 5- 2: Design parameters as outputs

	min	max
Well Spacing (Acres)	20	200
WAG Ratio	0.5	4
Alternating Frequency (Days)	30, 60, 90	
Alternating CO2 Size (% of PV)	0.1	2
Producing Well BHP (psia)	3000	4000

5. 2 Training an Artificial Neural Network and the Accuracy Analysis

The construction of WAG ANN was conducted in two stages in order to simplify the design process. In the first stage, expert system was built for only 60 days with fixed alternating CO_2 size. This network architecture provides the foundation to build more complicated networks which are universal expert systems in the second stage. In both stages, forward looking neural networks are also built along with inverse looking neural networks.

5. 2. 1 Stage-One: Expert System with Fixed Alternating Slug Size

A simple problem is studied in the first stage of the network construction. This network is developed with only 60 days alternating frequency maintaining unchanged alternating CO_2 size, 1% of pore volume. In order to train an ANN successfully, it is necessary to provide the network with as many data that cover most of reasonable scenarios as possible. But, generating these voluminous data using a commercial simulator requires tremendous computational time. This

network utilizes 239 cases that can include some of the most probable combinations of each variable.

Different network architectures were tried in this stage for the purpose of finding the most effective architecture for the WAG process. The networks utilize the multilayer cascade feed forward back propagation algorithm (newcf). The networks are also designed using the conjugate gradient back propagation with Fletcher-Reeves training function (traincgf) and the gradient descent with momentum weight and bias learning function (learngdm). Both forward and inverse networks utilize four hidden layers to deal with the complexity of problems. Transfer functions used in each hidden layers are in the order of tansig, logsig, tansig, and logsig while the purelin transfer function was used in the last layer.

Generated data are divided into three groups for the purpose of training, validation and testing. A total of 239 cases are separated in the following manner: 193 cases for training, 23 cases for testing, and another 23 cases for validation.

Forward looking neural network uses four reservoir characteristics and three design parameters as inputs to predict abandonment time and recovery efficiency. Table 5-3 and Figure 5-2 shows forward looking neural network architecture of the first stage.

Table 5- 3: Inputs and outputs of “stage-one” forward looking neural network

Inputs		Outputs	
Reservoir Characteristics	Formation Thickness (h) Porosity (Ø) Permeability (k) Initial Water Saturation (Swi)	**Reservoir Performance**	Abandonment Time (A.T.) Recovery Efficiency (R.E.)
Design Parameters	Well Spacing WAG Ratio Producing Well BHP		

Four functional links are added to the output layer to improve the accuracy of the network. This network is trained with 45 neurons in the first hidden layer, 30 neurons in the second layer, 20 neurons in the third layer and 15 neurons in the forth layer.

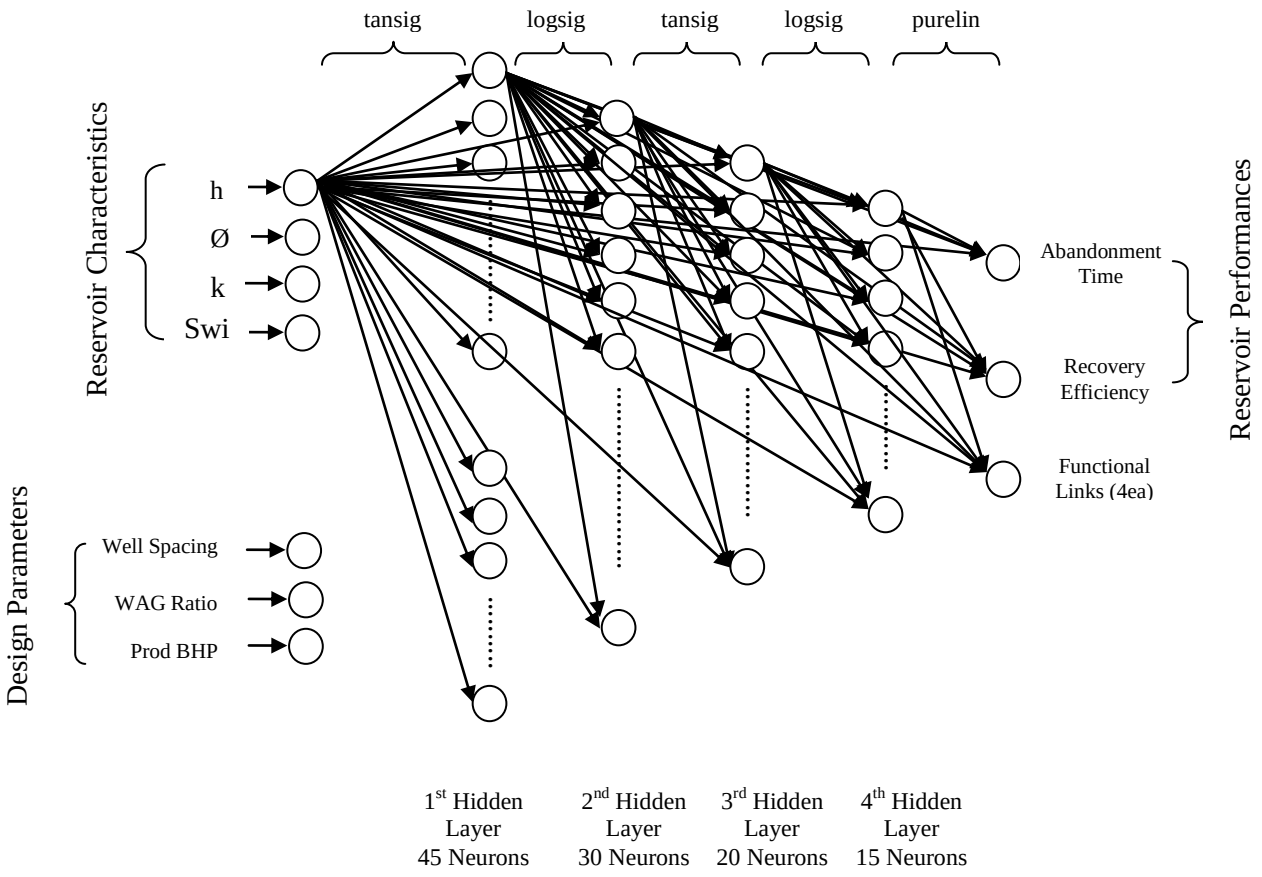

Figure 5- 2: Forward looking network architecture built in "stage-one"

This network cannot achieve the desired mean squared error of 10^{-4} and the overall performance or LMS error is 0.00118. The accuracy of the network is then analyzed by comparing the simulation outputs with the predicted ones. One of testing data sets of forward application is compared with the simulation results shown in Figure 5-3.

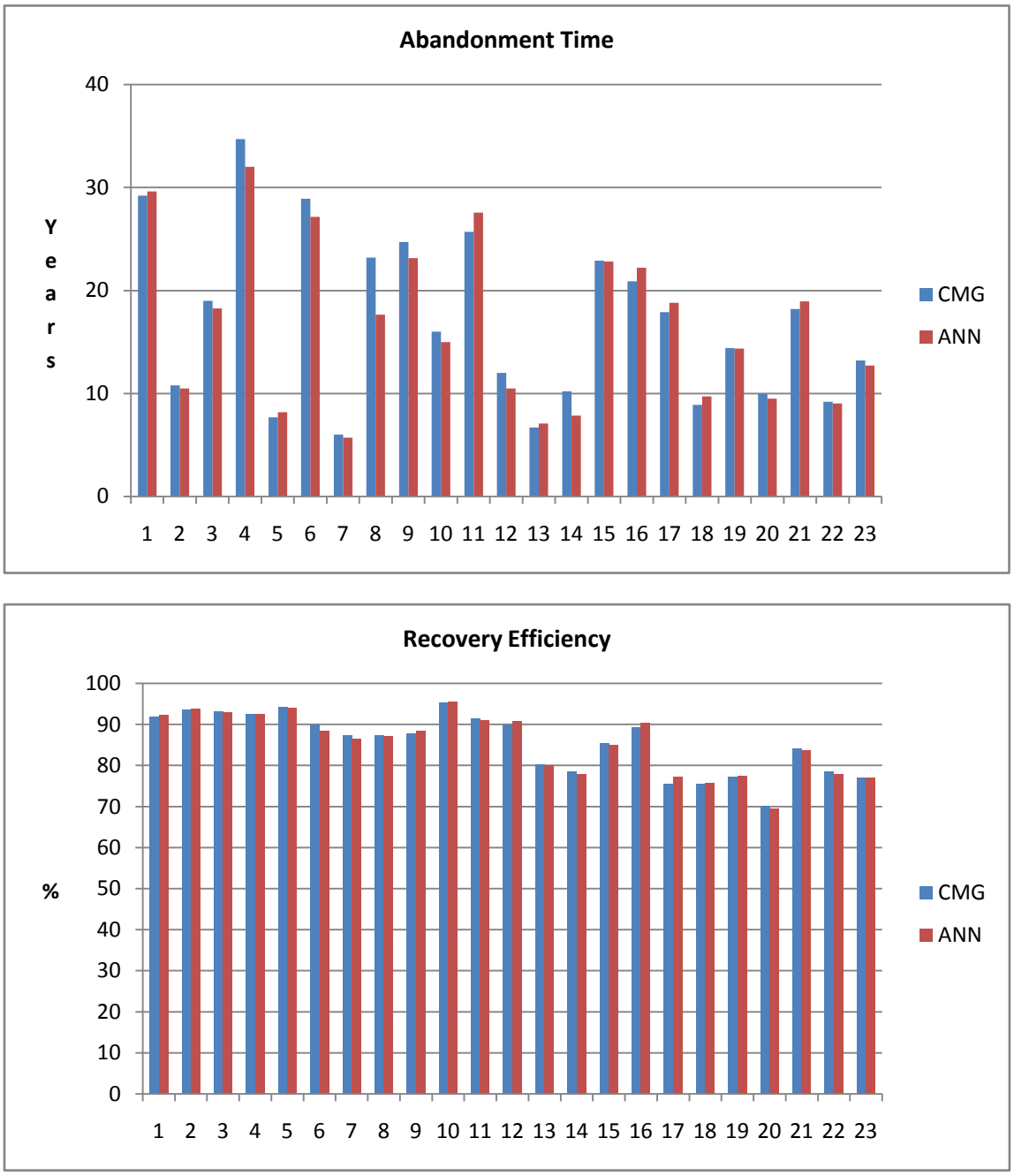

Figure 5- 3: "Stage-one" forward neural network performance

The absolute error is then calculated for each variable. The predicted abandonment time presents 0.35% of minimum and 12.6% of maximum error while recovery efficiency presents 0.008% of minimum and 2.4% of maximum error, respectively. Given similarity of values between simulation results and expected counterparts, this network can efficiently capture the relationships between oil recovery profile and two groups of inputs, which are the reservoir characteristics and design parameters.

For inverse neural network, inputs consist of four reservoir characteristics, two oil production profiles. This network predicts three design parameters that are well spacing, water-gas ratio and bottom hole pressure of a producing well. Inverse neural network architecture is shown in Table 5-4 and Figure 5-4.

Table 5- 4: Inputs and output of "stage-one" inverse looking neural network

Inputs		Outputs	
Reservoir Characteristics	Formation Thickness (h) Porosity (Ø) Permeability (k) Initial Water Saturation (Swi)	**Design Parameters**	Well Spacing WAG Ratio Producing Well BHP
Reservoir Performance	Abandonment Time (A.T.) Recovery Efficiency (R.E.)		

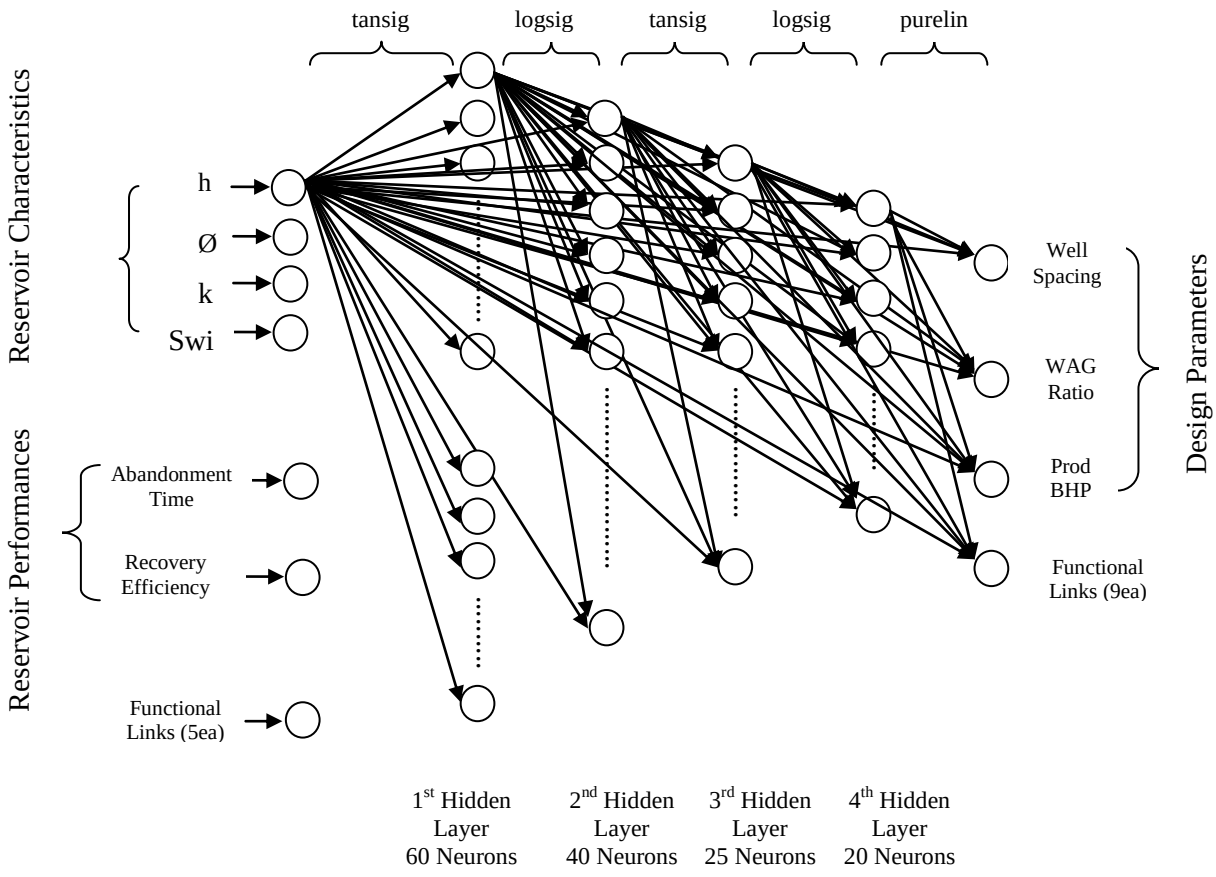

Figure 5- 4: Inverse looking network architecture built in "stage-one"

The network is trained with the training set but the LMS error is also estimated for the validation set. When the validation error is constant or grows after 1.0×10^{5} of epochs or the mean squared error reaches the goal of 1.0×10^{-4}, then network training procedure is stopped to avoid overtraining.

Inverse network was trained with 60 neurons in the first layer, 40 neurons in the second layer, 25 neurons in the third layer and 20 neurons in the forth layer. Different numbers of neurons and hidden layers were tested to determine optimum values. Too many numbers of neurons and hidden layers may result in over training.

The six utilized inputs are relatively small in order to predict three outputs compared to forward applications that utilize seven inputs to generate two outputs. Even if network should be able to recognize an interaction between output variables, more functional links need to be used for both input and output layers to improve the network accuracy due to the complexity of problems. Functional links used are summarized in Table 5-5.

Table 5- 5: Input and output layer functional links of "stage-one" inverse looking neural network

Inputs	Outputs
Abandonment time × Recovery efficiency × 0.1 Porosity × Initial water saturation Permeability × Formation thickness Recovery efficiency × Formation thickness (Permeability×Porosity×Thickness×Initial water saturation)^1/2	Well spacing × Abandonment time Well spacing × Recovery efficiency Well spacing × Permeability Well spacing × Formation thickness Well spacing × Initial water saturation WAG ratio × Abandonment time WAG ratio × Permeability Well spacing / WAG ration Well spacing × BHP

One of testing sets of inverse application is compared with simulations inputs and illustrated in Figure 5-5.

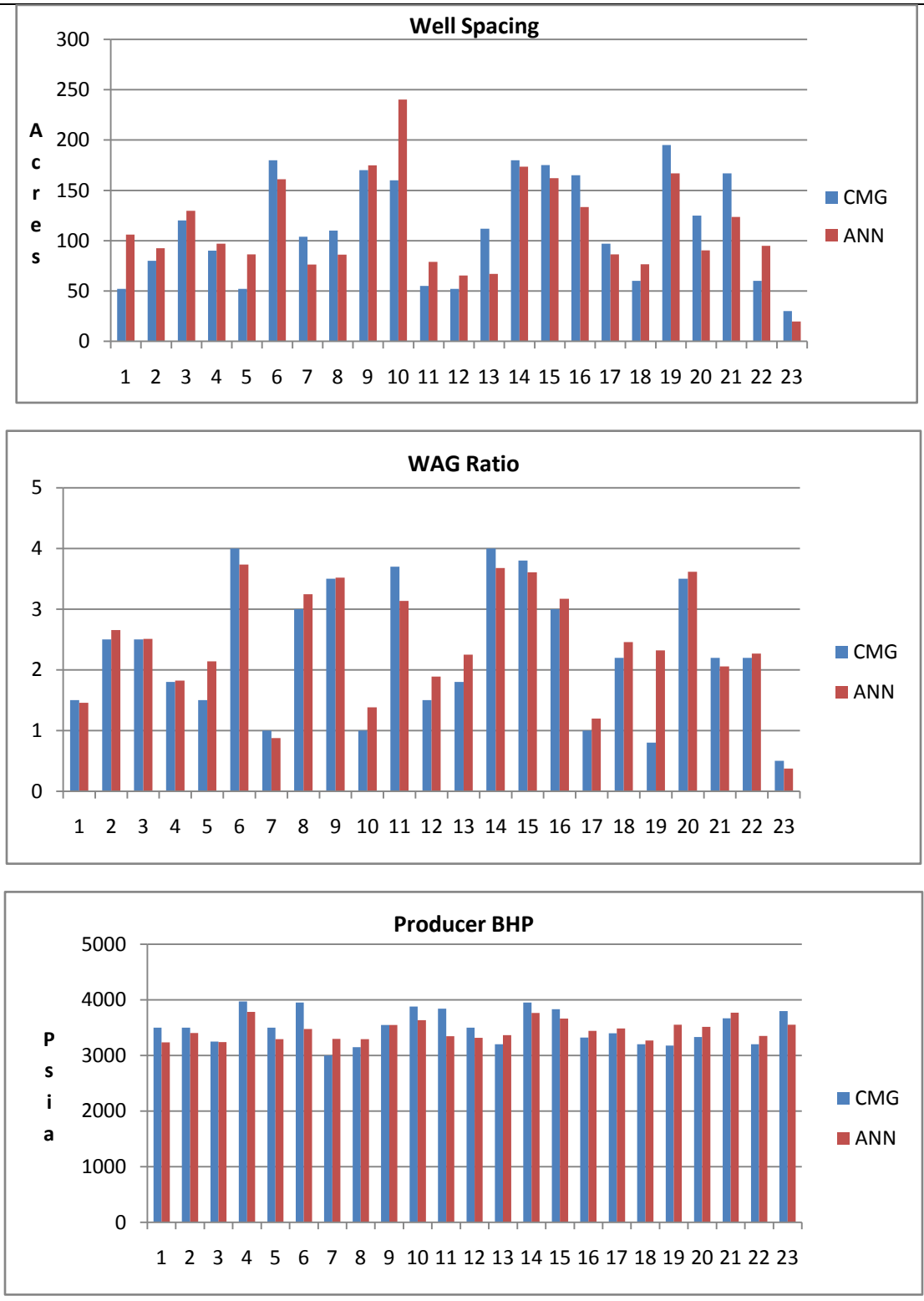

Figure 5- 5: “Stage-one” inverse neural network performance

Inverse network of this stage cannot also obtain the desired goal of 10^{-4} and LMS error is 0.016 which is more than one measured from forward network. The performance of the network is then evaluated by comparing the suggested development plans with the simulation inputs. The absolute error is calculated for each variable. The predicted well spacing presents 2.8% of minimum and 104.1% of maximum error while WAG ratio presents 0.48% of minimum and 42.7% of maximum error, respectively. Bottom hole pressure of a producing well shows 0.03% of minimum and 12.8% of maximum error that indicates higher accuracy compared to other two parameters. Based on LMS error and the absolute error compared to forward networks, inverse neural networks do not seem to effectively predict the operating conditions.

However, absolute errors cannot be the only criteria to evaluate the accuracy of the networks since they sometimes bring wrong conclusions. For instance, the range of well spacing is between 20 – 200 acres for this study. If the neural network forecasts a value of 40 for the 20 acres, that represents 100% of absolute error that is considered as a poor performance. Conversely, if the network predicts a value of 220 for the 200 acres, that represents only 10% of absolute error that is interpreted as a relatively good performance. The difference of absolute errors between two cases is 90% even though both cases have exactly same deviation of 20 acres.

Furthermore, respective outputs of inverse neural network do not always represent the overall performance of the networks since injection rates should be calculated using well spacing, WAG ratio, alternating frequency and alternating slug size. In other words, prediction of injection rates can be precise with good combination of those predicted four variables even though some of the variables have large absolute error. This observation implies that there should be other criteria to compensate a weak point of absolute error method.

Accordingly, network performance is further assessed by protocol implemented accuracy analysis based on abandonment time and recovery efficiency. These two variables are used as inputs of an inverse neural network, and then forward neural network re-predicts these two

variables using proposed operating schemes that were already generated from inverse application. Input variables of forward neural network are then directly utilized to run a commercial simulator to yield another pair of abandonment time and recovery efficiency. Protocol implemented accuracy analysis is schematically illustrated in Figure 5-6.

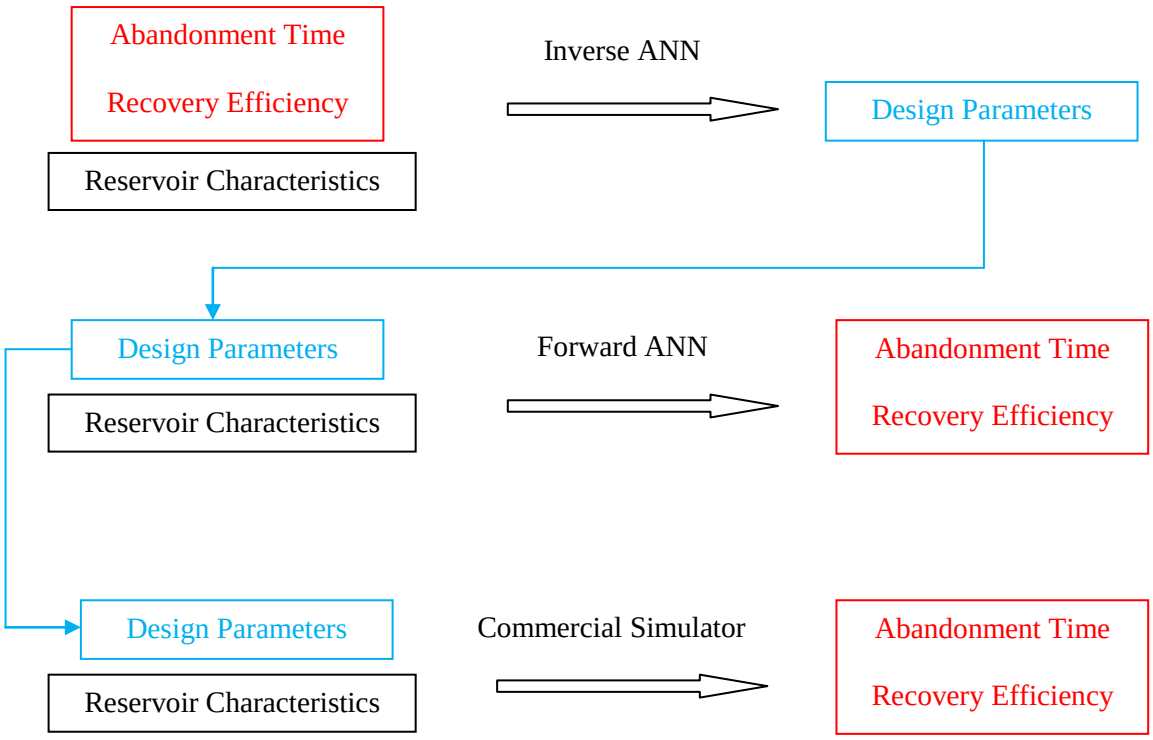

Figure 5- 6: Protocol implemented accuracy analysis purposes

The accuracy of forward neural network is analyzed by comparing abandonment time and recovery efficiency that are inputs of inverse neural network with ones re-generated from forward neural network. Since design parameters produced from inverse network are directly applied as

inputs of forward application, the accuracy of forward neural network is proportional to the closeness of those two variables between inverse and forward application expressed by blue and red columns in Figure 5-7.

In the same manner, the performance of inverse application can also be evaluated by the deviation of abandonment time and recovery efficiency. Those two variables are inputs of inverse network and compared against simulator outputs obtained using design parameters previously predicted from inverse applications. The suggested operating schemes from inverse neural network can be verified according to the similarity of abandonment time and recovery efficiency between inverse application and simulator illustrated by blue and green columns in Figure 5-7. Thus, inverse network performance can be reasonably analyzed in this way although the individual design parameters can present relatively large difference between real and predicted results. Once the network performance is confirmed by repeating a couple of times protocol implemented analysis, then design parameters of WAG process can successfully be forecasted from the inverse expert systems without any further recourse to accuracy analyses.

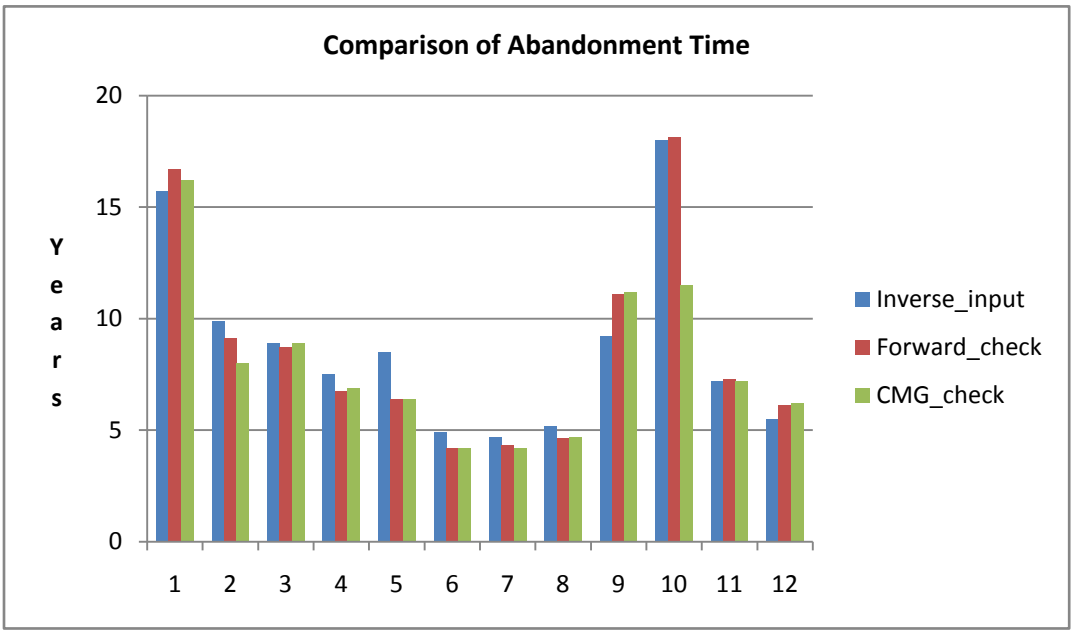

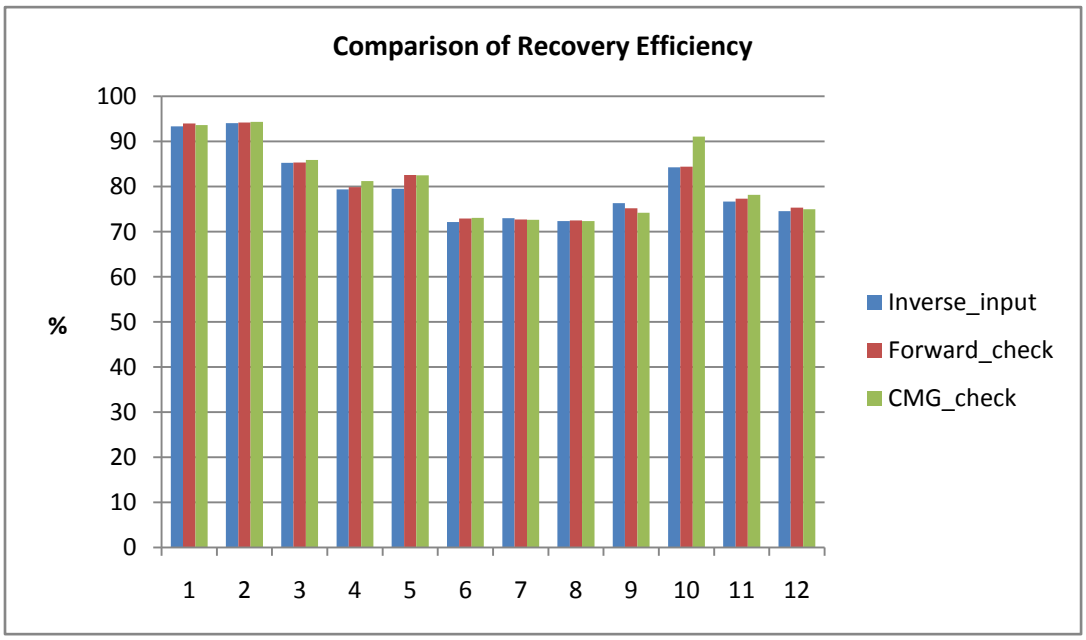

Figure 5- 7: Results of accuracy analysis

5. 2. 2 Stage-Two: Universal Expert System

In the second stage, the complexity of the network is increased by changing the alternating slug size. Three different networks are constructed for 30 days, 60 days and 90days of alternating frequency. As before, forward neural networks are also built along with inverse neural networks. Similar network architectures from previous stage are brought up to construct both forward and inverse neural networks.

In order to achieve better performance of this stage of networks, two different strategies are implemented. The first strategy is to introduce some functional links that help the networks find out more detailed connection between inputs and outputs. Different combinations of functional links are utilized for each three networks.

Another strategy is to decide the optimum number of cases used to train each network. Even though the networks seem to predict more accurate outputs with as many cases that cover almost all scenarios as possible, there exists the optimum number of cases in each three networks to avoid memorizing problems and also to make training process efficiently. 30 days network utilizes 145 cases that are divided in the following form: 117 cases for training, 14 cases for testing and another 14 cases for validation. 60 days network uses 192 cases that are divided into 154 cases for training, 19 cases for testing and another 19 cases for validation. 90 days network utilizes 155 cases that are divided into 125 cases for training, 15 cases for testing and another 15 cases for validation.

Table 5- 6: Inputs and outputs of "stage-two" forward looking neural network

Inputs		Outputs	
Reservoir Characteristics	Formation Thickness (h) Porosity (Ø) Permeability (k) Initial Water Saturation (Swi)	**Reservoir Performance**	Abandonment Time (A.T.) Recovery Efficiency (R.E.)
Design Parameters	Well Spacing WAG Ratio Alternating CO_2 Size Producing Well BHP		

Forward neural networks use four reservoir characteristics and four design parameters as inputs to predict abandonment time and recovery efficiency. Table 5-6 and Figure 5-8 illustrates forward neural network architecture commonly used in all three networks of this stage.

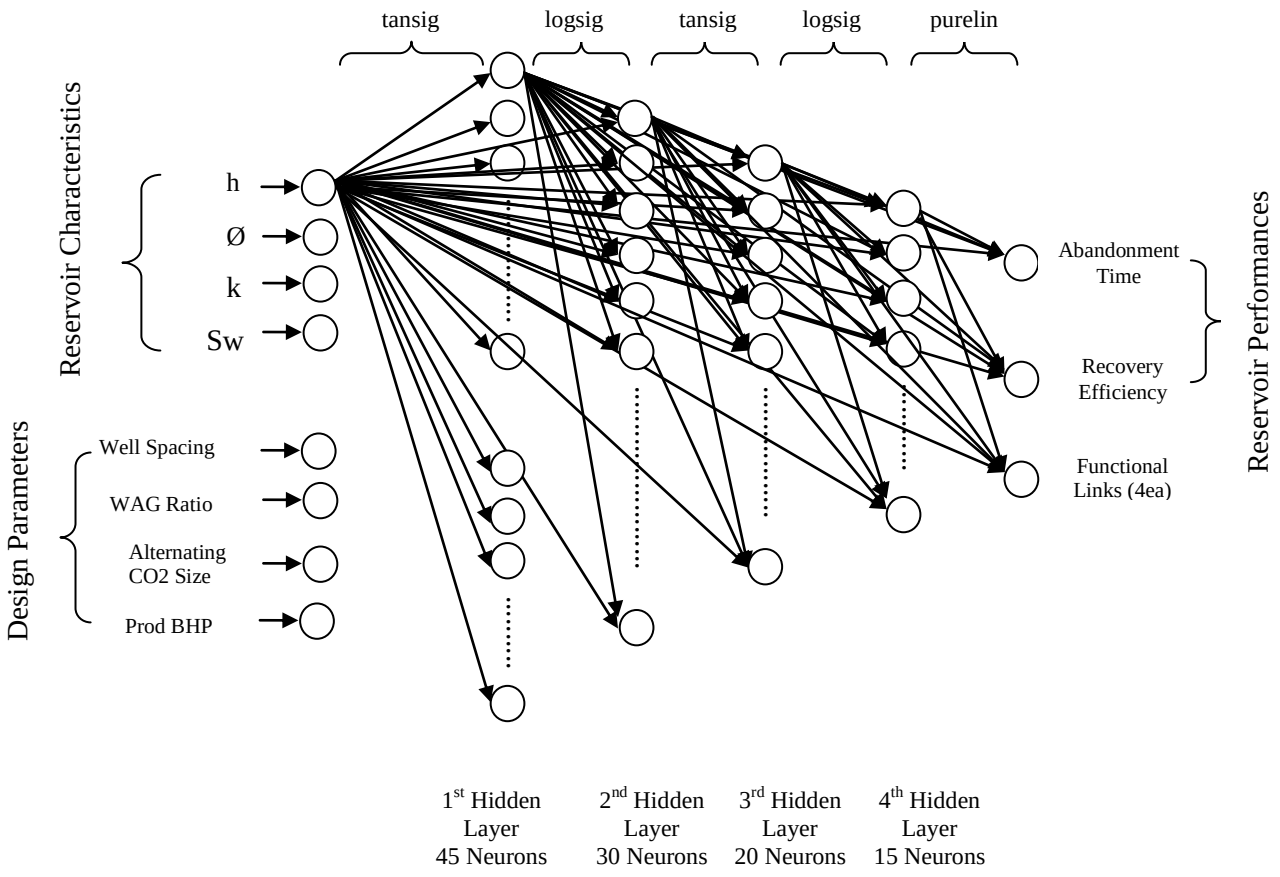

Figure 5- 8: Forward looking network architecture built in "stage-two"

Three networks present similar value of the least mean squared (LMS) error, 0.0007~0.0008. The accuracy of forward neural network is then evaluated based on abandonment time and recovery efficiency. One of testing data sets of each three forward neural networks is shown in Figure 5-9, 5-10 and 5-11 respectively.

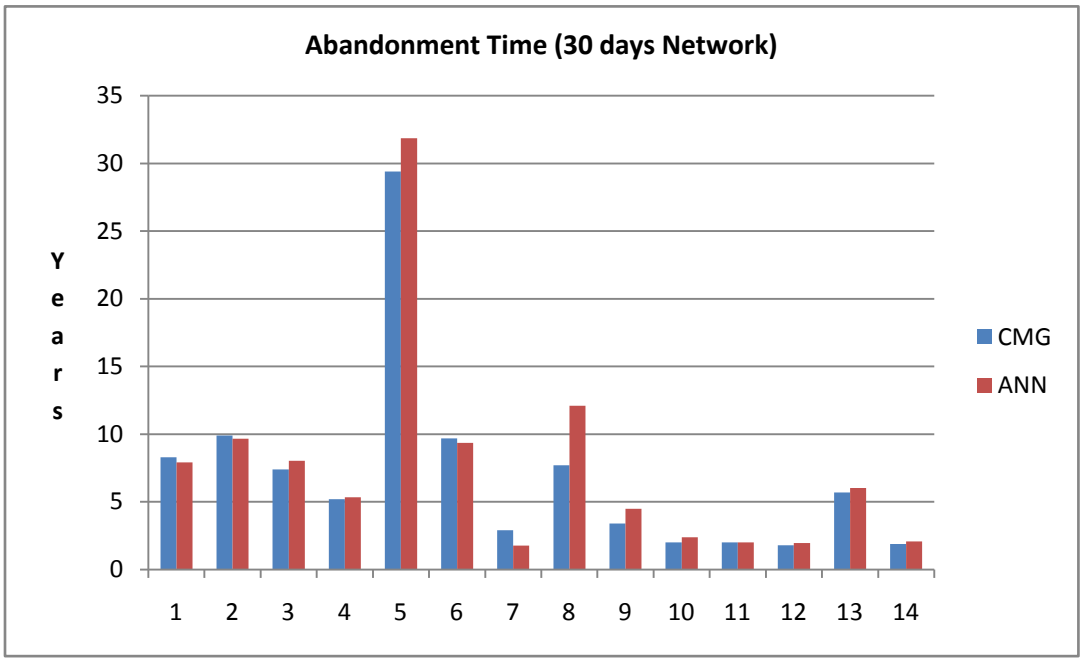

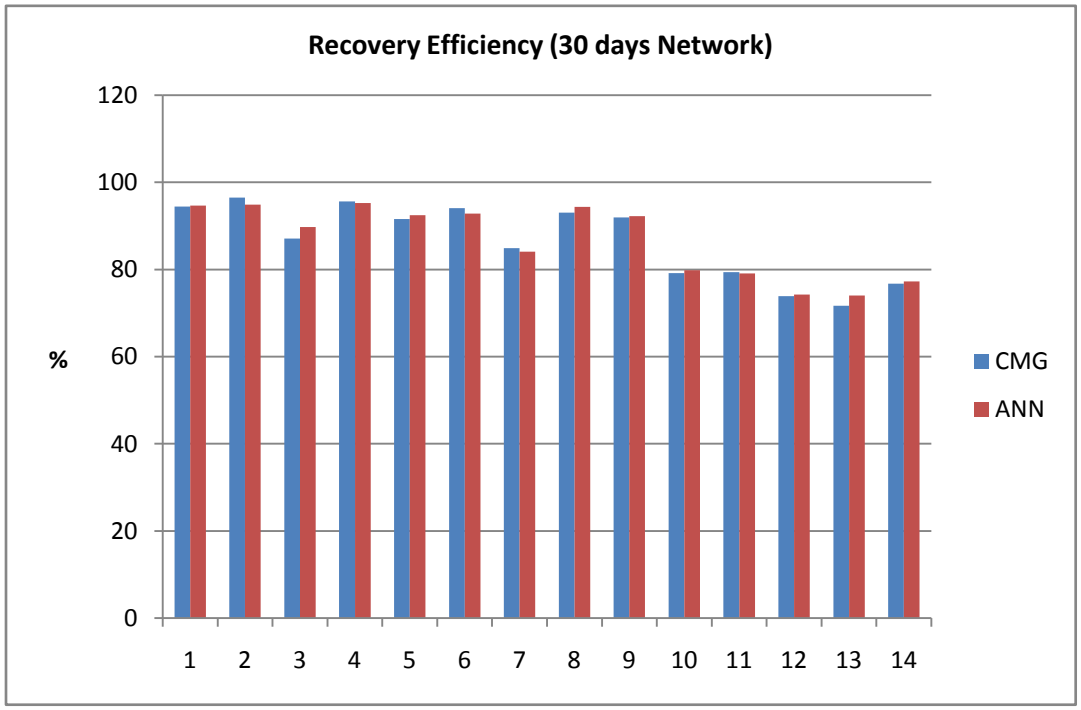

Figure 5- 9: 30 Days forward neural networks performance

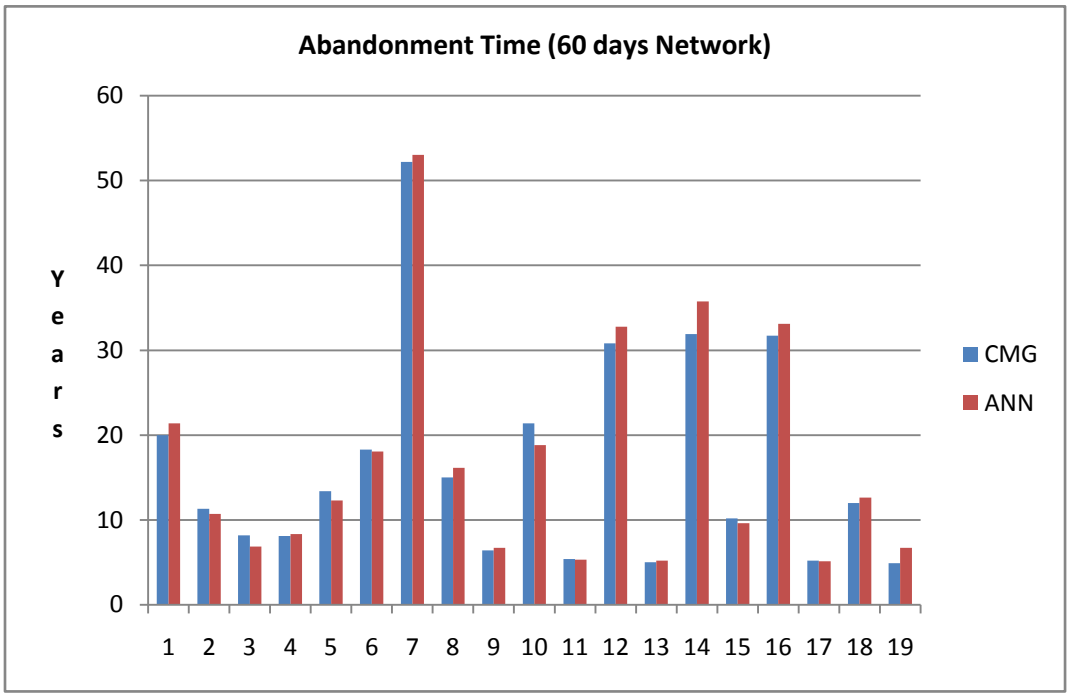

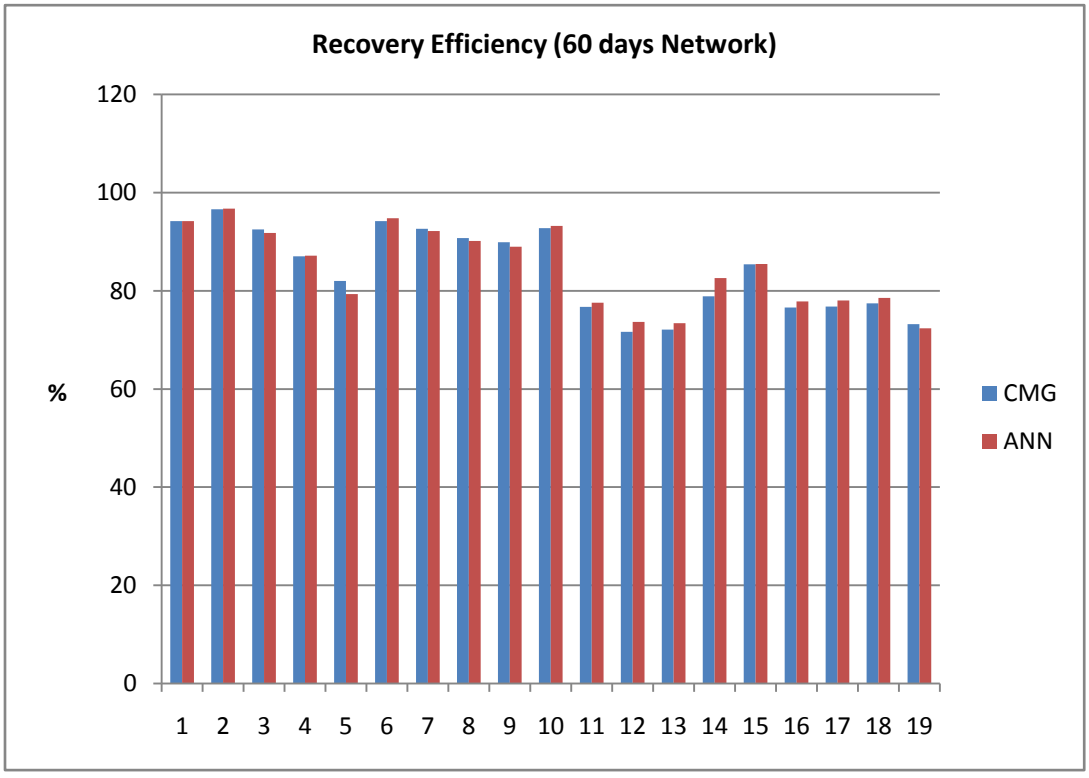

Figure 5- 10: 60 Days forward neural networks performance

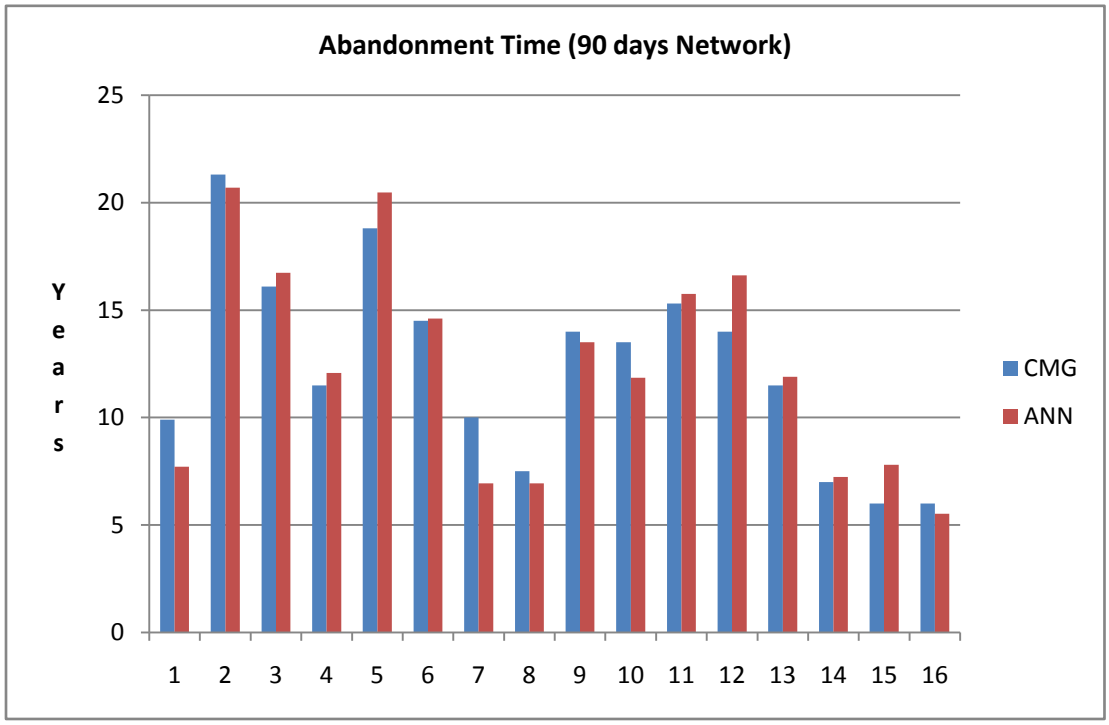

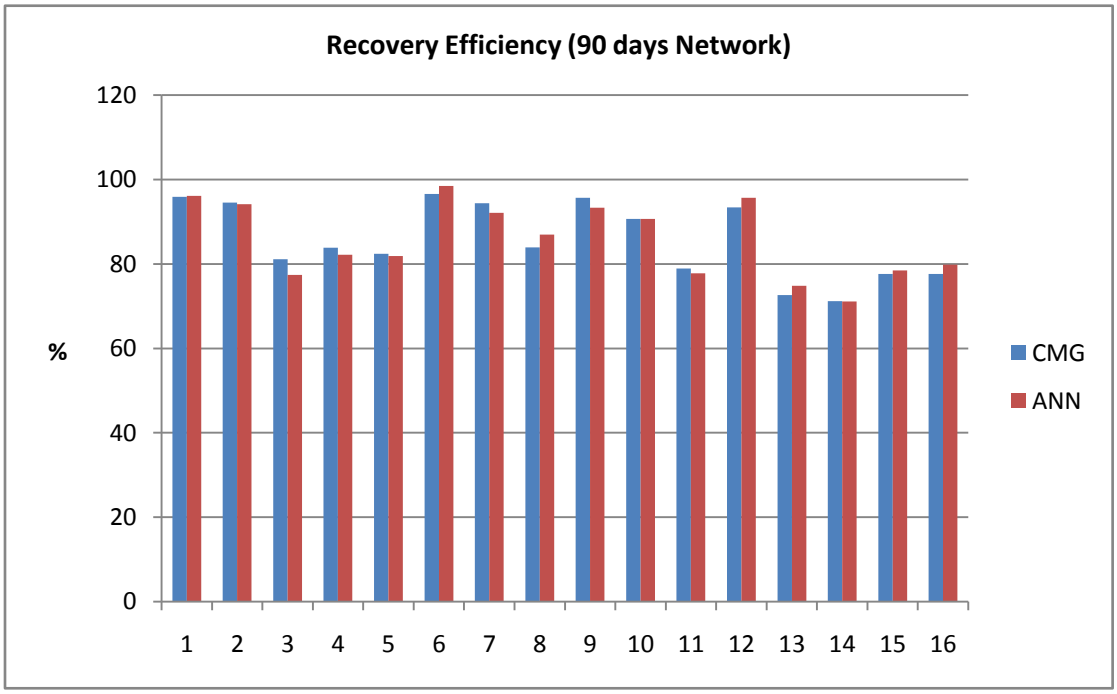

Figure 5- 11: 90 Days forward neural networks performance

The absolute errors of the predicted abandonment time and recovery efficiency are summarized in Table 5-7. The absolute error indicates that three networks achieve similar extent of the accuracy.

Table 5- 7: The absolute error of forward neural network of "stage-two"

(%)

Output \ Network		30 Days	60 Days	90 Days
Abandonment Time	Min	0.2	1.1	0.7
	Max	38.9	36.8	30.5
	Ave	14.5	7.6	10.2
Recovery Efficiency	Min	0.2	0.01	0.05
	Max	3	4.6	4.6
	Ave	1.1	1.2	1.8

Inverse neural network utilizes four reservoir characteristics, abandonment time and recovery efficiency as inputs in order to forecast four field operating parameters that are well spacing, WAG ratio, alternating CO_2 size and bottom hole pressure of a producing well. This networks deal with more complicated problems due to increased number of outputs compared to previous stage inverse applications. Inverse neural network architecture is shown in Table 5-8 and Figure 5-12.

Table 5- 8: Inputs and output of "stage-two" inverse looking neural network

Inputs		Outputs	
Reservoir Characteristics	Formation Thickness (h) Porosity (Ø) Permeability (k) Initial Water Saturation (Swi)	**Design Parameters**	Well Spacing WAG Ratio Alternating CO_2 Size Producing Well BHP
Reservoir Performance	Abandonment Time (A.T.) Recovery Efficiency (R.E.)		

In all three networks, the ANN structure maintains the same format including the number of hidden layers, the number of neurons and transfer functions. Networks are trained with 60 neurons in the first layer, 40 neurons in the second layer, 20 neurons in the third layer and 15 neurons in the forth layer. Networks also utilize transfer function in the order of tansig, logsig, tansig, logsig and purelin. However, combinations of functional links used in three networks are different, and furthermore input layer functional links are added to help learning process. The appropriate selection of those functional links plays an important role to achieve good network performance of second stage.

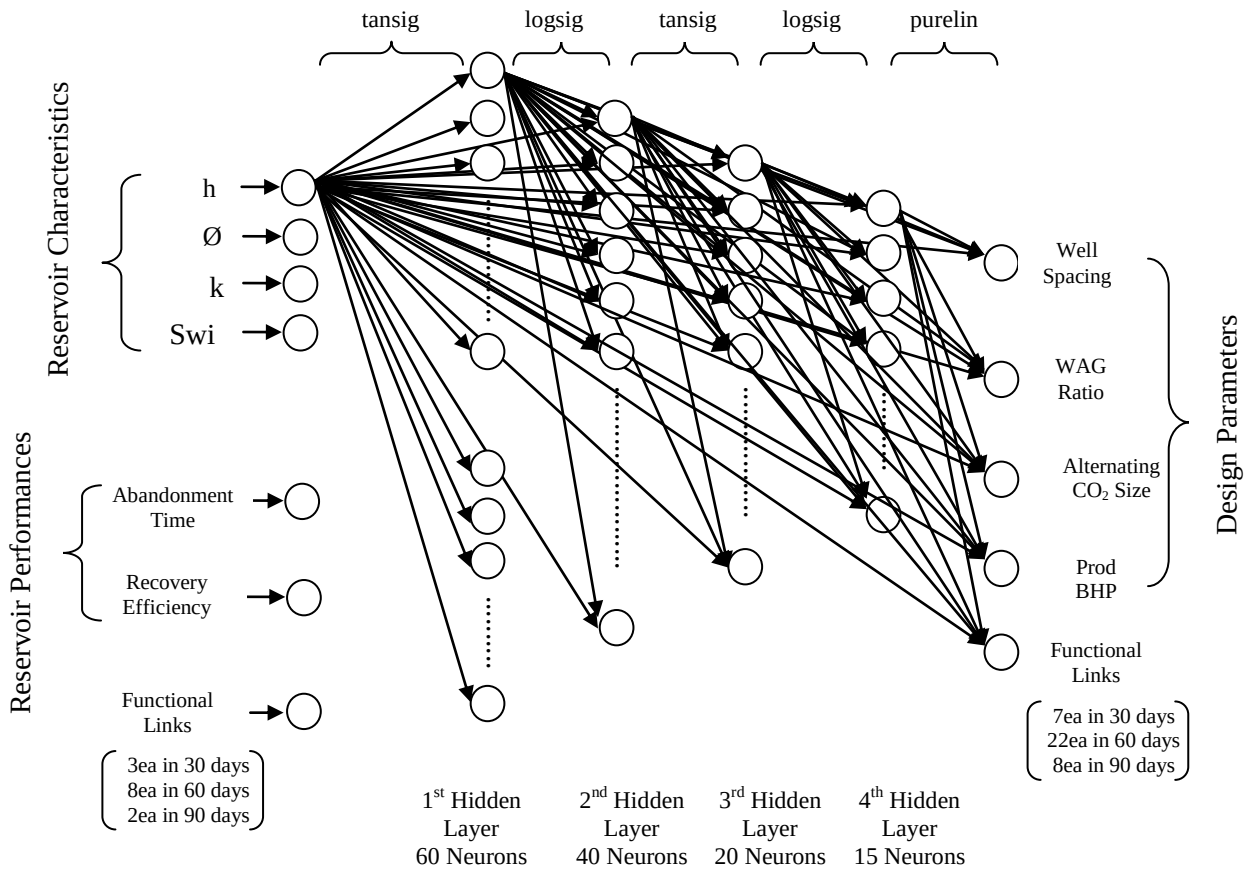

Figure 5- 12: Inverse looking network architecture built in "stage-two"

Table 5-9 summarizes input and output layer functional links used in each three inverse neural networks. It can be noticed that abandonment time is the most frequently used variable to generate functional links for both input layer and output layer. Since a simulator produces different values of abandonment time with respect to the reservoir characteristics and operating conditions, abandonment time is the most appropriate parameter to help the network realize the difference of each case used to train and thus diminish the error. Ultimate recovery efficiency, on the other hand, can be similar within certain reservoir characteristics and it sometimes complicates the network training.

Table 5- 9: Input and output layer functional links of inverse looking neural network

	Input Layer	Output Layer
30 Days	Abandonment time × Recovery efficiency Abandonment time × Formation thickness Abandonment time × (k×Ø×h×Swi)^1/2	Well spacing × Abandonment time Well spacing × Recovery efficiency Well spacing × Permeability WAG ratio × Recovery efficiency WAG ratio × Permeability Alternating CO_2 size × Abandonment time Abandonment time
90 Days	Abandonment time × Recovery efficiency Abandonment time × (k×Ø×h×Swi)^1/2	Distance between injection wells Distance between injection and producing well Well spacing × Abandonment time Well spacing × Recovery efficiency Well spacing × Permeability WAG ratio × Abandonment time Alternating CO_2 Size × Abandonment time Abandonment time

Table 5- 10: Input and output layer functional links of inverse looking neural network

	Input Layer	Output Layer
60 Days	Abandonment time × Recovery efficiency Abandonment time × Permeability Abandonment time × Porosity Abandonment time × Formation thickness Recovery efficiency × Permeability Recovery efficiency × Porosity Recovery efficiency × Formation thickness Abandonment time × (k×Ø×h×Swi)^1/2	Well spacing × Abandonment time Well spacing × Recovery efficiency Well spacing × Permeability Well spacing × Porosity Well spacing × Formation thickness Well spacing × Initial water saturation WAG ratio × Abandonment time WAG ratio × Recovery efficiency WAG ratio × Permeability WAG ratio × Porosity WAG ratio × Formation thickness WAG ratio × Initial water saturation Alternating CO_2 size × Abandonment time Alternating CO_2 size × Permeability Alternating CO_2 size × Porosity Alternating CO_2 size × Formation thickness Well spacing / WAG ratio Well spacing × WAG ratio Well spacing / Alternating CO_2 Size Well spacing × Prod BHP Alternating CO_2 size × WAG ratio WAG ratio × Prod BHP

The LMS error of inverse network is 0.015 ~ 0.027 that is larger than forward network. Since the LMS error is not the only criterion to determine the accuracy of networks, the performance of each inverse application is assessed by comparing the predicted operating conditions with the ones used for simulators shown in Figure from 5-13 to 5-18. It is observed that in some cases, predicted ones are above or below the limits when the actual operating parameters are close to either upper or lower limits. In each run, same network can produce little different results since they choose different data sets in a random way for the purpose of validation, training and test. But it is obvious that overall performance of each run is similar based on the accuracy analysis. Three more predictions from each inverse application are added in appendix A, B and C.

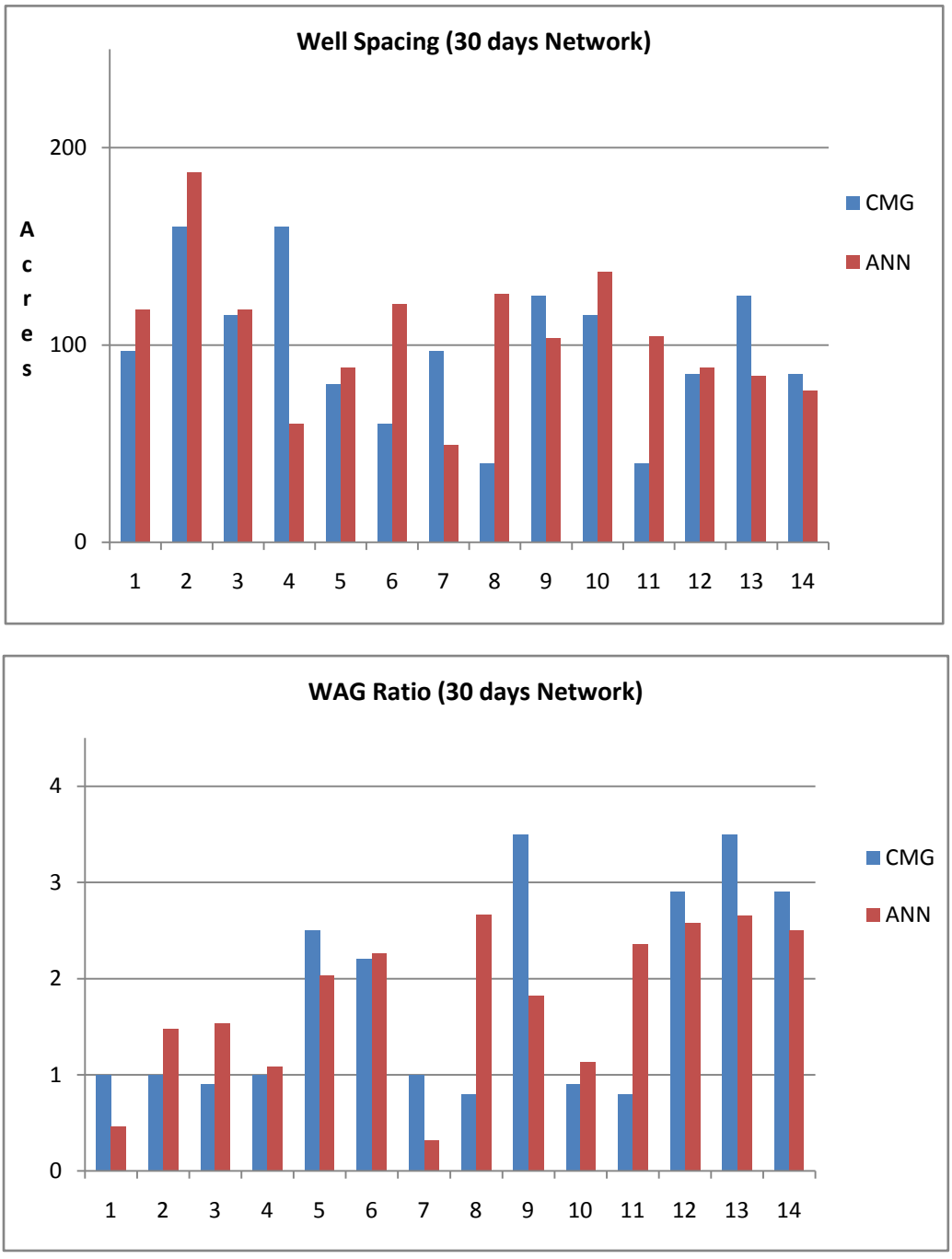

Figure 5- 13: 30 Days inverse neural networks performance

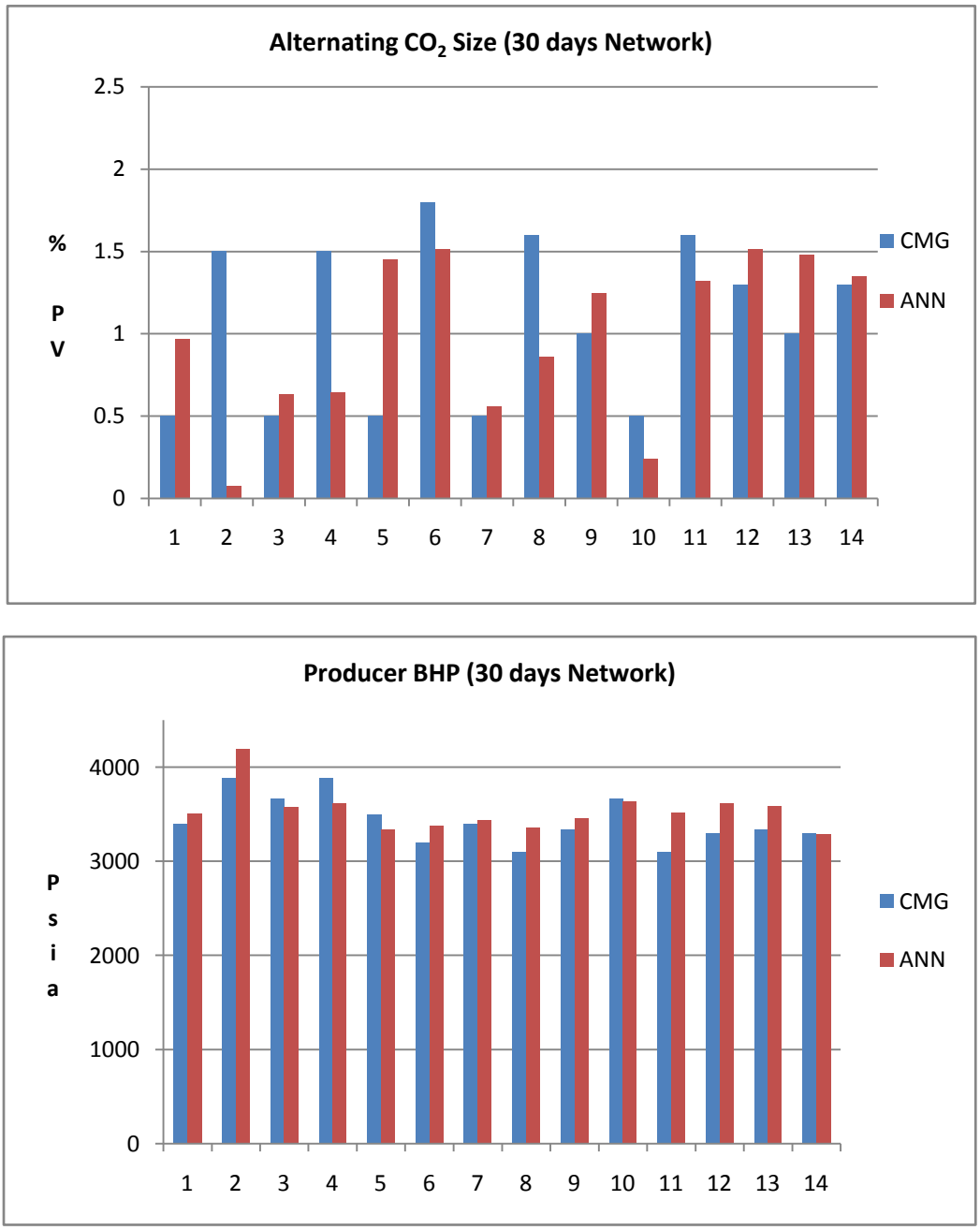

Figure 5- 14: 30 Days inverse neural networks performance

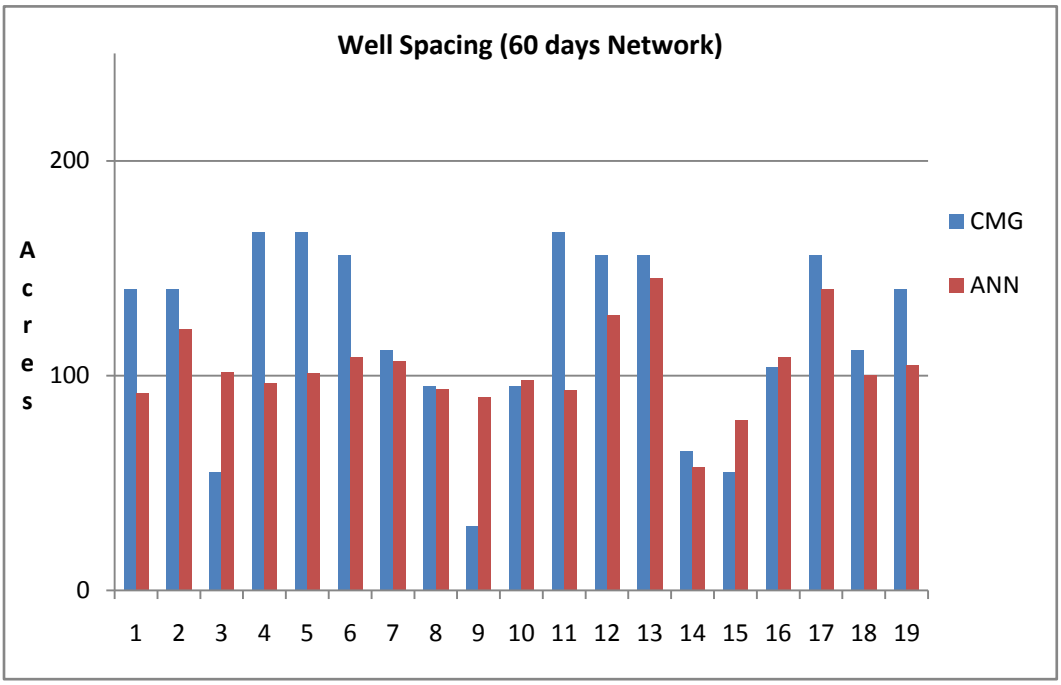

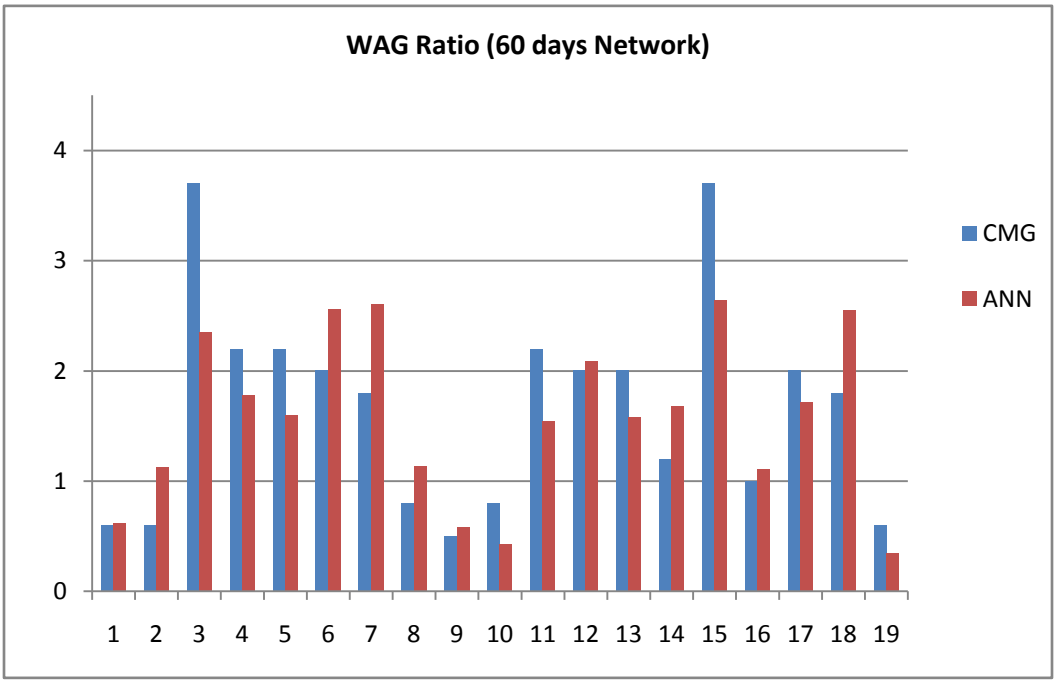

Figure 5- 15: 60 Days inverse neural networks performance

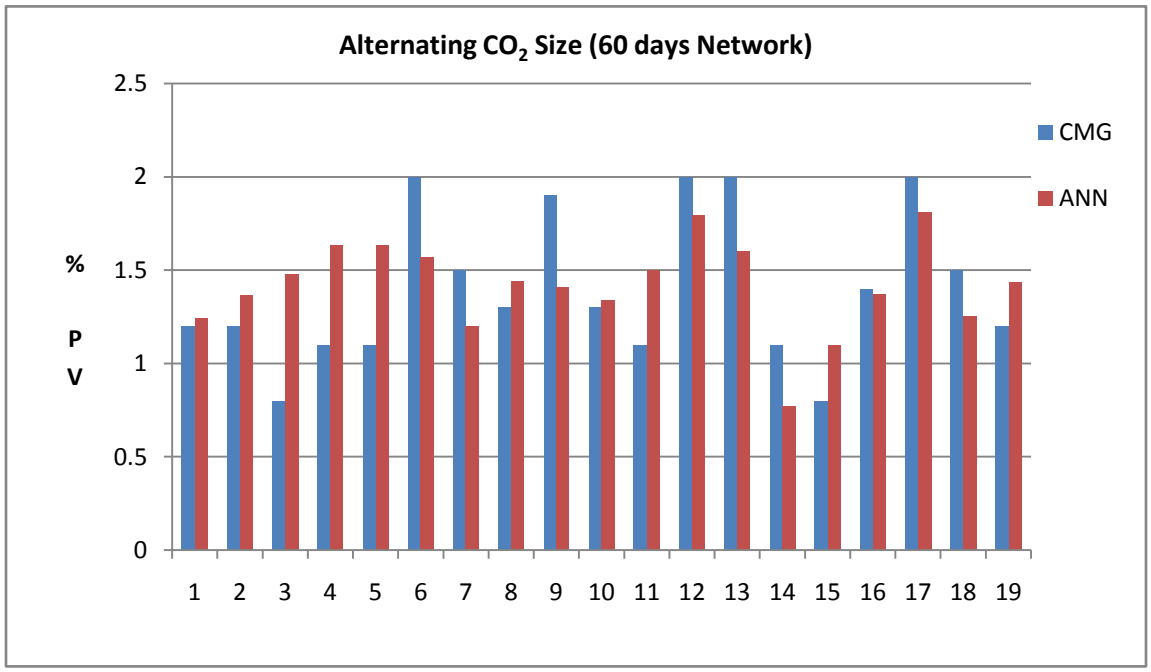

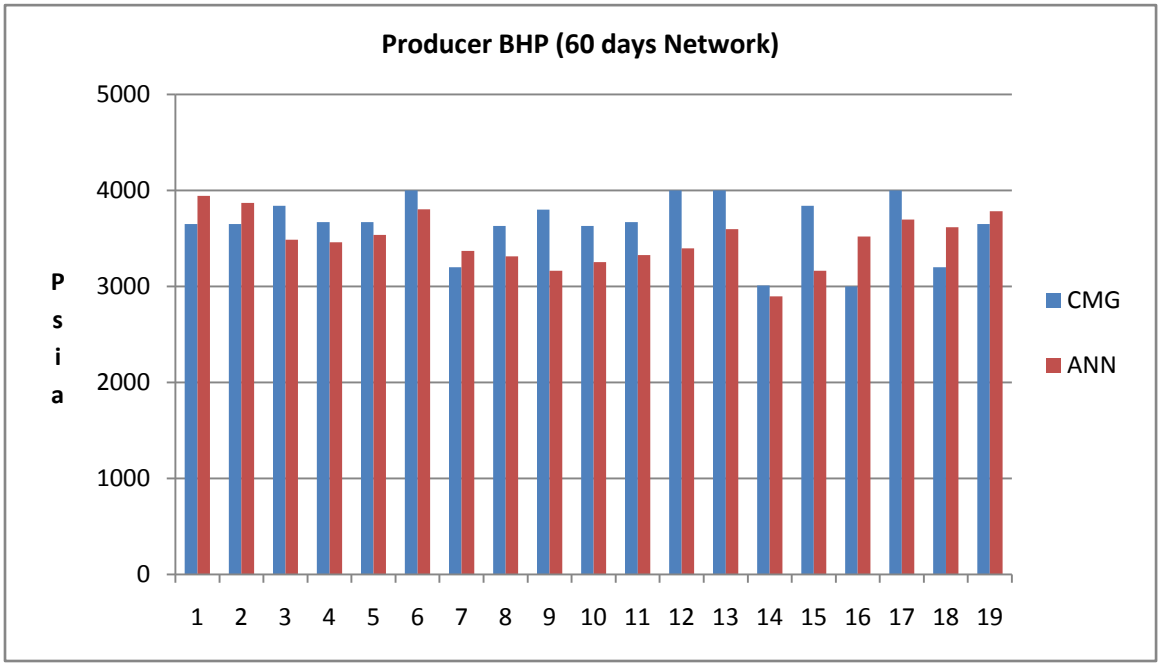

Figure 5- 16: 60 Days inverse neural networks performance

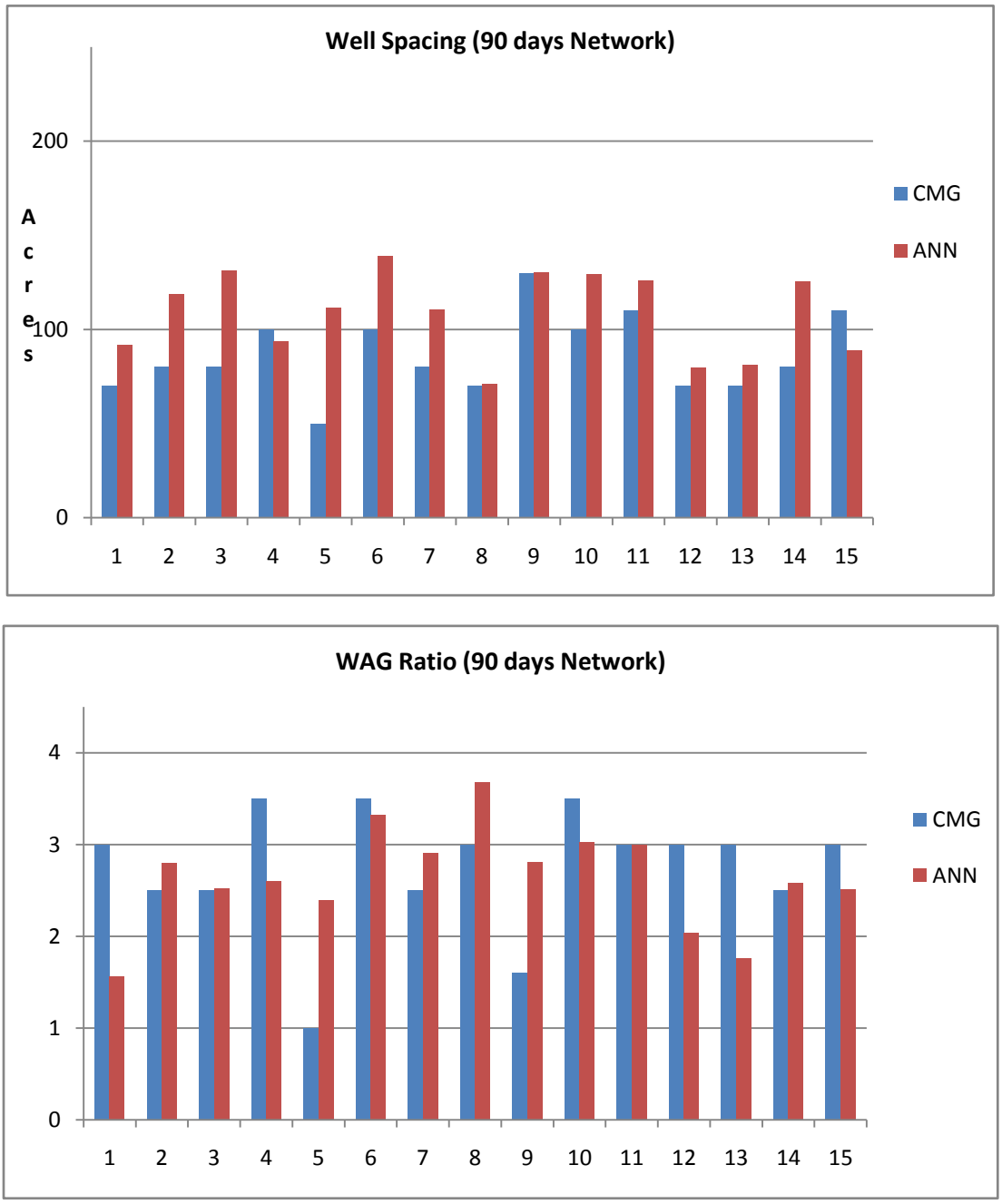

Figure 5- 17: 90 Days inverse neural networks performance

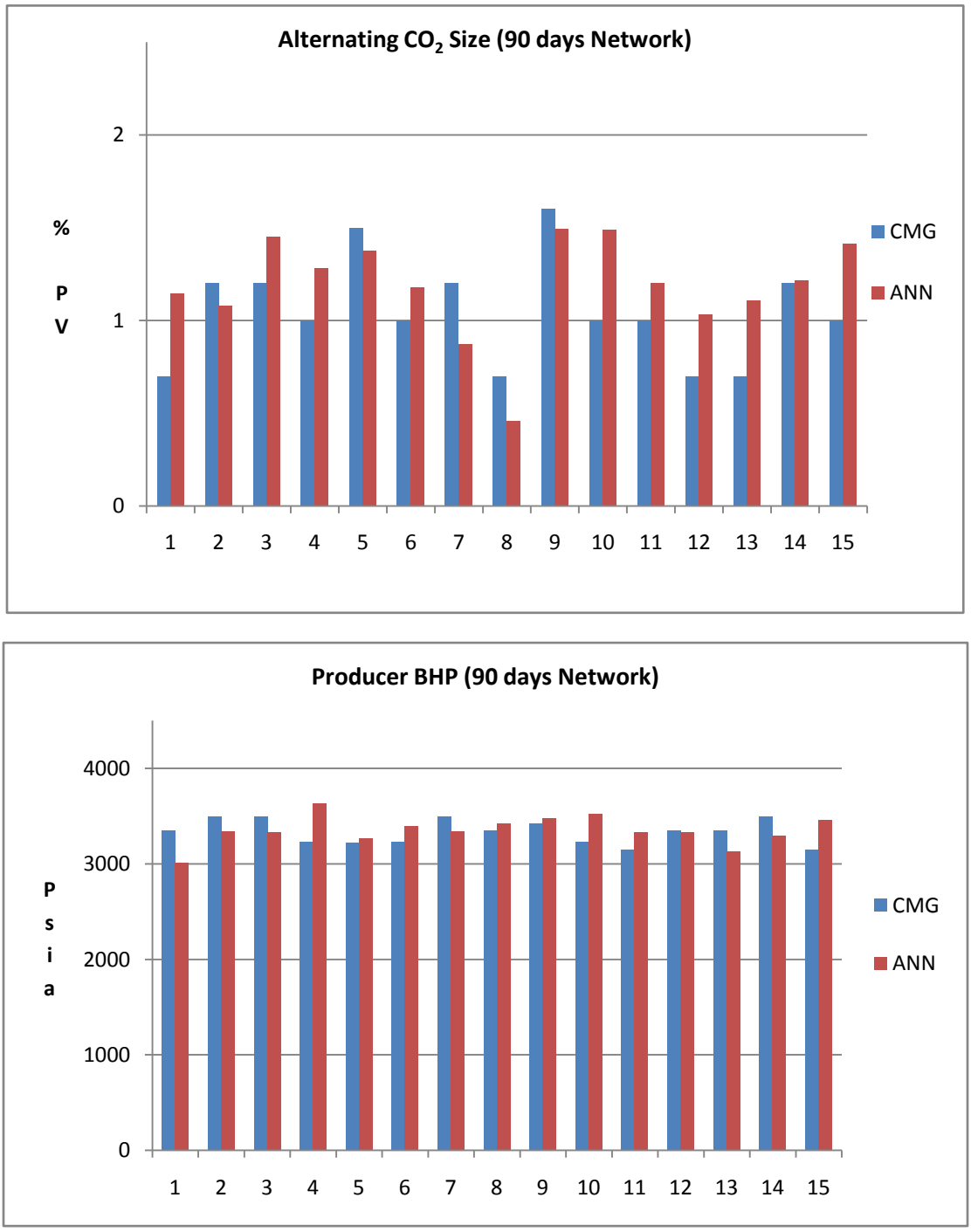

Figure 5- 18: 90 Days inverse neural networks performance

The absolute errors are then calculated for each four outputs and shown in Table 5-10. Based on the absolute errors, network prediction of BHP of a producing well has the smallest error and the rest of three outputs show similar range of error.

Table 5- 11: The Absolute error of inverse neural network of "stage-two"

(%)

Output \ Network		30 Days	60 Days	90 Days
Well Spacing	Min	2.4	1.3	0.1
	Max	214.4	199.9	64.2
	Ave	51.6	36.5	33.4
WAG Ratio	Min	2.9	3.1	0.05
	Max	232.4	87.0	139.5
	Ave	58.6	30.3	30.1
Alternating CO_2 Size	Min	3.8	2.1	1.5
	Max	190.4	84.6	63.7
	Ave	49.9	26.1	29.0
BHP of a Producing Well	Min	0.3	3.6	0.6
	Max	13.3	17.5	12.5
	Ave	5.4	9.5	5.7

Compared to previous inverse application, the absolute errors tend to exhibit more wide range, for instance, the absolute error of WAG ratio in 30 days network varies from 2.9% up to

232.4 %. In order to further analyze the network performance, protocol implemented accuracy analysis is used based on abandonment time and recovery efficiency. In this method, forward neural network and a simulator regenerate abandonment time and recovery efficiency using the operating conditions that were previously predicted from inverse neural network. If forward neural networks can predict oil production profile that are similar to the input of inverse neural network, then the accuracy of forward neural network can be confirmed. In the same manner, the performance of inverse application can be verified by similarity of those two values between the input of inverse network and the results from a simulator. Figure 5-19 through 5-21 and Table 5-11 through 5-13 shows the accuracy analysis of 30 days, 60 days and 90 days networks, respectively.

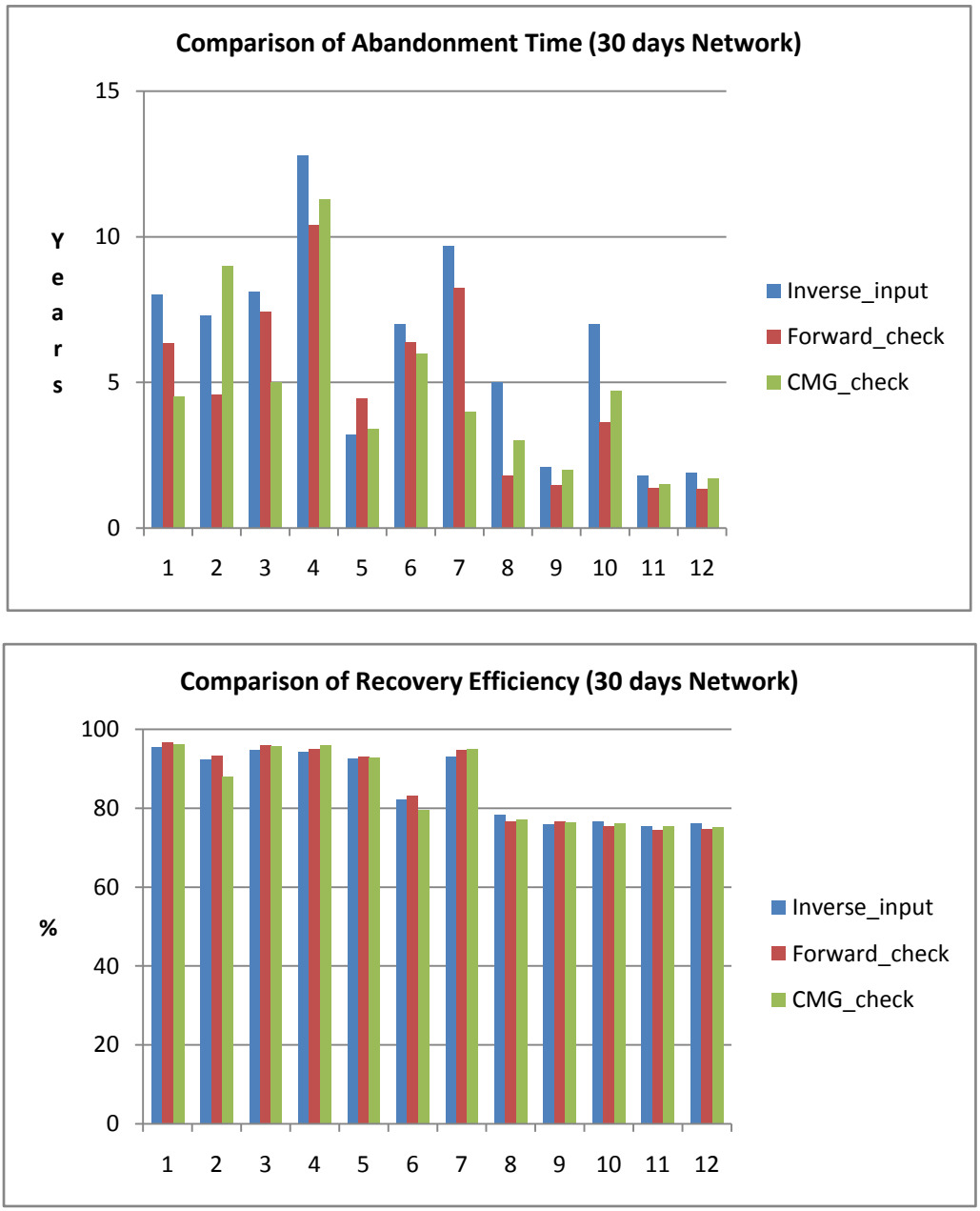

Figure 5- 19: Accuracy analysis on 30 days network performance

Table 5- 12: The accuracy analysis on 30 days network performance

	Deviations			
	Forward Neural Network		Inverse Neural Network	
	Abandonment Time (years)	Recovery Efficiency (%)	Abandonment Time (years)	Recovery Efficiency (%)
1	1.7	1.3	3.5	0.7
2	2.7	1.0	1.7	4.3
3	0.7	1.2	3.1	0.8
4	2.4	0.8	1.5	1.7
5	1.3	0.5	0.2	0.3
6	0.6	1.2	1	2.5
7	1.5	1.7	5.7	1.9
8	3.2	1.9	2	1.3
9	0.6	0.7	0.1	0.5
10	3.4	1.0	2.3	0.4
11	0.4	0.9	0.3	0.04
12	0.5	1.4	0.2	1.0
Ave	1.6	1.1	1.8	1.3

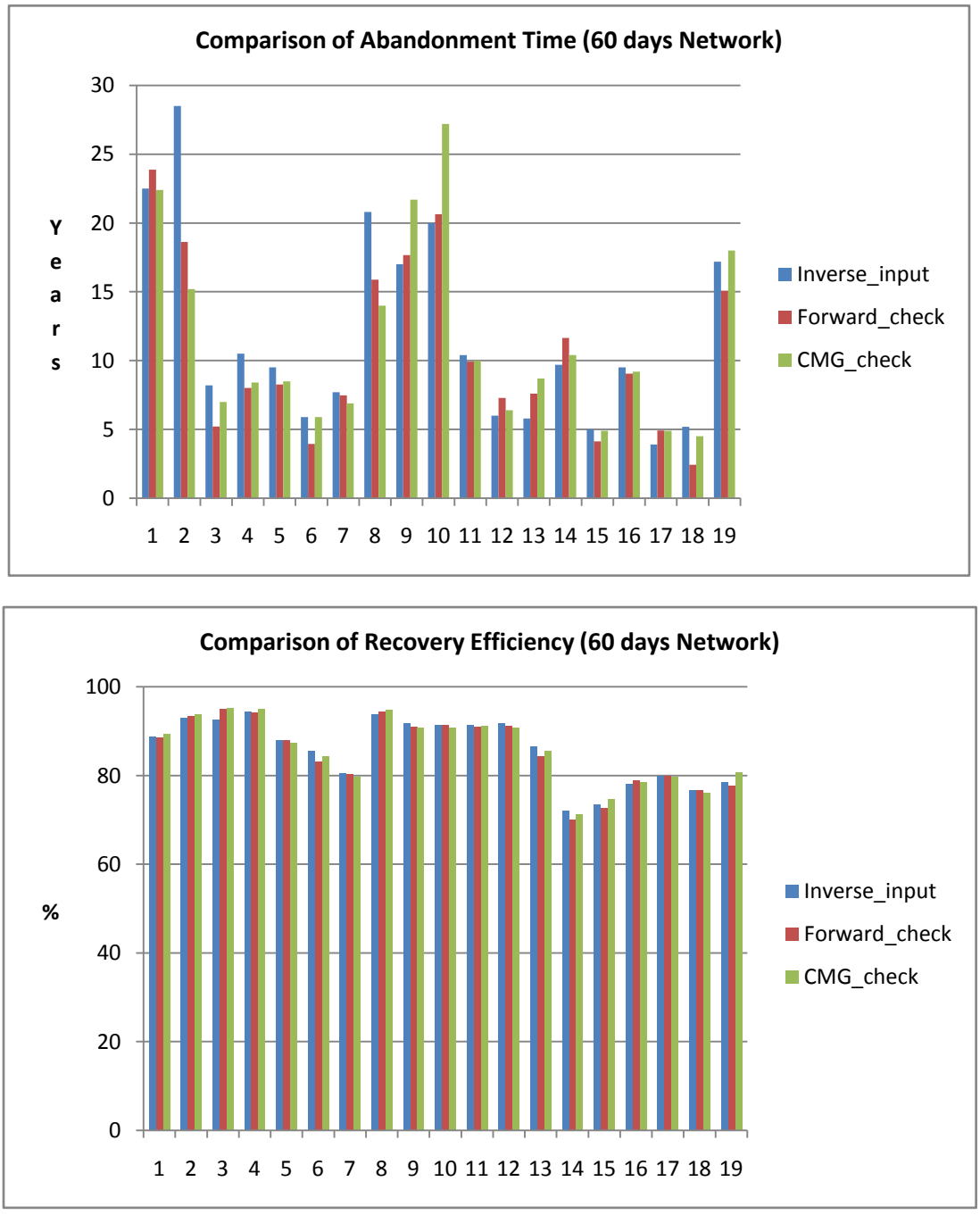

Figure 5- 20: Accuracy analysis on 60 days network performance

Table 5- 13: The accuracy analysis on 60 days network performance

	Deviations			
	Forward Neural Network		Inverse Neural Network	
	Abandonment Time (years)	Recovery Efficiency (%)	Abandonment Time (years)	Recovery Efficiency (%)
1	1.4	0.1	0.1	0.6
2	9.9	0.4	13.3	0.9
3	2.9	2.5	1.2	2.6
4	2.5	0.1	2.1	0.6
5	1.2	0.2	1	0.4
6	1.9	2.4	0	1.3
7	0.2	0.2	0.8	0.7
8	4.9	0.5	6.8	0.9
9	0.7	0.8	4.7	0.9
10	0.6	0.08	7.2	0.6
11	0.5	0.4	0.4	0.3
12	1.3	0.4	0.4	1.0
13	1.8	2.3	2.9	1.0
14	1.9	2.0	0.7	0.7
15	0.9	0.7	0.1	1.4

Table 5-12: The accuracy analysis on 60 days network performance

	Deviations			
	Forward Neural Network		Inverse Neural Network	
	Abandonment Time (years)	Recovery Efficiency (%)	Abandonment Time (years)	Recovery Efficiency (%)
16	0.4	0.8	0.3	0.4
17	1.0	0.1	1.0	0.3
18	2.8	0.01	0.7	0.6
19	2.1	0.8	0.8	2.3
Ave	2.0	0.8	2.3	0.9

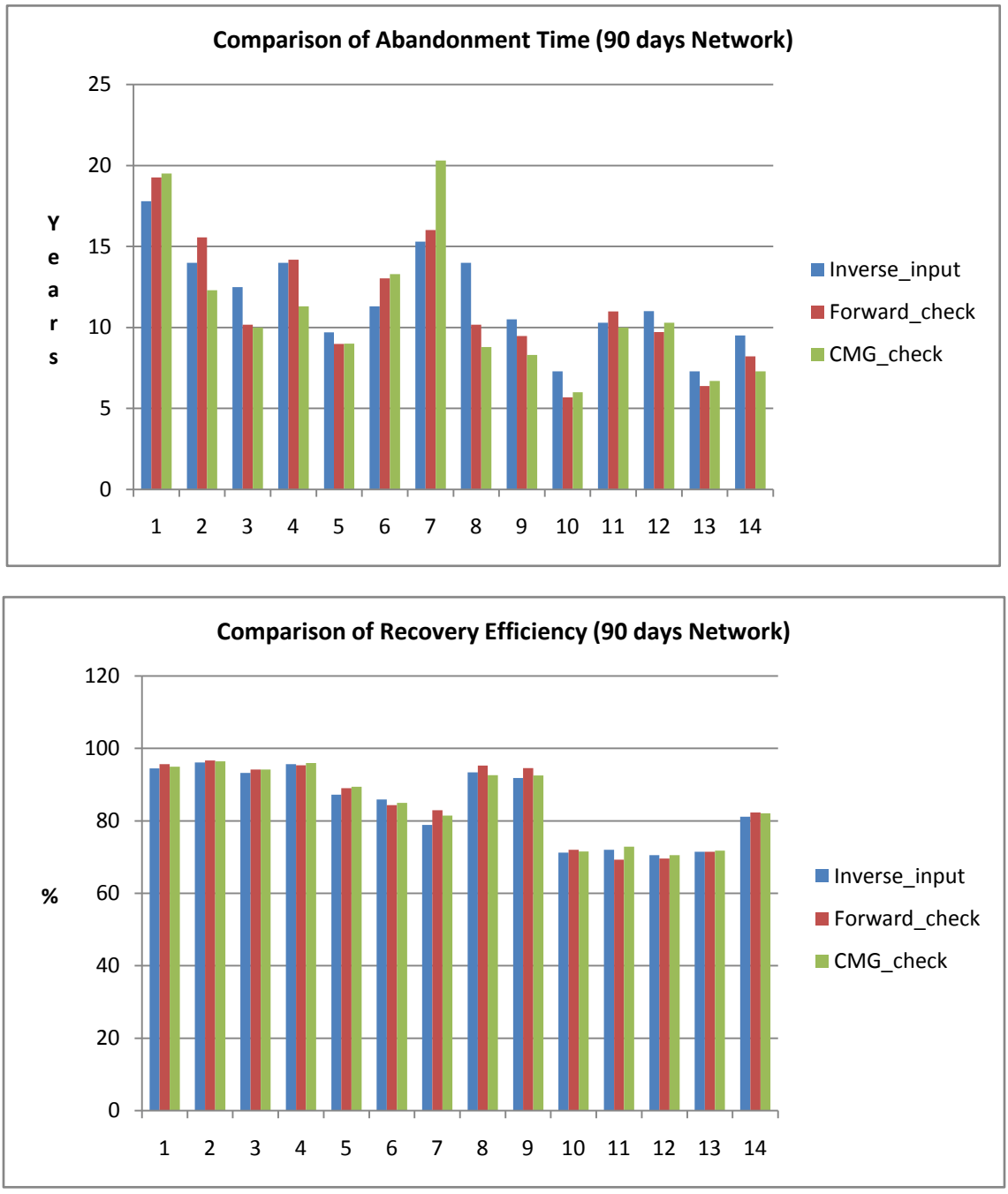

Figure 5- 21: Accuracy analysis on 90 days network performance

Table 5- 14: The accuracy analysis on 90 days network performance

	Deviations			
	Forward Neural Network		Inverse Neural Network	
	Abandonment Time (years)	Recovery Efficiency (%)	Abandonment Time (years)	Recovery Efficiency (%)
1	1.5	1.2	1.7	0.5
2	1.6	0.5	1.7	0.3
3	2.3	0.9	2.5	0.9
4	0.2	0.3	2.7	0.3
5	0.7	1.8	0.7	2.2
6	1.7	1.6	2	1.0
7	0.7	4.0	5	2.5
8	3.8	1.9	5.2	0.8
9	1.0	2.7	2.2	0.7
10	1.6	0.8	1.3	0.3
11	0.7	2.8	0.3	0.8
12	1.3	0.9	0.7	0.01
13	0.9	0.03	0.6	0.3
14	1.3	1.15	2.2	0.9
Ave	1.4	1.5	2.1	0.8

In general, the LMS error and the absolute error indicate that forward applications possess higher accuracy and inverse counterparts seem to have relatively low accuracy. However, based on results of the protocol implemented accuracy analyses, it is observed that two applications achieve similar network performance within acceptable margin of error. Therefore, suggested field operating schemes from inverse expert systems should be able to help the reservoir engineers find out the optimum production scenarios of water-alternating-gas processes.

Chapter 6

CONCLUSIONS AND RECOMMENDATIONS FOR FUTURE WORK

The networks were constructed to suggest the optimum field operating parameters of water-alternating-gas process where three respective neural network architectures were trained using the data generated by a commercial simulator. Black-oil formulation was selected and minimum miscibility conditions were included in the model. Sensitivity analyses were implemented to minimize the numerical dispersion resulting in a 15×15 Cartesian grid with a five spot well pattern.

The following observations and conclusions were made from this study:

- Permeability has a strong influence on recovery efficiency in a WAG application. This study utilize 10 md as a low limit and 500 md as a high limit permeability
  - Reservoirs with a low limit permeability present higher recovery efficiency than ones with a high limit permeability
  - Reservoirs with a low limit permeability show consistent amount of recovery efficiency, while reservoirs with a high limit permeability generally exhibit high recovery efficiency when low value of WAG ratio is utilized
  - In reservoirs with a high limit permeability, the simulation model sometimes encounters in convergence problems
- Recovery efficiency is directly proportional to porosity and inversely proportional to initial water saturation
- Formation thickness does not affect the recovery efficiency even though gravitational effect is included from 4 layering in the model

- In general, shorter abandonment time is observed as injection rates of both phases are increased, but there exists an optimum value of injection rate
  - Excessive injection rate leads to operational problems
  - Minimal injection rate extends the life of the project
- An artificial neural network was effectively constructed for WAG process using a multilayer cascade feed forward back propagation algorithm
- This study suggests three respective networks with respect to 30 days, 60 days and 90 days of alternating frequency
- Each network was built using similar network architectures except functional links
- Following strategies were implemented to decrease the error, to maximize the accuracy of the networks and to increase efficiency of training process:
  - Determining an optimum number of neurons and hidden layers in each networks
    - Too many number of neurons and hidden layers do not improve network performance but require longer computational time
    - Too small number of neurons and hidden layers deteriorate network accuracy
  - Selecting appropriate functional links for each three networks to find out the complicated relationship between inputs and outputs of networks
  - Deciding an optimum number of cases to avoid the memorization related issues
- The performance of networks was evaluated based on three criteria
  - The least mean squared(LMS) error
  - The absolute error: comparing predicted results from networks with the ones from a simulator
  - Accuracy analysis: accuracy of the network performance is further analyzed based on recovery efficiency and abandonment time, which are regenerated from forward network and a simulator using design parameters previously predicted from inverse

applications. Forward applications are assessed by closeness of two variables between inverse and forward applications. In the same manner, inverse applications are also evaluated by comparing those two variables used for inverse network with ones regenerated from a simulator

- Generally the LMS error and the absolute error indicate that forward applications exhibit better performance than inverse counterpart. However, protocol implemented accuracy analysis show that there is no significant difference of accuracy between forward and inverse network. Thus, inverse expert systems are able to propose field development strategies of WAG processes within acceptable margin of error

Following perspectives were generated during the study, which can help suggesting more flexible field development plans under diverse reservoir characteristics complementing the current work.

- This study was only associated with one type of black-oil. But, different networks can be constructed according to different black-oil and volatile-oil systems. A similar procedure followed to train current networks can be effectively used for networks dealing with other types of oil
- The relative permeability data for present study is one typical example of the sandstone rock properties. Network can be constructed using different water-oil and gas-oil relative permeability curves of several rock types
- Even though 5-spot well pattern is typically utilized in WAG process, it is worth generating networks to study various well patterns such as 4-spot, inverted 5-spot, 9-spot and inverted 9-spot
- Types of injection gas used in WAG process can include other gases such as hydrocarbon gases or N_2

- The study can be expanded to include the simultaneous water alternating gas injection process (SWAG)

Bibliography

Ali, J. K.: Neural Networks, A New Tool for the petroleum Industry?, SPE Paper 27561, 2006

Bedrikovetsky, P., Andrade, G.M., Ferreira, L.E.A.: Optimization of Miscible Water-Alternate-CO_2 Injection, SPE Paper 36133, 1996

Carcoana, Aurel: Applied Enhanced Oil Recovery, Library of Congress Cataloging-in-Publication Data, Prentice-Hall, Inc., New Jersey, ISBN 0-13-044272-0, 1992

Christensen, J. R., Stenby, E.H., Skauge, A.: Review of WAG Field Experience, SPE Paper 71203, 2001

Corey, A. T.: The Interrelation between Gas and Oil Relative Permeabilities, Producers Monthly, 1954

Craft, B. C. and Hawkins, M. F.: Applied Petroleum Reservoir Engineering, PRENTICE-HALL CHEMICAL ENGINEERING SEREIS, Prentice-Hall, Inc., New Jersey, 1959

Dandekar, Abhijit Y.: Petroleum Reservoir Rock and Fluid Properties, Taylor & Francis Group, CRC Press, ISBN 0-8493-3043-2, 2006

Demuth, H., Beale M. and Hagan, M.: Neural Network Toolbox 5 User's Guide, The Math Works, Inc., Natick, Massachusetts, 2007

Ertekin, Turgay., Abou-Kassem, Jamal H., King, Gregory R.: Basic Applied Reservoir Simulation, SPE Text Book Series, Richardson, Texas, ISBN 1-55563-089-8, 2001

Fausett, Laurene: Fundamentals of Neural Networks, Prentice-Hall, Inc., New Jersey, ISBN 0-13-334186-0, 1994

Green, Don W and Willhite, G. Paul: Enhanced Oil Recovery, SPE Textbook Series Vol. 6. Richardson, Texas, ISBN 1-55563-077-4, 1998

Hagan, M., Demuth, H. and Beale, M.: Neural Network Design, PWS pub., 1st Edition, Boston, ISBN 7-111-10841-8, 1996

Lake, Larry W.: Enhanced Oil Recovery, Prentice-Hall, Inc., New Jersey, ISBN 0-13-281601-6, 1989

learnartificailneuralnetworks.com: Neural Networks, Artificial Intelligence Technologies Tutorial, 2007

Maren, A., Harston, C and Pap, R.: Handbook of Neural Computing Applications, Academic Press, Inc., San Diego, ISBN 0-12-546090-2, 1990

Minakowski, Claudia Helena Parada: An Artificial Neural Network Based Tool-Box for Screening and Designing Improved Oil Recovery Methods, The Pennsylvania State University, 2008

Patterson, D. W.: Artificial Neural Networks, Theory and Applications, Prentice-Hall, Inc., Singapore, ISBN 0-13-295353-6, 1996

Rogers, John D. and Grigg, Reid B.: A Literature Analysis of the WAG Injectivity Abnormalities in the CO_2 Process, SPE Paper 59329, 2000

Stalkup, Fred I. Jr.: Miscible Displacement, SPE Monograph Volume 8, Henry L. Doherty Series, Dallas, ISBN 0-89520-319-7, 1983

Stosur, J. J. George: The Potential of Enhanced Oil Recovery, International Journal of Energy Research, 2007

Teletzke, G. F., Patel, P. D. Chen, A. L.: Methodology for Miscible Gas Injection EOR Screening, SPE Paper 97650, 2005

Yellig, W. F. and Metcalfe, R. S.: Determination and Prediction of CO2 Minimum Miscibility Pressure, Journal of Petroleum Technology, 1980

Appendix A

Inverse Application for 30 Days

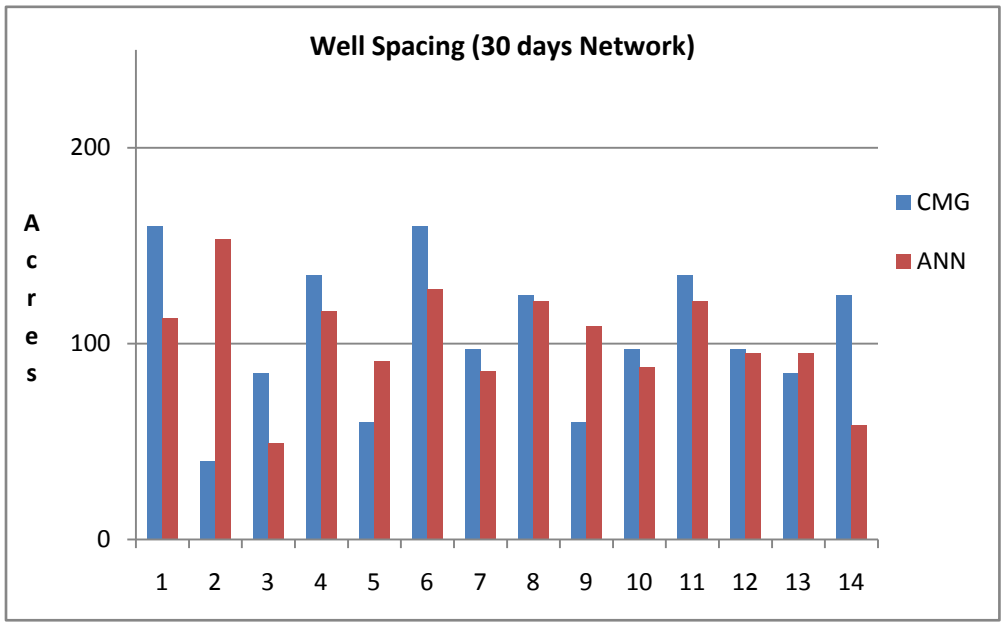

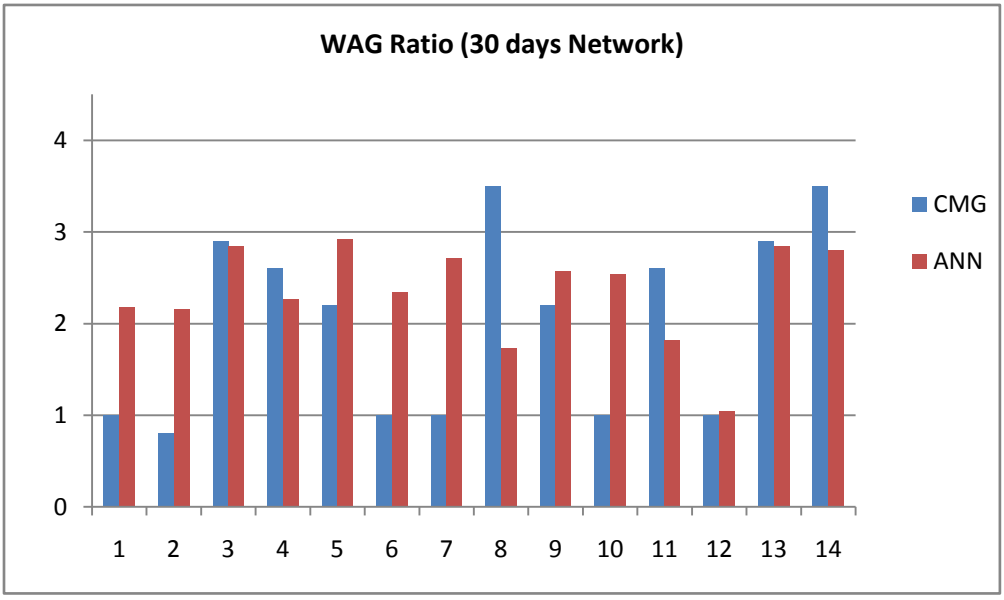

Figure A- 1: 30 Days inverse neural networks performance

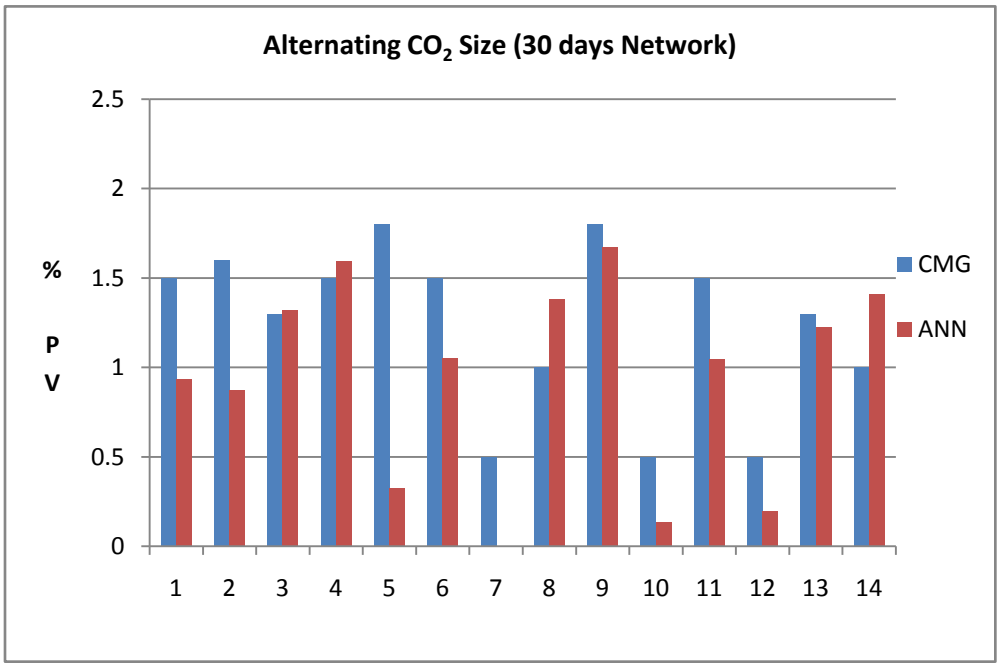

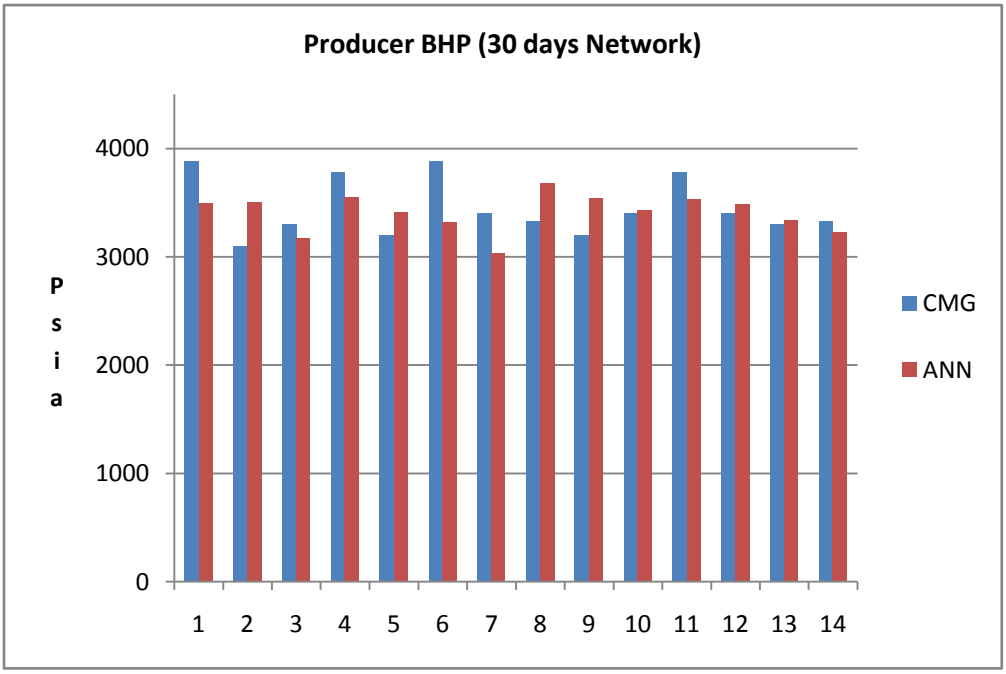

Figure A- 2: 30 Days inverse neural networks performance

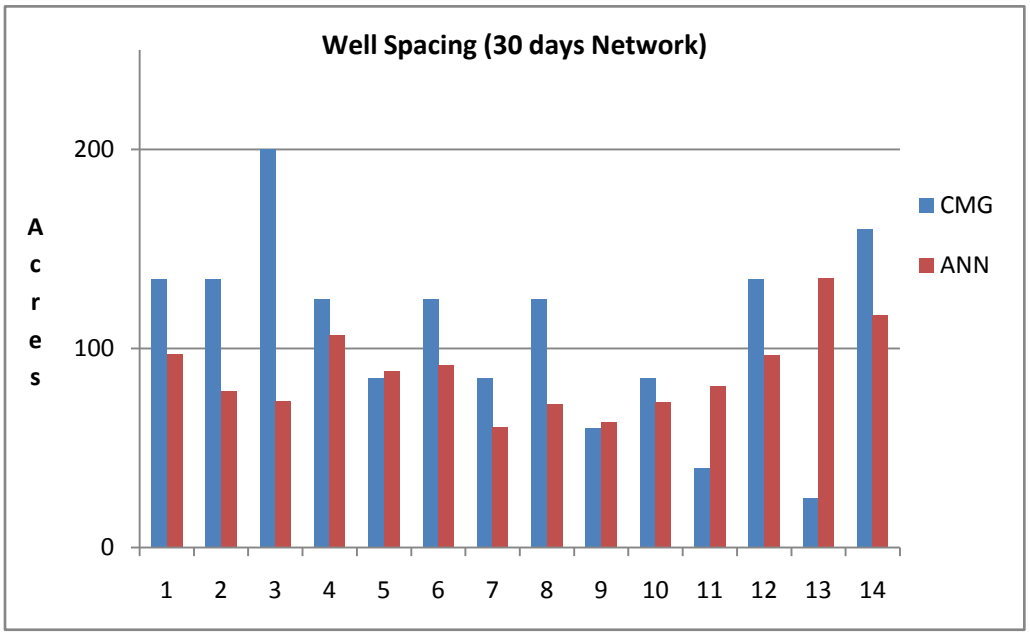

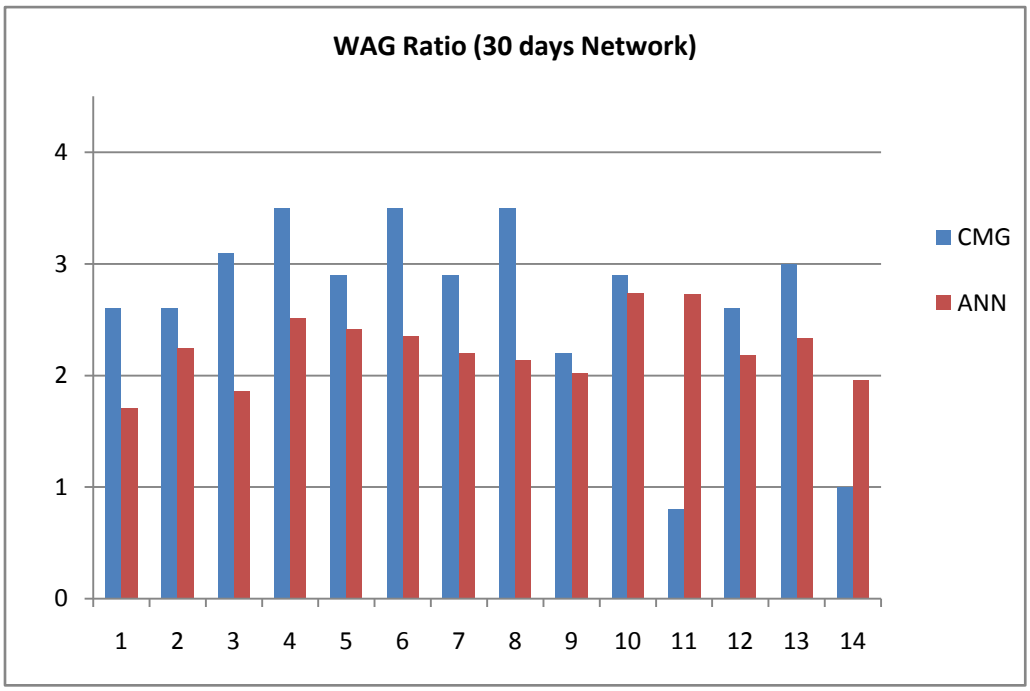

Figure A- 3: 30 Days inverse neural networks performance

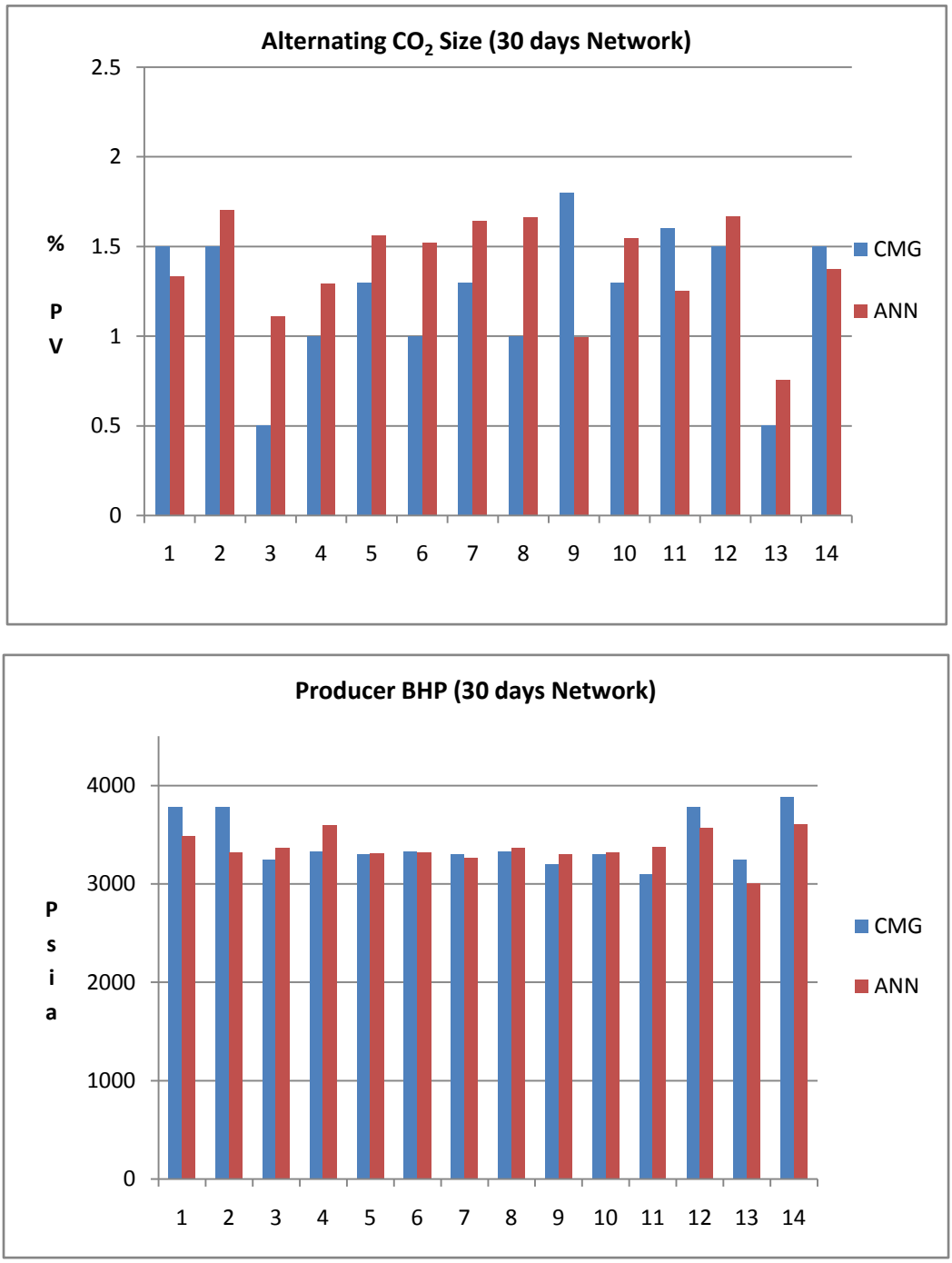

Figure A- 4: 30 Days inverse neural networks performance

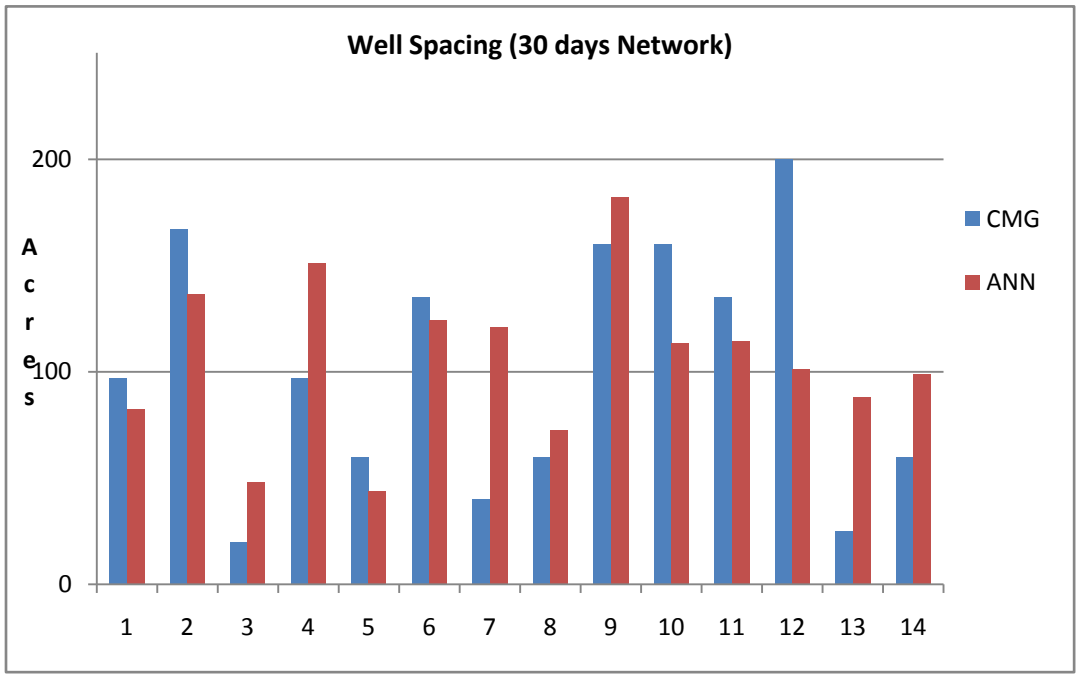

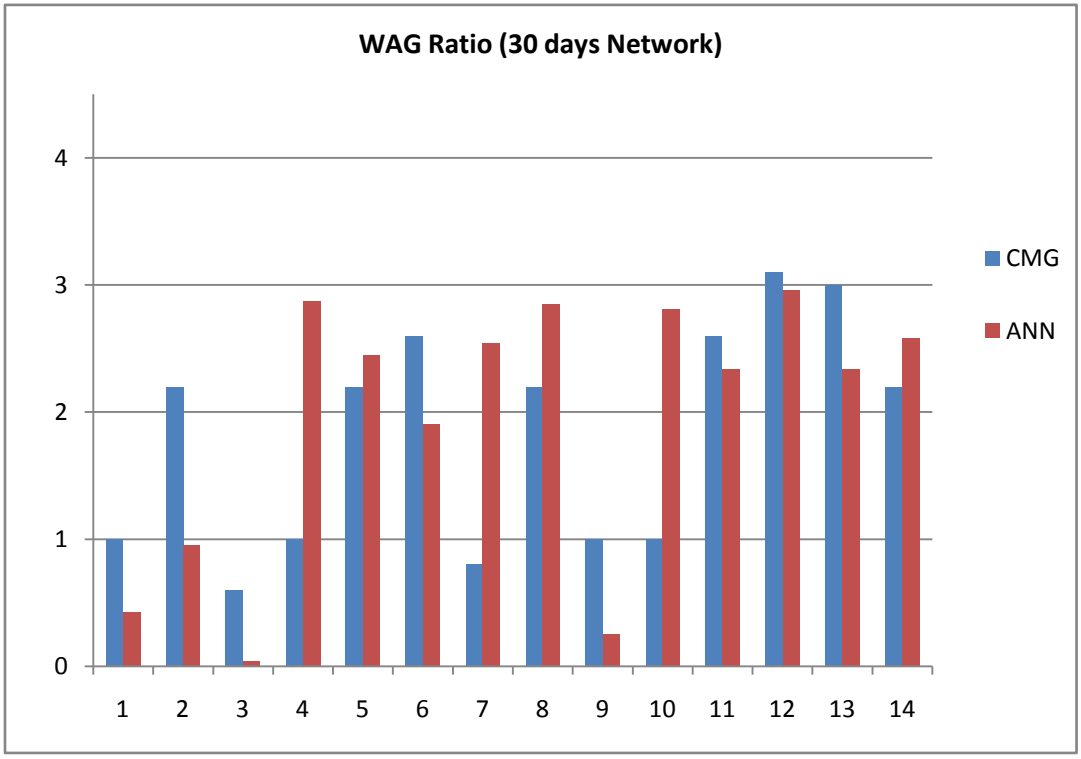

Figure A- 5: 30 Days inverse neural networks performance

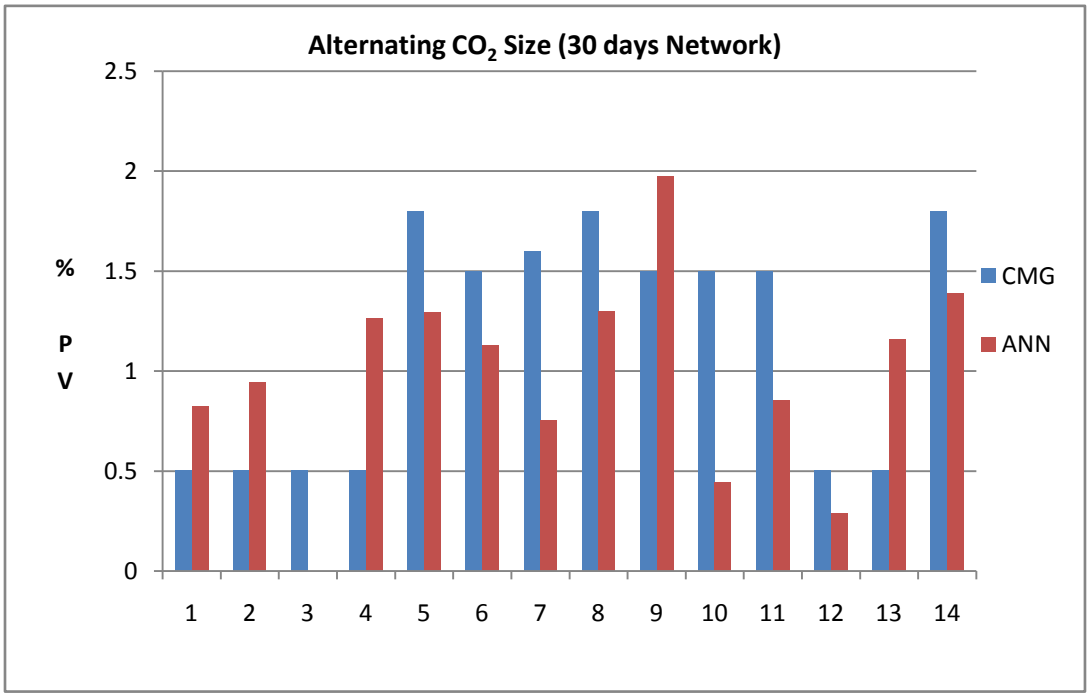

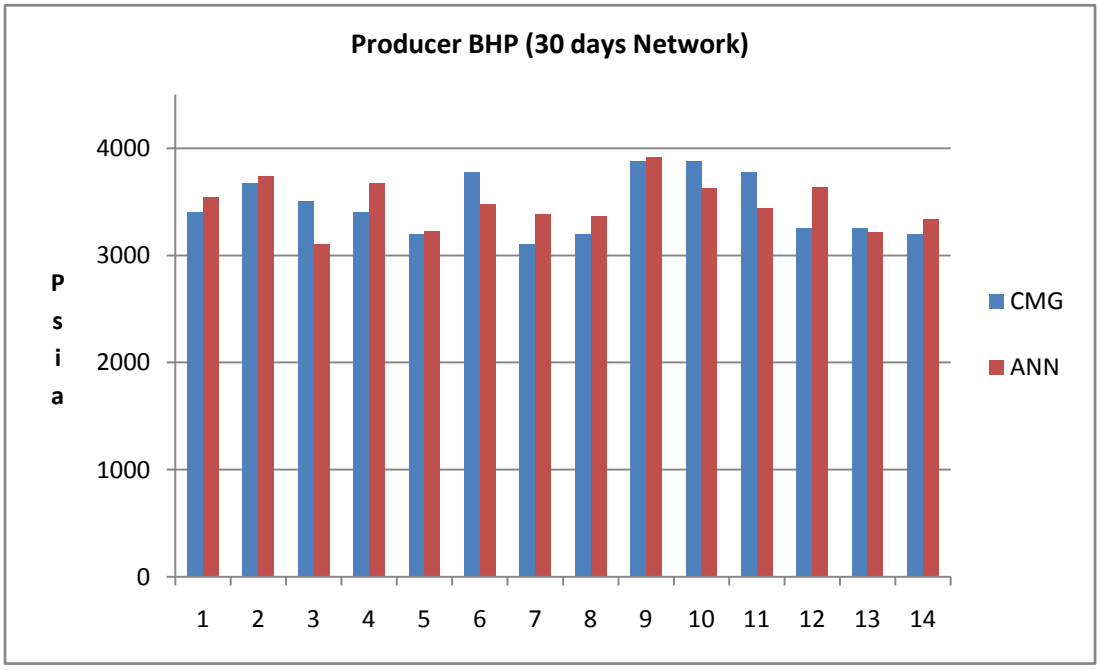

Figure A- 6: 30 Days inverse neural networks performance

Appendix B

Inverse Application for 60 Days

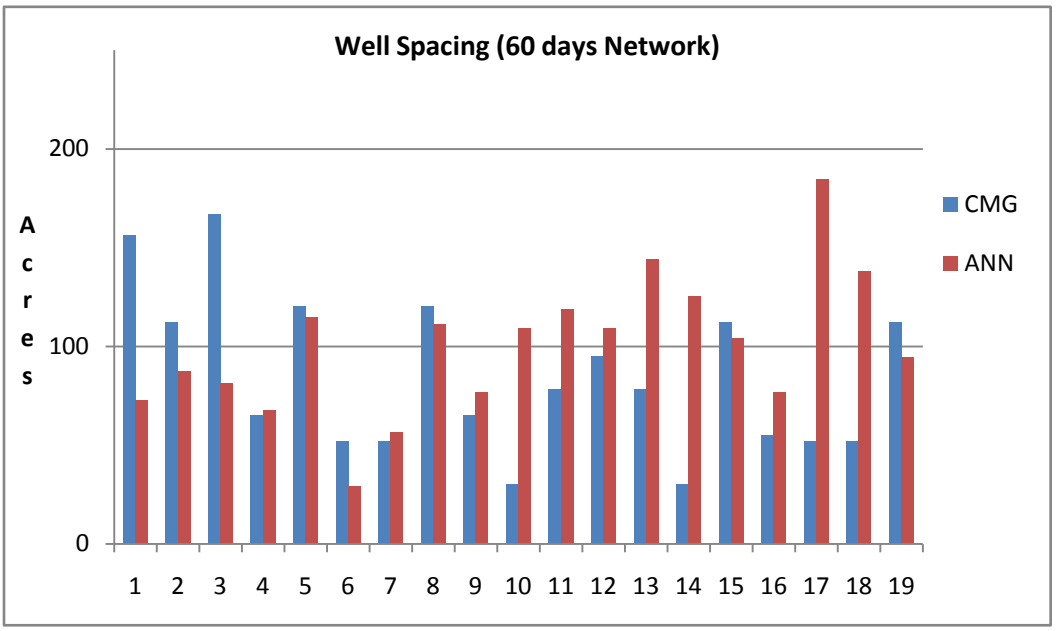

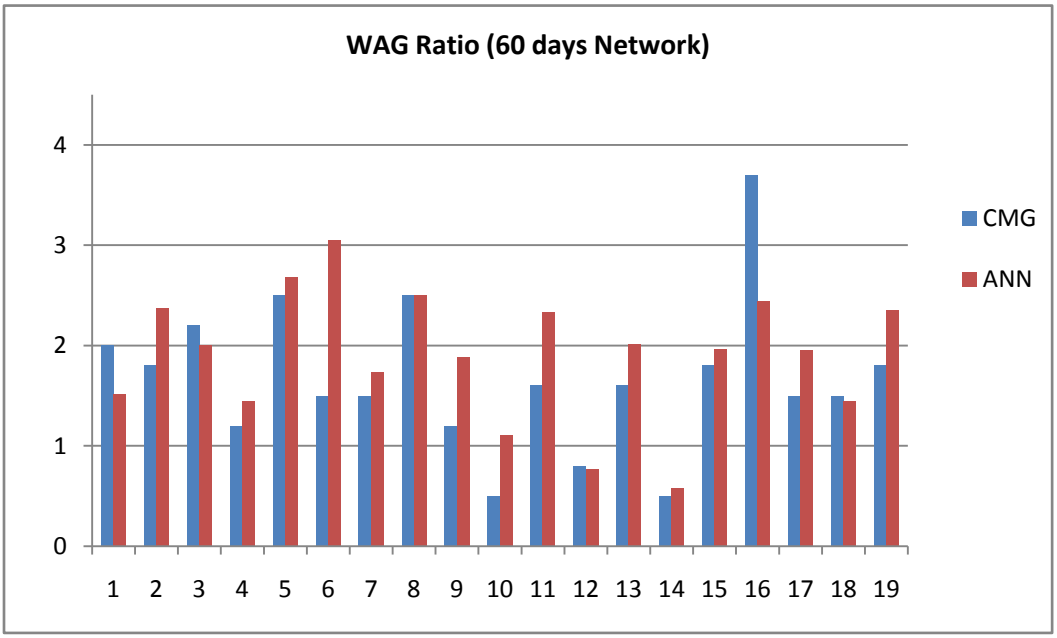

Figure B- 1: 60 Days inverse neural networks performance

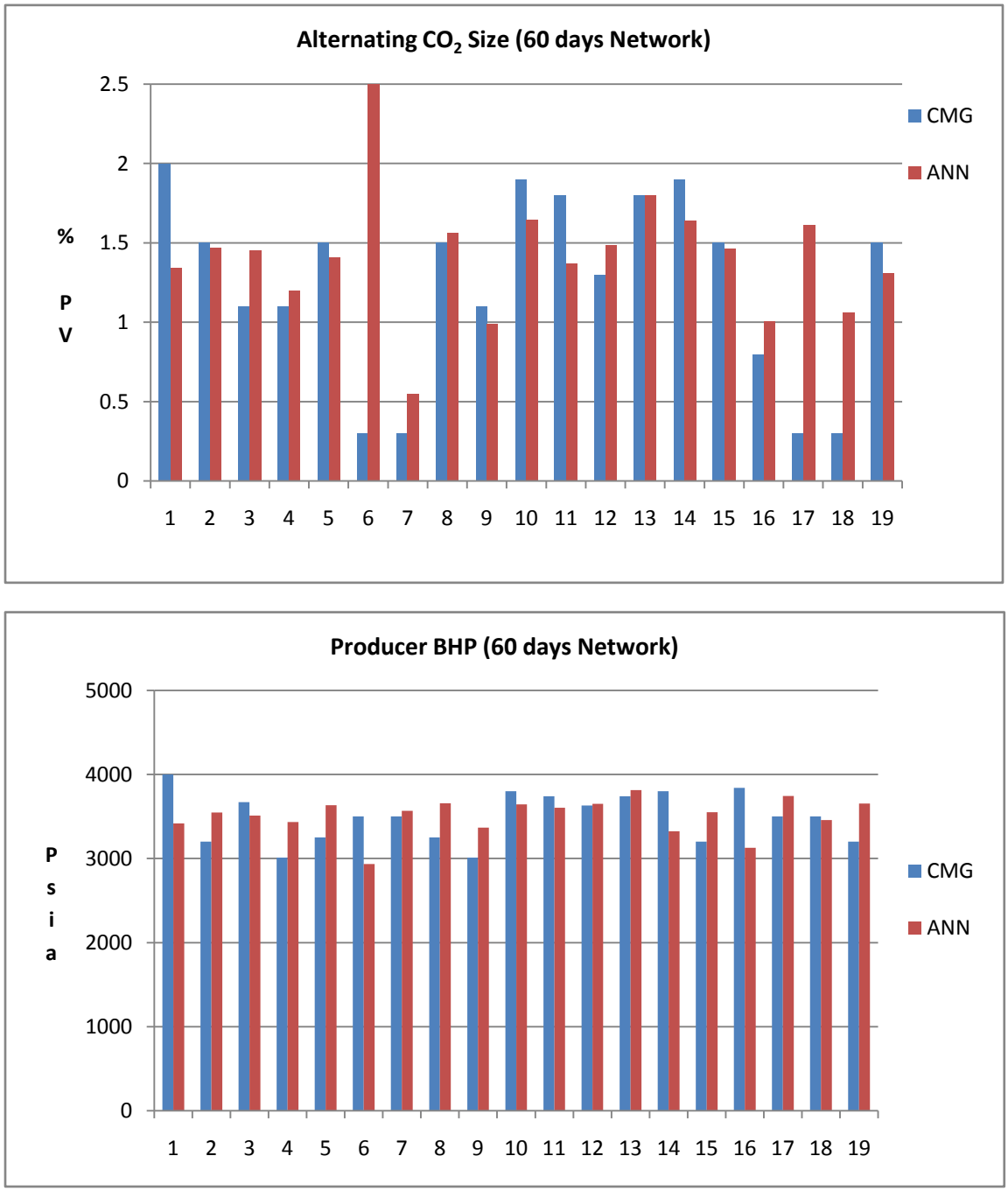

Figure B- 2: 60 Days inverse neural networks performance

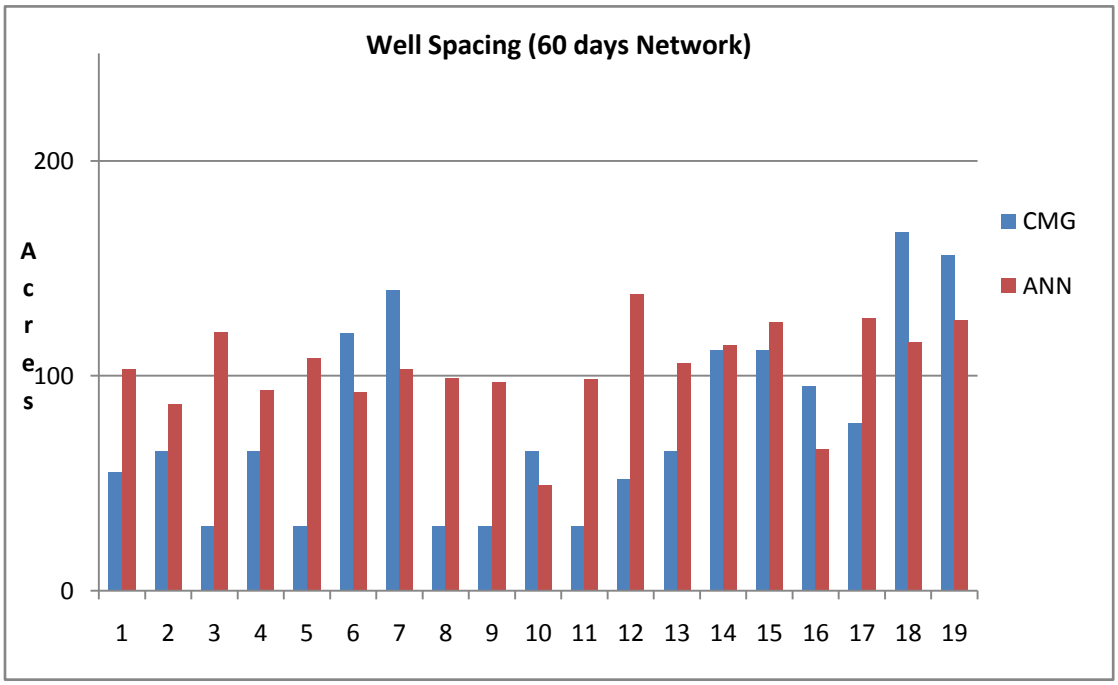

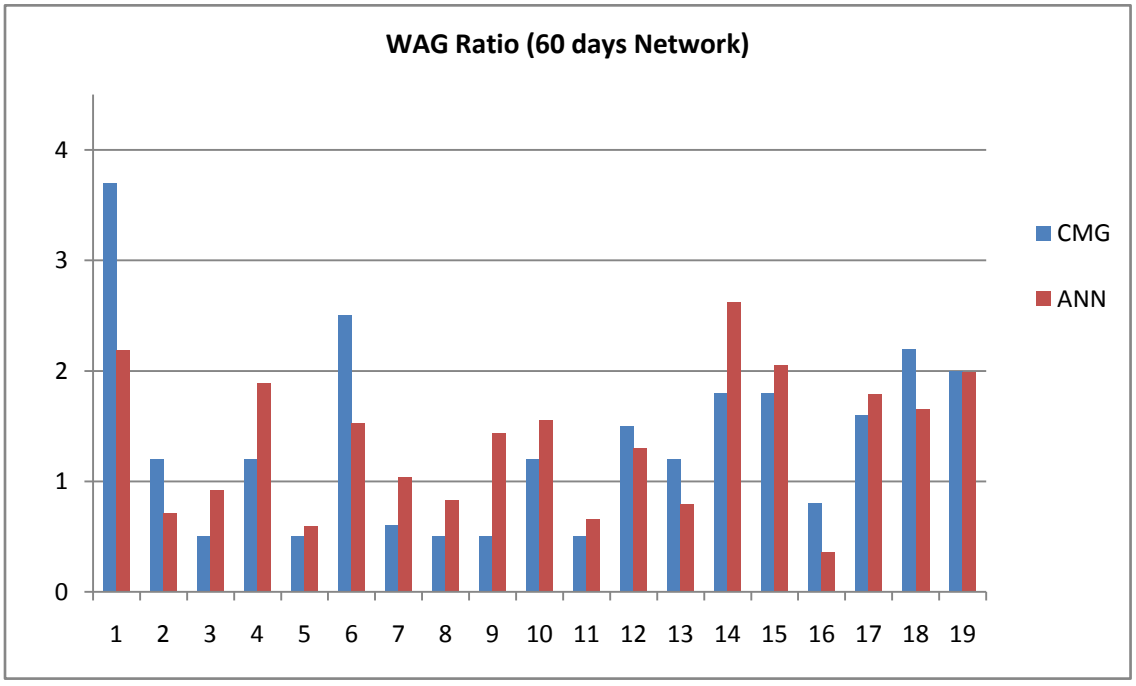

Figure B- 3: 60 Days inverse neural networks performance

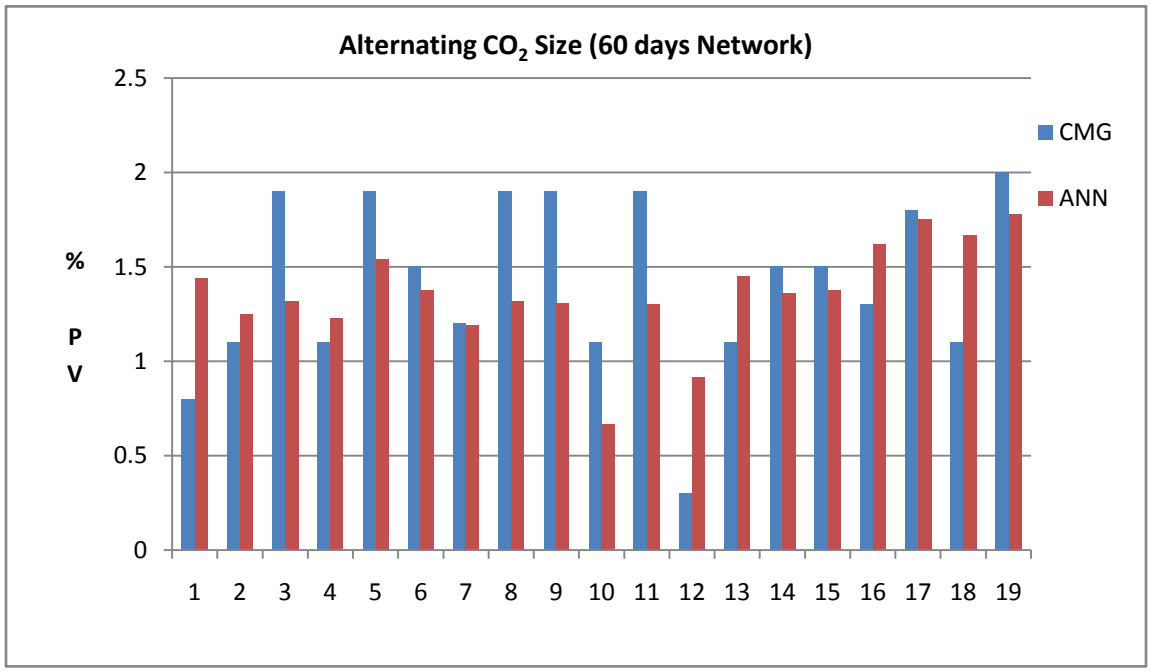

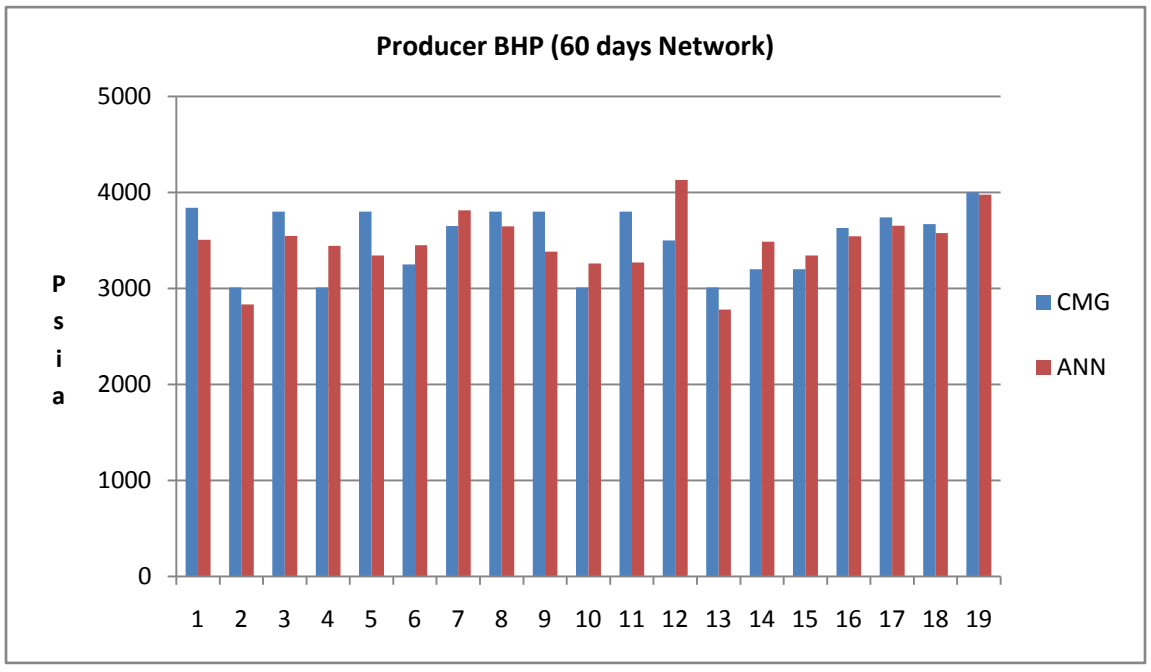

Figure B- 4: 60 Days inverse neural networks performance

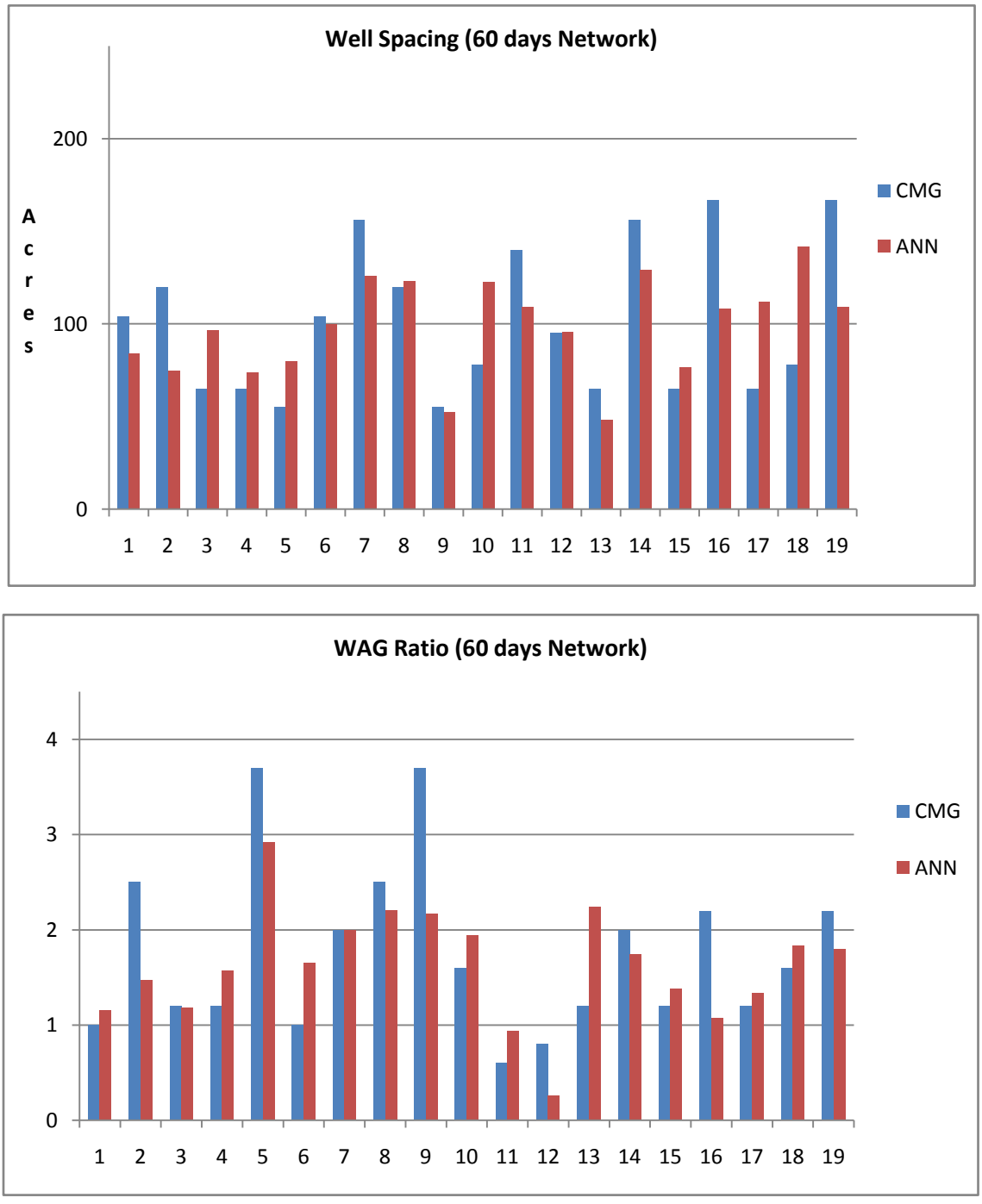

Figure B- 5: 60 Days inverse neural networks performance

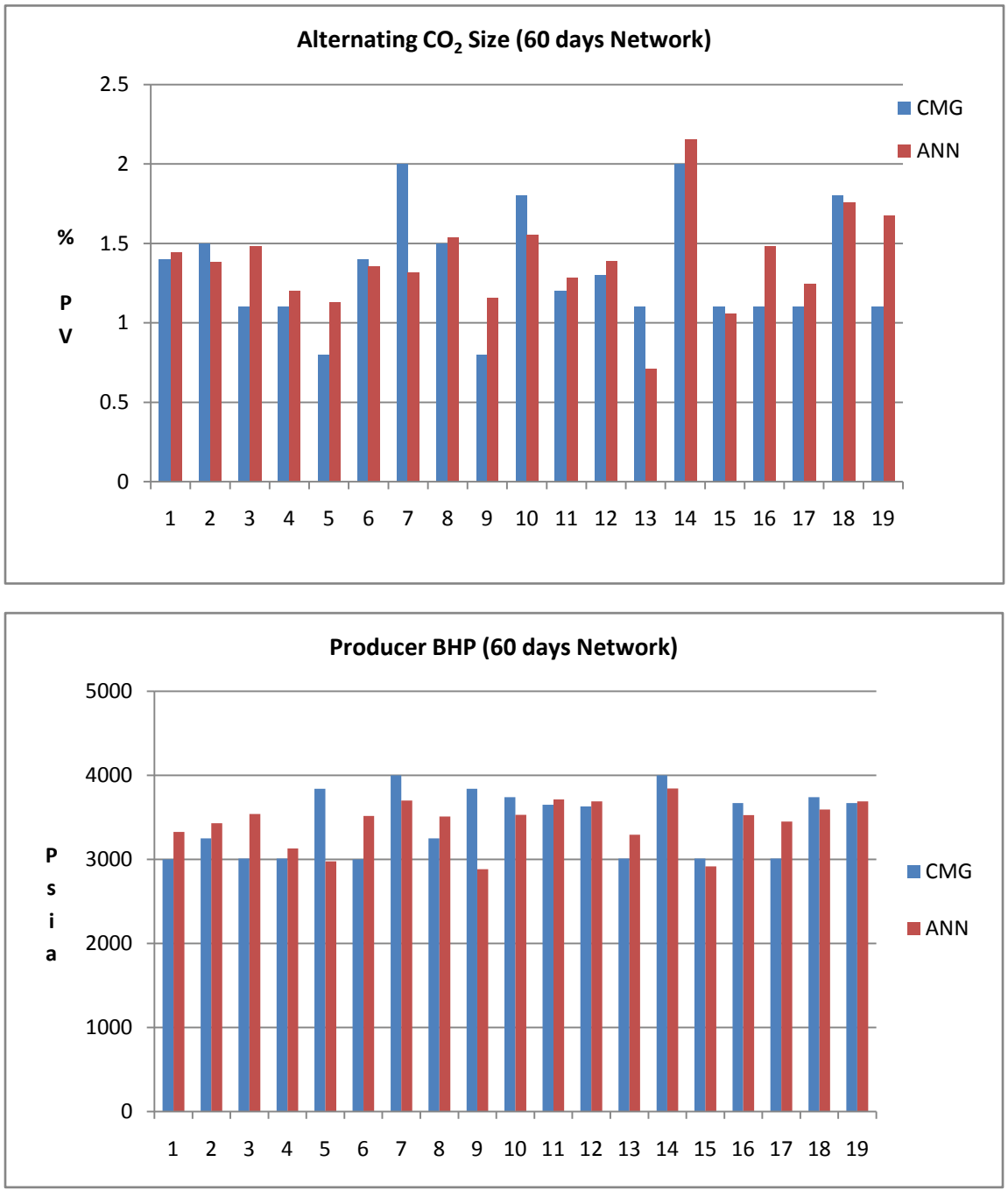

Figure B- 6: 60 Days inverse neural networks performance

Appendix C

Inverse Application for 90 Days

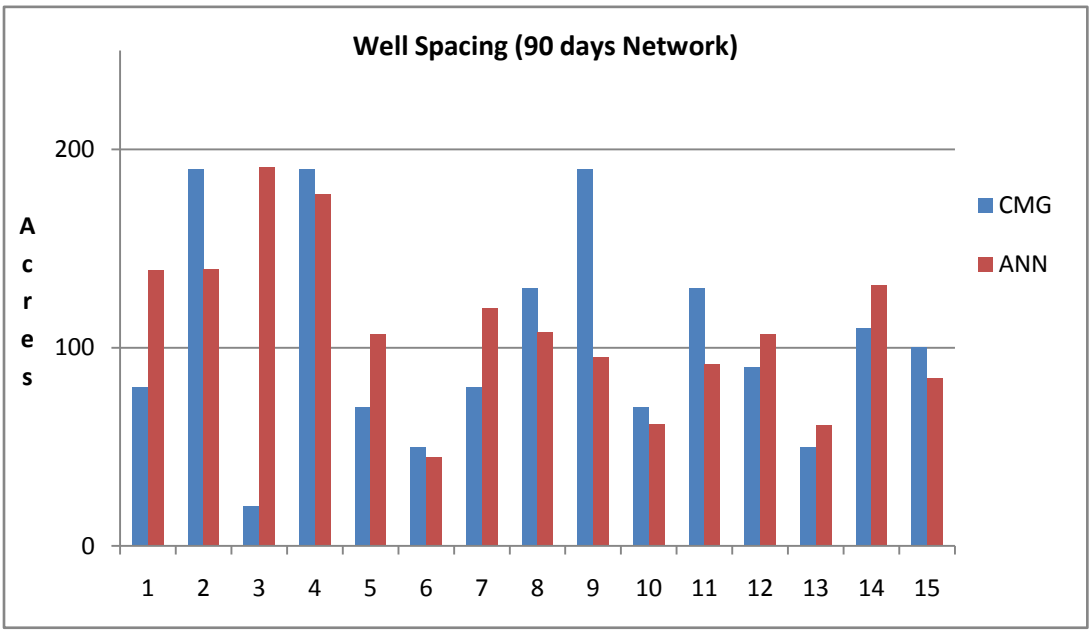

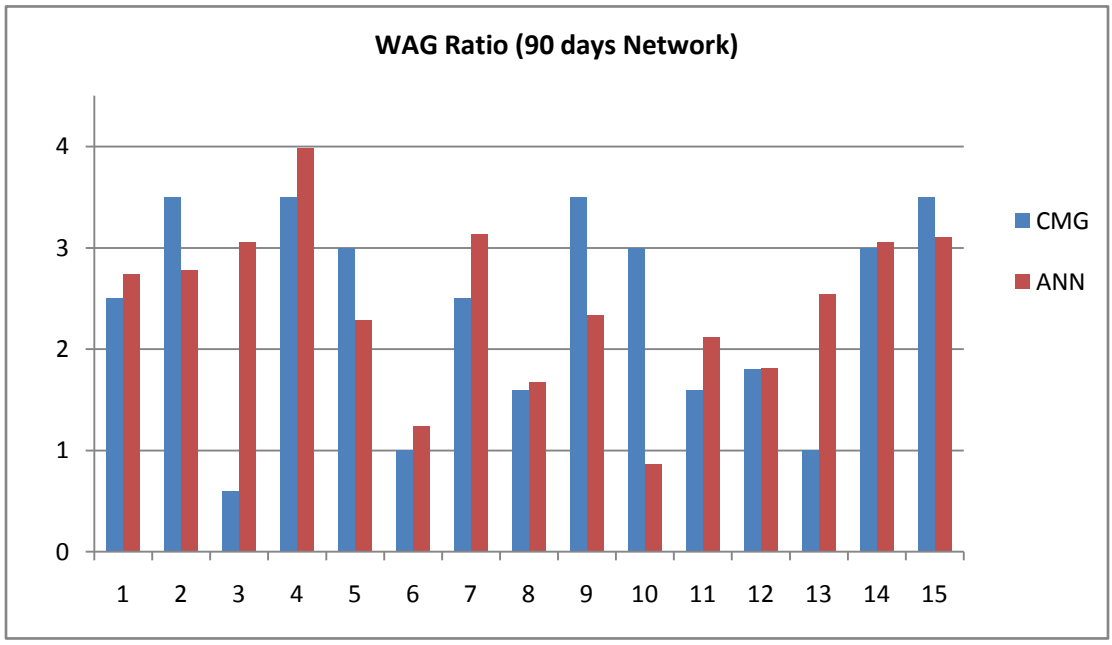

Figure C- 1: 90 Days inverse neural networks performance

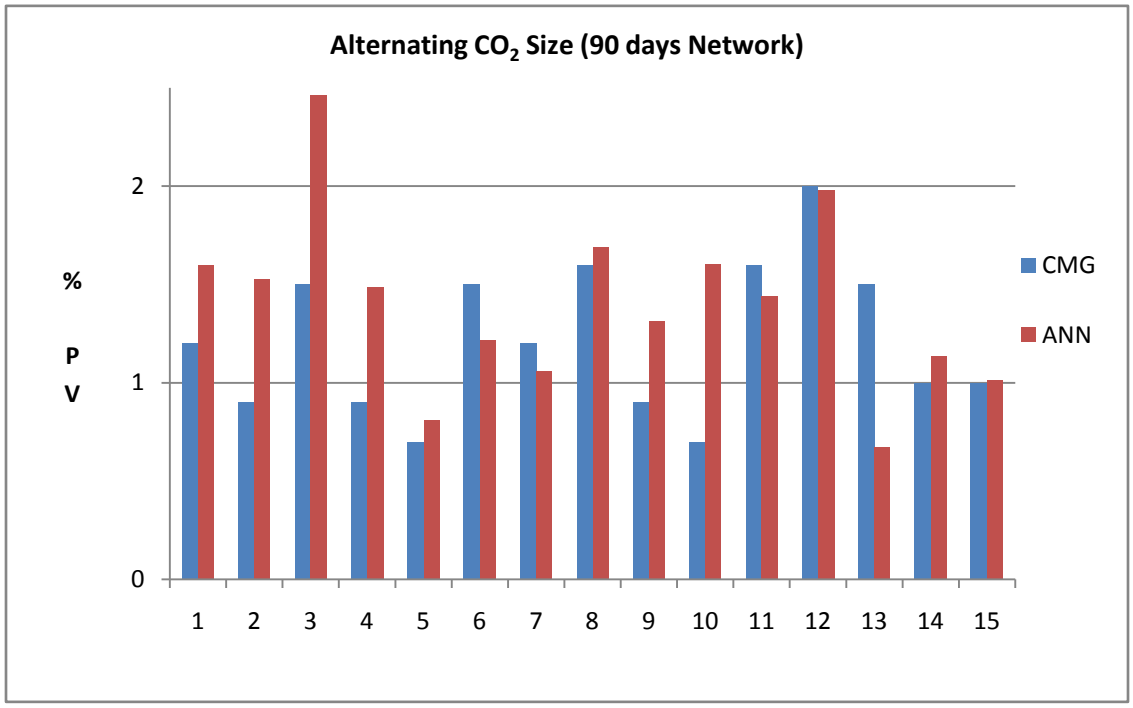

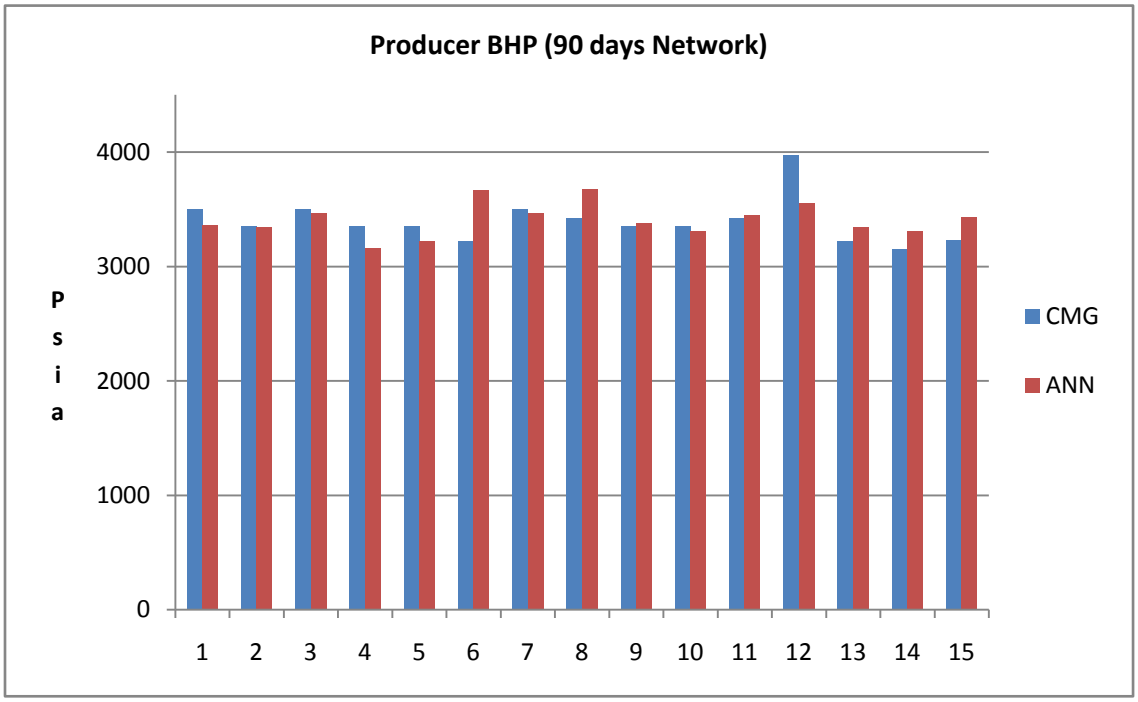

Figure C- 2: 90 Days inverse neural networks performance

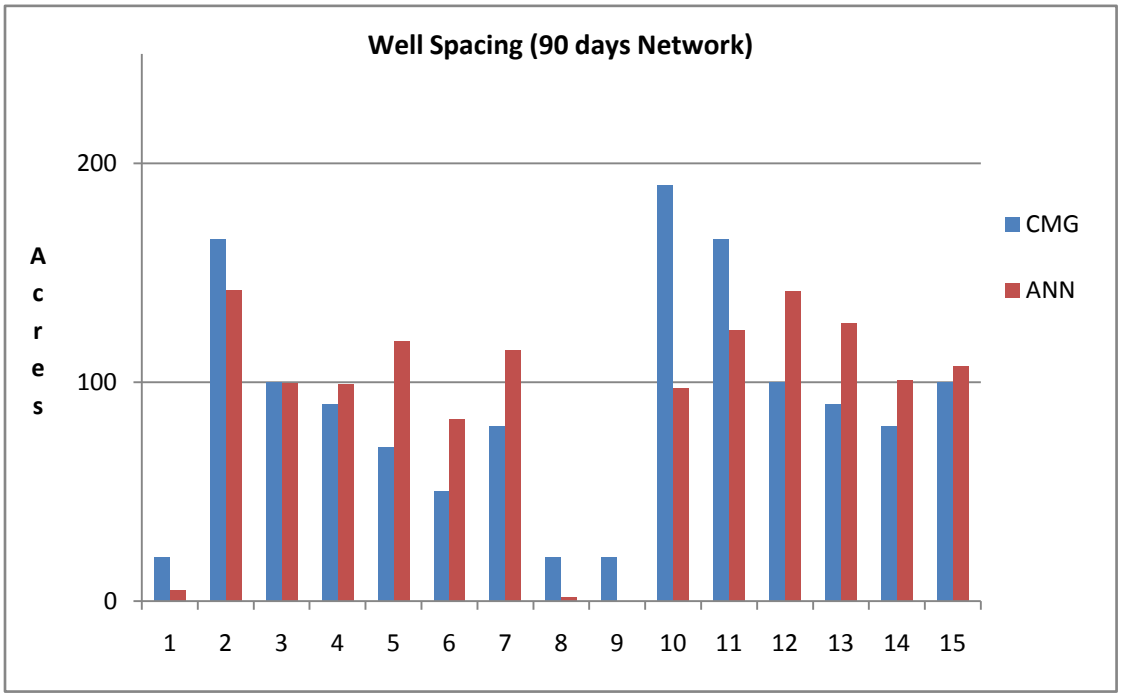

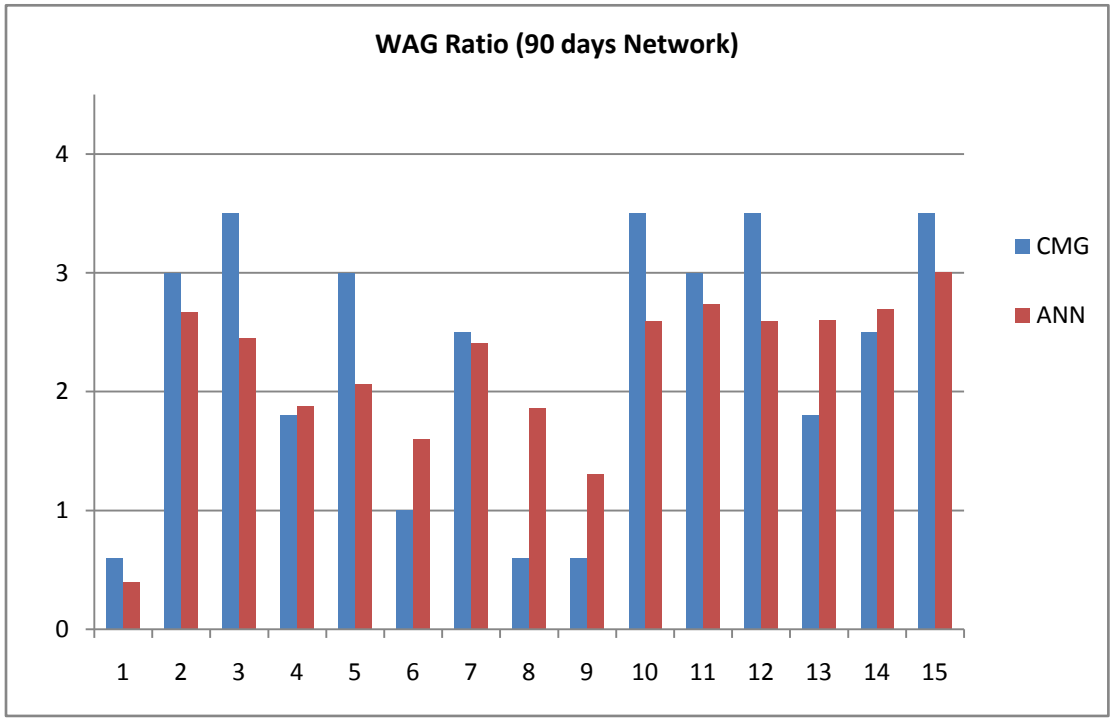

Figure C- 3: 90 Days inverse neural networks performance

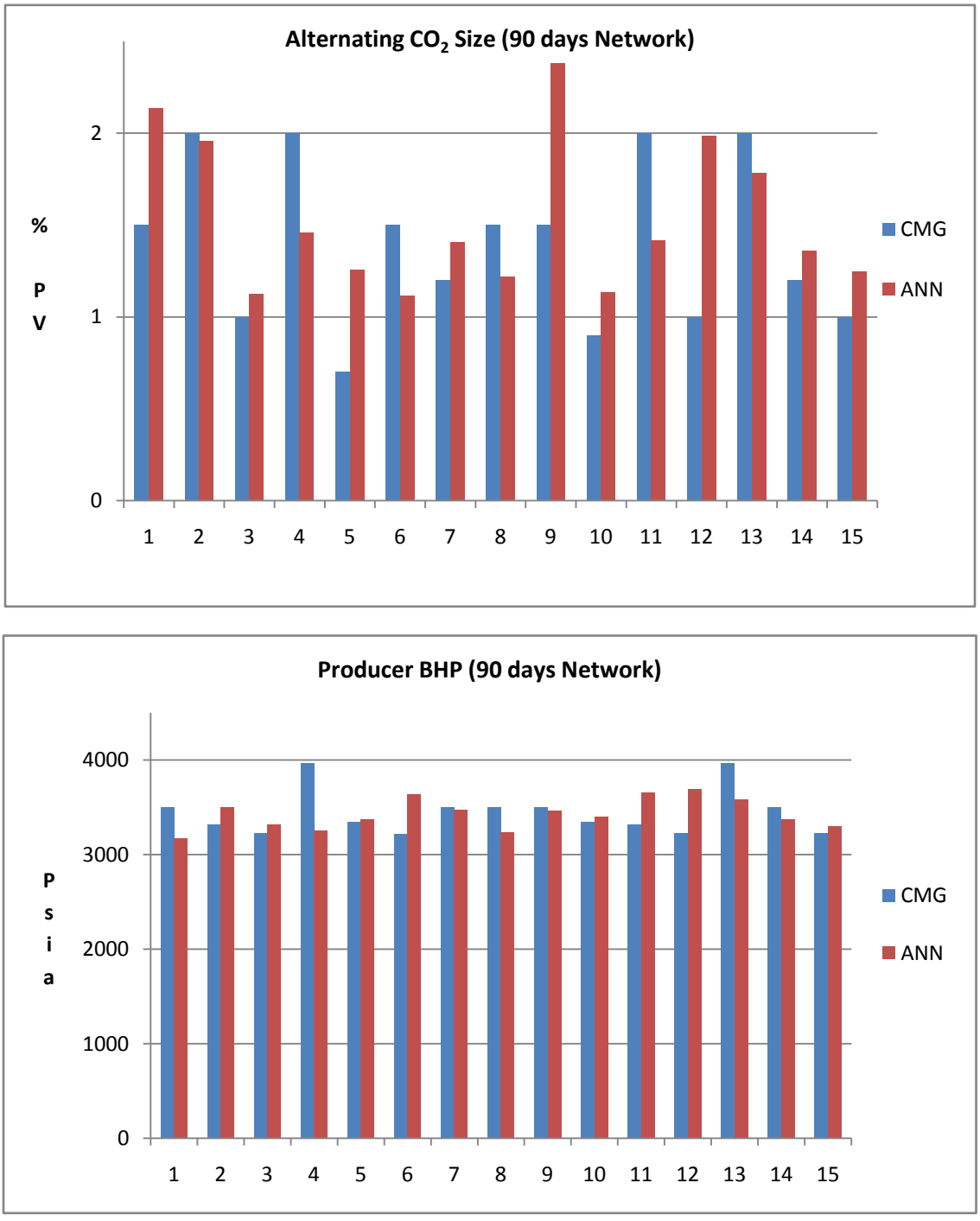

Figure C- 4: 90 Days inverse neural networks performance

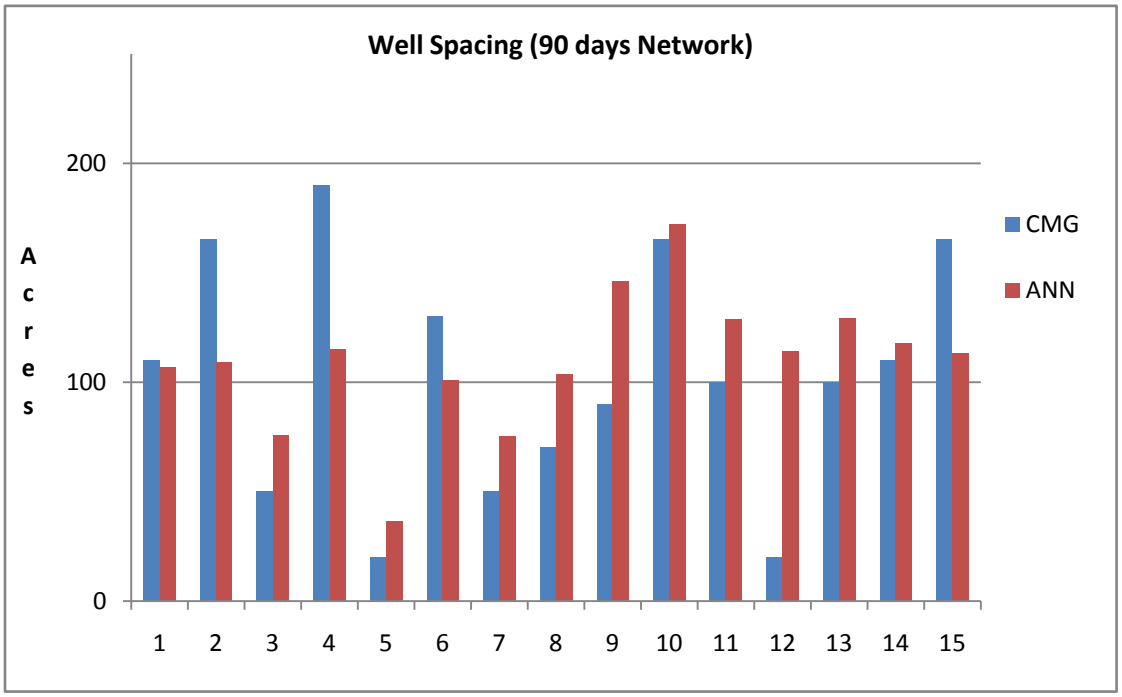

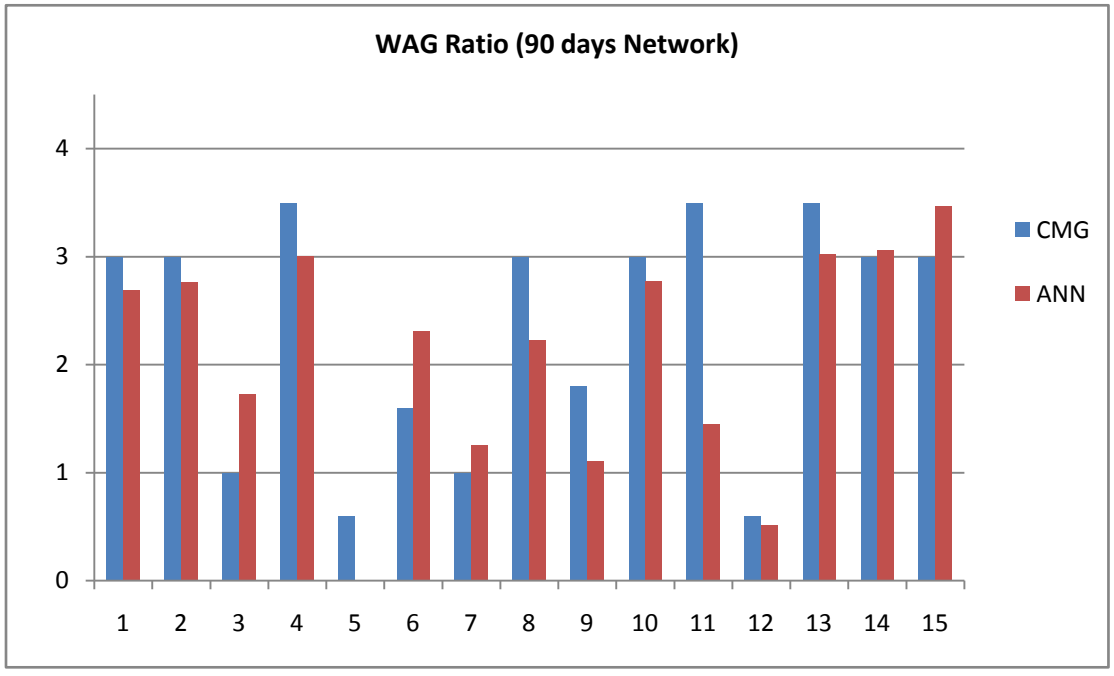

Figure C- 5: 90 Days inverse neural networks performance

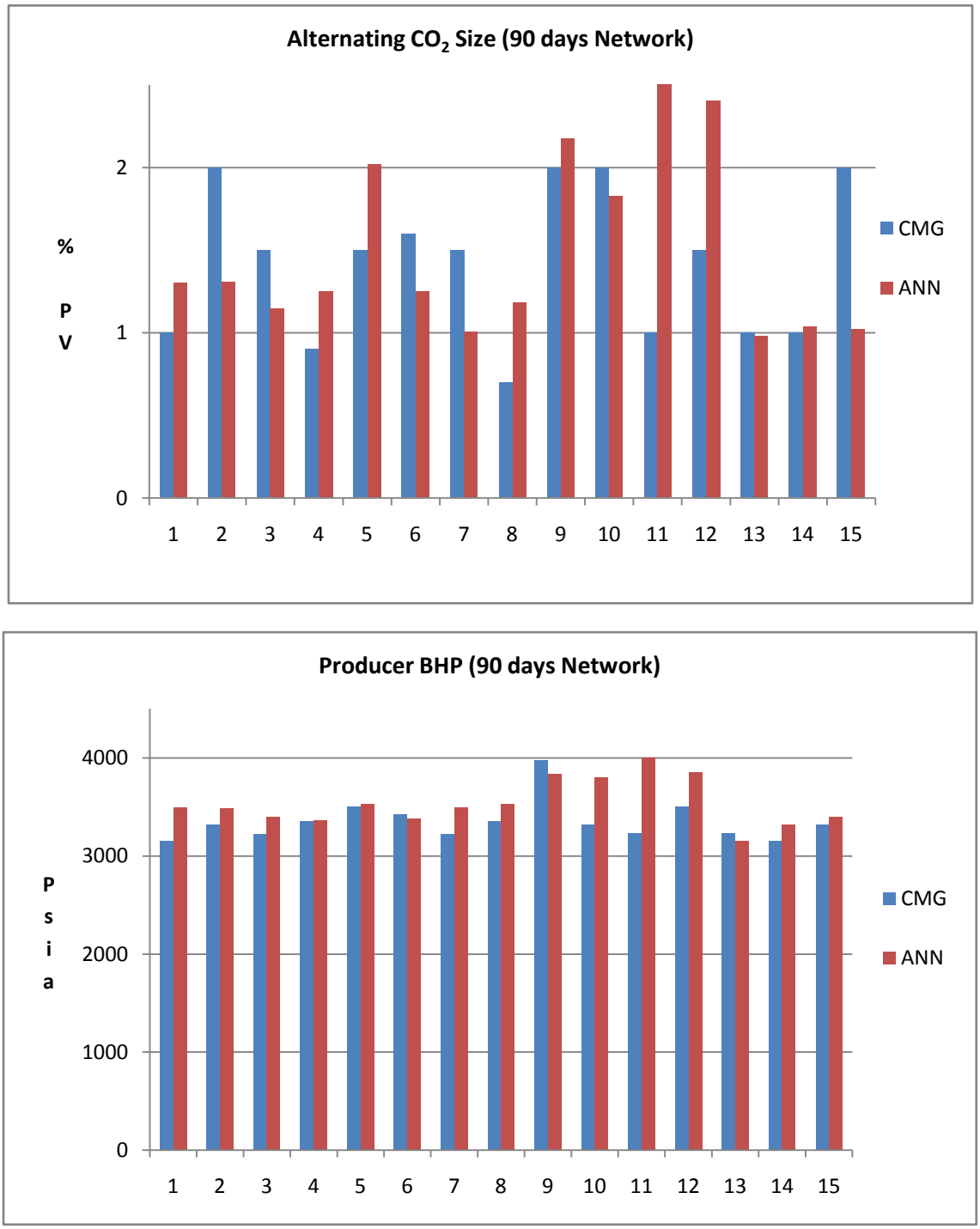

Figure C- 6: 90 Days inverse neural networks performance